STRUCTURAL AND FUNCTIONAL STUDIES OF AN ATYPICAL OMPR/PHOB TRANSCRIPTIONAL REGULATOR, CHXR, FROM *CHLAMYDIA TRACHOMATIS*

By

John Hickey

Submitted to the graduate degree program in Molecular Biosciences and the Graduate Faculty of the University of Kansas in partial fulfillment of the requirements for the degree of Doctor of Philosophy.

_____
Chairperson (Scott Hefty, Ph.D.)

_____*
(Audrey Lamb, Ph.D.)

_____*
(Susan Egan, Ph.D.)

_____*
(Yoshiaki Azuma, Ph.D.)

_____*
(Roberto De Guzman, Ph.D.)

_____*
(Russ Middaugh, Ph.D.)

*Committee Members

Date Defended: 04/08/2011

The Dissertation Committee for John Hickey certifies that this is the approved version of the following dissertation:

STRUCTURAL AND FUNCTIONAL STUDIES OF AN ATYPICAL OMPR/PHOB TRANSCRIPTIONAL REGULATOR, CHXR, FROM *CHLAMYDIA TRACHOMATIS*

_____
Chairperson (Scott Hefty, Ph.D.)

Date approved: 4/22/2011

SUMMARY

Chlamydia infections have an immense impact on public health and are associated with diverse disease manifestations including atherosclerosis, blindness, and sterility. The chlamydial developmental cycle is intrinsically linked with the ability of the organism to cause disease. The mechanisms that regulate the developmental cycle are poorly understood; however, transcription appears to play a governing role. An OmpR/PhoB subfamily response regulator termed ChxR exhibits expression patterns that indicate an important role during the developmental cycle. Previously, ChxR was demonstrated to interact with its own promoter and facilitate the transcriptional activation of the *chxR* gene. To begin to understand the functional role of ChxR, I identified the DNA sequence recognized by ChxR to identify its gene targets. Primarily using gel mobility shift assays, I determined that ChxR interacts with, and has differential affinity for six binding sites in the *chxR* promoter region. Using the DNA sequences from these binding sites, I elucidated the ChxR cis-acting recognition sequence.

Additionally, I was interested in elucidating the ChxR mechanism of transcriptional activation. Usually as a result of phosphorylation, OmpR/PhoB response regulators form homodimers through a receiver domain as an integral step in transcriptional activation. Dimer formation facilitates an interaction of the effector domain interaction with DNA and transcriptional machinery to regulate transcription. ChxR is an atypical OmpR/PhoB response regulator because it is active in the absence of phosphorylation. We hypothesized that the intra- and intermolecular interactions involved in forming a transcriptionally competent ChxR protein are distinct from the canonical phosphorylation (activation) paradigm in the OmpR/PhoB response regulator subfamily. Using biochemical techniques, I demonstrated that ChxR forms homodimers through the receiver domain and the effector domain interacts with DNA similar to

phosphorylation-induced and transcriptionally active OmpR/PhoB response regulators. Additionally, the structures of the two domains were solved to direct functional studies to identify the residues important in homodimer formation, interaction with DNA, and interaction with RNA polymerase machinery. Both structures had unique features that are not found in other OmpR/PhoB subfamily members. The combination of these results suggests that ChxR is a member of the OmpR/PhoB subfamily, although many of the characteristics of the subfamily are not shared in ChxR.

This work is dedicated to my parents and wife
for their unwavering love and support

ACKNOWLEDGEMENTS

The person I would like to thank first is my graduate mentor Dr. Scott Hefty. Under his expert tutelage, I developed my skill as a research scientist. He was always there when I had a question regarding an experimental approach or information within the literature. I am very grateful for my time in his laboratory. Additionally, I would like to thank all of the graduate students, undergraduates, and technicians in the lab that facilitated my research and development as a scientist.

I would also like to thank my committee members: Dr. Audrey Lamb, Dr. Susan Egan, Dr. Yoshiaki Azuma, Dr. Roberto De Guzman, Dr. Emily Scott, and Dr. Russ Middaugh. Each has had an impact not only on my development as a scientist throughout my graduate career, but in my research as well. Whether it was through collaboration on a project, or critical analysis of data, or through the use of equipment and reagents, the guidance I received was invaluable to my accomplishments.

I would like to thank my family and friends for their support and encouragement over the last 5 years. My parents, Vicki and Mike Hickey, were elated when I informed them of my decision to peruse a graduate degree. Sadly, my mother passed away during my first semester in graduate school. She had an enormous impact on my life and even though she will not see me receive my degree, I know that she would be very proud of my accomplishments. I would also like to thank my wife Sarah for her unvarying love and support. I am very lucky to have found someone who always encourages me and drives me to become a better person.

TABLE OF CONTENTS

Collaborator's Contributions:

Dr. Scott Hefty performed the quantitative-PCR in Fig. 1.4 and generated the figure. Lindsey Weldon performed the immunoblot in Fig. 2.2B and the ChIP-PCR assay in Fig. 2.3. Lei Hu performed the circular dichroism analysis in Fig. 3.2. Dr. Asokan Anbanandam determined the NMR secondary structure of the ChxR effector domain (Fig. 4.6) and assisted in the chemical shift titration experiment (Fig. 4.7A). The structure of the receiver domain (Fig. 3.4) and the effector domain (Fig. 4.3) were solved with the guidance of Dr. Audrey Lamb and Dr. Scott Lovell.

Chapter I

Health Impact of *Chlamydia*

Chlamydiae are obligate intracellular bacteria that proliferate through a phylum-defining biphasic developmental cycle. Phylogenetic analysis indicates that chlamydiae diverged from other bacteria approximately two billion years ago and became obligate intracellular pathogens approximately 700 million years ago (Horn, Collingro et al. 2004). When chlamydiae first began to infect humans is unknown, but references to the symptoms of infection were recorded over 4,800 years ago (al-Rifai 1988). *Chlamydia* spp. of today (*C. pneumoniae* and *C. trachomatis*) have immense and distinct impacts on public health.

The diverse and chronic diseases correlated with *C. pneumoniae* infection are a result of the immune response to the organism. *C. pneumoniae* is primarily associated with an acute upper respiratory tract infection resulting in an estimated 10% of community-acquired pneumoniae and 5% of bronchitis cases (Grayston 2000; Blasi 2004). *C. pneumoniae* infections have also been correlated with multiple diseases including atherosclerosis, Alzheimer's disease, and arthritis (Yucesan and Sriram 2001; Villareal, Whittum-Hudson et al. 2002; Campbell and Kuo 2004; Itzhaki, Wozniak et al. 2004). The initial infection by the bacteria occurs primarily in lung epithelial cells, which promotes a proinflammatory response from the host (Rasmussen, Eckmann et al. 1997). Cytokine production and secretion recruit macrophages to the site of infection. Macrophages have been shown to be susceptible to infection by *C. pneumoniae* and are proposed to be the transport mechanisms in the dissemination of the bacteria (Gaydos, Summersgill et al. 1996). Disseminated *C. pneumoniae* has been detected in a variety of cells including aortic smooth muscle cells and neurons (Campbell and Kuo 2004; Appelt, Roupas et

al. 2008). The immune response to the organism in these tissues is thought to accelerate the development of the aforementioned diseases. For example, *C. pneumoniae*-infected macrophages secrete matrix metalloproteinases and express tissue factors, which promote platelet and fibrin aggregation (thrombosis) and can lead to atherosclerosis.

C. trachomatis is the leading cause of preventable blindness in the world. The World Health Organization considers trachoma to be endemic in tropical and subtropical countries (Thylefors, Negrel et al. 1995; Polack, Brooker et al. 2005). These countries are primarily located in Africa and the Middle East in poor living and hygienic conditions. The organism is primarily transmitted from the ocular secretions of an infected person to a new host through flies or direct person-person contact (Thomson, Holden et al. 2008). Following exposure, the organism propagates within the conjunctival epithelium. The symptoms associated with an acute infection are usually limited to conjunctivitis. Repeat infections, however, can lead to corneal scarring and blindness if left untreated. The estimated 41 million people that have trachoma and 1-3 million people that are blind as a result of *C. trachomatis* infection demonstrate the critical need to improve sanitary conditions and public awareness within endemic areas (Resnikoff, Pascolini et al. 2004; Haddad 2010).

In addition to an ocular infection, *C. trachomatis* is the most commonly reported sexually transmitted bacterial infection in the world. 89 million cases are reported worldwide annually (Gerbase, Rowley et al. 1998), with 1.2 million of these cases originating in the U.S. (CDC 2010). However, the number of cases is likely much higher due to undiagnosed infections and a high (~90%) asymptomatic rate (Stevens-Simon and Sheeder 2005). *C. trachomatis* infection of the genital tract can result in a variety of conditions, including pelvic inflammatory disease in women, which can lead to sterility and ectopic pregnancy (Stephens 2003; Bebear and de

Barbeyrac 2009). The costs of detecting, treating, and preventing *C. trachomatis* infection has been estimated at $1.5 billion annually in the U.S., further exacerbating the impact of the organism (Gaydos, Cartwright et al. 2010).

Similar to *C. pneumoniae*, the pathology associated with *C. trachomatis* infection is primarily immune mediated. The adaptive and innate immune systems respond to the organism at the site of infection (epithelial layer of the eye or genital tract) by producing and secreting proinflammatory cytokines (Roan and Starnbach 2008). The chronic secretion of these cytokines can lead to the diverse pathologies associated with *C. trachomatis* infection (Burton, Rajak et al. 2011).

The Chlamydial Developmental Cycle

The pathogenic mechanisms utilized by *Chlamydia* are still undefined. However, the growth of this obligate intracellular bacteria and its ability to maintain the characteristic biphasic developmental cycle are intrinsically linked with the immune-mediated pathology associated with *Chlamydia* infections (Stephens 2003). Unlike other pathogenic bacteria, invasion by *Chlamydia* does not elicit an immediate immune response (Eckmann, Kagnoff et al. 1993; Rasmussen, Eckmann et al. 1997). Only after the early stages of the developmental cycle (>20 hours post infection (hpi)), does the infected cell begin to produce and secrete proinflammatory chemokines and cytokines, with maximal secretion occurring 48-72 hpi. The direct correlation between the progression of the chlamydial developmental cycle and the initiation and amplification of the immune response indicates a critical need to elucidate the steps of the cycle and develop therapies that would prevent its progression.

The biphasic developmental cycle in *Chlamydia* consists of two morphologically and phenotypically distinct forms of the organism: the elementary body (EB) and the reticulate body (RB) (Fig. 1.1). EBs are the metabolically inert, infectious form of *Chlamydia*. EBs are relatively small (0.2-0.3 μm) and have cystine-rich proteins (OmpA, OmcA, and OmcB) in their outer membrane that result in a highly crosslinked outer surface (Hatch, Allan et al. 1984). This structural rigidity facilitates survival in the extracellular environment.

EBs begin the developmental cycle by attaching to and then invading eukaryotic host cells (Hatch 1999). Upon entry, EBs are internalized within a membrane-bound parasitophorous vacuole, termed an inclusion. The bacteria actively modulate the inclusion to prevent fusion with lysosomes and late endosomes. Depending on the serovar of *C. trachomatis*, approximately 2-8 hours post infection (hpi) EBs differentiate into RBs. RBs are larger than EBs (0.5-1.6 μm) and are the non-infectious, metabolically active form of the organism. The RBs then reproduce through binary fission. Through poorly defined mechanisms and unknown signals, secondary differentiation begins and RBs asynchronously convert into EBs (~18-24 hpi). The bacteria are then released from the cell, either through host cell lysis or extrusion (~48-72 hpi) (Hybiske and Stephens 2007). The timing of these events in the developmental cycle of *C. pneumoniae* are extended compared to *C. trachomatis*, as the bacteria do not begin to replicate until ~19 hpi or exit the host cell until 72-96 hpi (Vandahl, Birkelund et al. 2004; Mukhopadhyay, Good et al. 2006).

An important deviation to the developmental cycle is the formation of enlarged, pleomorphic RBs, which are associated with a persistent infection (Hogan, Mathews et al. 2004).

FIG. 1.1 *Chlamydia* proliferate through a biphasic developmental cycle. The chlamydial developmental cycle consists of a primarily extracellular, metabolically inactive, and infectious form termed elementary body (EB) converting intracellularly (~2-8 hpi) into the metabolically active, replicative, and non-infectious form called a reticulate body (RB). After numerous rounds of RB replication, asynchronous reciprocal conversion (RB into EB) occurs (~18-24 hpi), and EBs are released to infect new cells (~48-72 hpi). Nutrient starvation or the presence of antibiotics during the developmental cycle causes *Chlamydia* to enter a persistent state, which is reversible when the stress is removed.

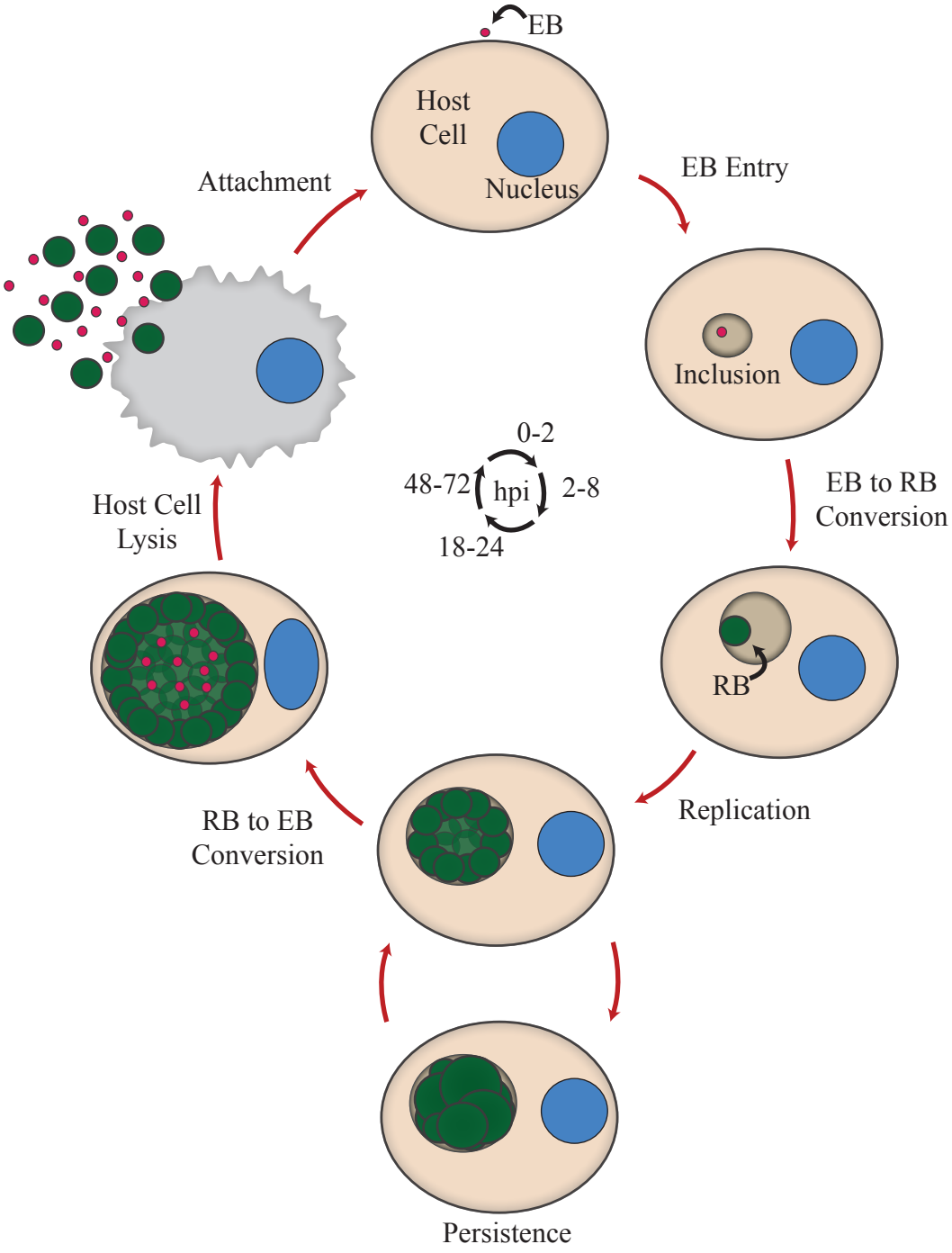
EB
Host
Cell
Nucleus
EB Entry
Inclusion
EB to RB
Conversion
RB
Replication
RB to EB
Conversion
Host Cell
Lysis
Attachment
0-2
2-8
18-24
48-72
hpi
Persistence

Chlamydial persistence is described as a viable but non-replicating growth phase of the organism that has a long-term relationship with the host (Beatty, Morrison et al. 1994), and is achieved through nutrient deprivation or the presence of antibiotics but is reversible when the stress is removed (Roan and Starnbach 2008). Persistence during an infection elicits a sustained inflammatory response from the immune system, which is thought to be a key factor in the *Chlamydia*-induced pathology (Rasmussen, Eckmann et al. 1997).

Mechanisms of Transcriptional Regulation in *Chlamydia*

Due to the current absence of a developed system for specific genetic manipulation in *Chlamydia*, relatively little is known regarding the signals and components that regulate the chlamydial developmental cycle. However, transcriptional regulation has a governing role in the developmental cycle (Belland, Zhong et al. 2003; Nicholson, Olinger et al. 2003; Abdelrahman and Belland 2005). Two independent microarray analyses have been performed at multiple time points during the developmental cycle of *C. trachomatis*, which identified many temporally expressed genes (Belland, Zhong et al. 2003; Nicholson, Olinger et al. 2003). The Nicholson *et al*. analysis indicated that approximately 71% of the open reading frames (612 in *C. trachomatis*) are initially transcribed during the EB to RB conversion, and are constitutively expressed throughout the developmental cycle. Genes within this group are associated with basic cellular functions that facilitate growth. The microarray analysis also determined that multiple temporal gene clusters comprise the middle (~18 hpi) and late (~24-36 hpi) stages of the developmental cycle and account for approximately 20% of the open reading frames (186 in *C. trachomatis*) in the chlamydial genome. Gene products of the middle cluster are involved in a variety of cellular

processes including membrane maintenance, energy metabolism, and protein folding. In contrast, gene products of the late cluster are involved in chromosome condensation, arming the bacteria for the next round of infection, and allowing the bacteria to survive in the extracellular environment upon exiting the host cell (Hefty and Stephens 2007).

The temporal gene expression observed throughout the developmental cycle is not a result of alternative sigma factors in *Chlamydia*. Three sigma factors are encoded in the chlamydial genome: σ^{54}, σ^{28}, and σ^{66}. In other bacteria, σ^{54} is involved in nitrogen assimilation, however, only two genes (*CT652.1* and *CT683*), which encode hypothetical proteins, have been linked with this alternative sigma factor in *Chlamydia* (Mathews and Timms 2000). Similarly, the other alternative sigma factor in *Chlamydia*, σ^{28}, has been shown to transcribe a small number of genes (*hctB*, *tsp*, *tlyC_1*, *dnaK*, *pgk*, and *bioY*) (Yu, Kibler et al. 2006). These genes encode proteins that are involved in a variety of cellular processes including protein folding (DnaK) and glycolysis (PgK). Importantly, HctB is the only gene product from these six genes that has been shown to directly influence transcription of other genes (Brickman, Barry et al. 1993). *hctB* is one of the last genes to be expressed during the developmental cycle and is one of the two genes (with *hctA*) that encode histone-like proteins. HctA and HctB are associated with DNA condensation and transcriptional silencing during the final events of the RB-to-EB conversion (Belland, Zhong et al. 2003).

The primary sigma factor in *Chlamydia*, σ^{66}, is homologous to the general housekeeping sigma factor in *E. coli* (σ^{70}), and is responsible for the expression of most of the constitutively expressed genes (Fahr, Douglas et al. 1995; Hatch 1999; Hefty and Stephens 2007; Niehus, Cheng et al. 2008). Notably, most of the middle and late stage genes are preceded by σ^{66} promoter elements. The association of σ^{66} with many of the temporally expressed middle and late

gene clusters, and the absence of evidence linking the two alternative sigma factors with the expression of these gene clusters, provides strong evidence that additional factors, such as transcriptional activators and repressors, are necessary to regulate their expression. Identifying these factors is critical to our understanding of the mechanisms that generate infectious *Chlamydia*. Furthermore, therapies could be developed that would inhibit the function of these factors, potentially preventing the bacteria from becoming infectious and preventing or limiting the diseases associated with a chlamydial infection.

Recent studies have begun to identify and characterize diverse mechanisms of transcriptional regulation in *Chlamydia*. Non-coding RNAs and DNA topology have been shown to influence transcription; although, only three genes have been demonstrated to be directly regulated through these two mechanisms (Niehus, Cheng et al. 2008; Abdelrahman, Rose et al. 2010). Transcription factors have also been identified in *Chlamydia*, but have only been associated with a small number of genes. Two species-specific transcription factors are associated with amino acid uptake or biosynthesis. ArgR from *C. pneumoniae* is an arginine-dependent repressor that is predicted to control arginine uptake during the developmental cycle by regulating the *glnPQ* operon (Schaumburg and Tan 2006). TrpR is a tryptophan biosynthesis repressor from *C. trachomatis* that is associated with the transcriptional regulation of the *trpRBA* operon (Akers and Tan 2006).

In contrast to these two species-specific transcriptional regulators, a two-component signal transduction system has been identified in both species of *Chlamydia*. The two-component system consists of a sensor kinase (CtcB) and a cognate transcription factor (CtcC) (Koo and Stephens 2003). CtcC shares primary sequence homology to the NtrC/DctD subfamily of response regulators, which interact with σ^{54} to regulate the expression of genes involved in

nitrogen assimilation. Currently, no genes have been directly linked with this two-component system but as CtcC is presumed to interact with σ^{54}, the two genes (*CT652.1* and *CT683*) that have been linked with σ^{54} could also be targets for this two-component system.

In combination, alternative sigma factors, non-coding RNA, DNA topology, and the currently identified transcription factors do not account for the expression of most of the 186 genes comprising the middle and late gene clusters. ChxR, a transcription factor present in all species of *Chlamydia*, interacts with many of the middle and late gene protomers and is therefore an important factor in the progression of the developmental cycle (Koo, Walthers et al. 2006; Spedding 2009). ChxR shares homology to the OmpR/PhoB subfamily of response regulators, however many of the characteristics of these proteins are not conserved in ChxR. The focus of this research is to define the mechanism of ChxR transcriptional regulation.

Two-Component Signal Transduction Systems

Two-component signal transduction systems provide important mechanisms for the modification of many physiological functions within an organism, generally through an alteration of gene expression. Two-component systems are abundant in bacteria but are absent in mammals (Hoch 2000). These systems modulate many different processes in bacteria including sporulation, chemotaxis, and differentiation (Stock, Robinson et al. 2000). These systems have also been shown to regulate the expression of virulence factors within pathogenic bacteria and are essential for their growth (Gooderham and Hancock 2008; Gotoh, Eguchi et al. 2010). Therefore, current research is aimed at identifying and characterizing the components of these

systems. A primary goal of this research is to develop novel antimicrobial agents that inhibit the function of two-component systems and consequently, the expression of their gene targets.

The prototypical two-component system consists of a membrane-bound sensor histidine kinase and a cognate response regulator (Fig. 1.2). Upon sensing stimuli, the sensor kinase undergoes an autophosphorylation event at a conserved histidine in its cytosolic domain. This phosphoryl group is then transferred to a conserved aspartate in the cognate response regulator. Phosphorylation stabilizes the active conformation of the response regulator, which enhances its functional activity. The functions of response regulators are diverse, with some of these proteins modulating intracellular processes through protein-protein interactions or through enzymatic reactions; however the majority of response regulators contain a DNA-binding domain that alters gene expression in response to phosphorylation (Gao and Stock 2009).

Response regulators that contain a DNA-binding domain are generally classified into three subfamilies depending upon how the protein interacts with DNA. Each subfamily is named after its two archetypes and includes NarL/FixJ, NtrC/DctD, and OmpR/PhoB. The DNA binding domain of the NarL/FixJ subfamily contains four-helices and interacts with DNA through a helix-turn-helix motif (Maris, Sawaya et al. 2002). The NtrC/DctD subfamily also interacts with DNA through a helix-turn-helix motif, but requires an ATPase domain to hydrolyze ATP in order to activate transcription (Wedel and Kustu 1995). The OmpR/PhoB subfamily is the largest subfamily and comprises ~48% of all identified DNA-binding response regulators (Martinez-Hackert and Stock 1997; Galperin 2006). Members of this subfamily are composed of a receiver domain that contains the site of phosphorylation and is involved in homodimerization, and an effector domain that interacts with DNA through a subfamily-defining winged helix-turn-helix motif.

FIG. 1.2 A prototypical two-component signal transduction system. Upon sensing stimuli, the histidine kinase (HK) transfers a phosphoryl group to a conserved Asp in the receiver domain of a cognate response regulator (RR). Phosphorylation generally promotes dimerization and facilitates the effector domain to bind DNA and interact with RNA polymerase machinery. (Figure adapted from (Gao and Stock 2009))

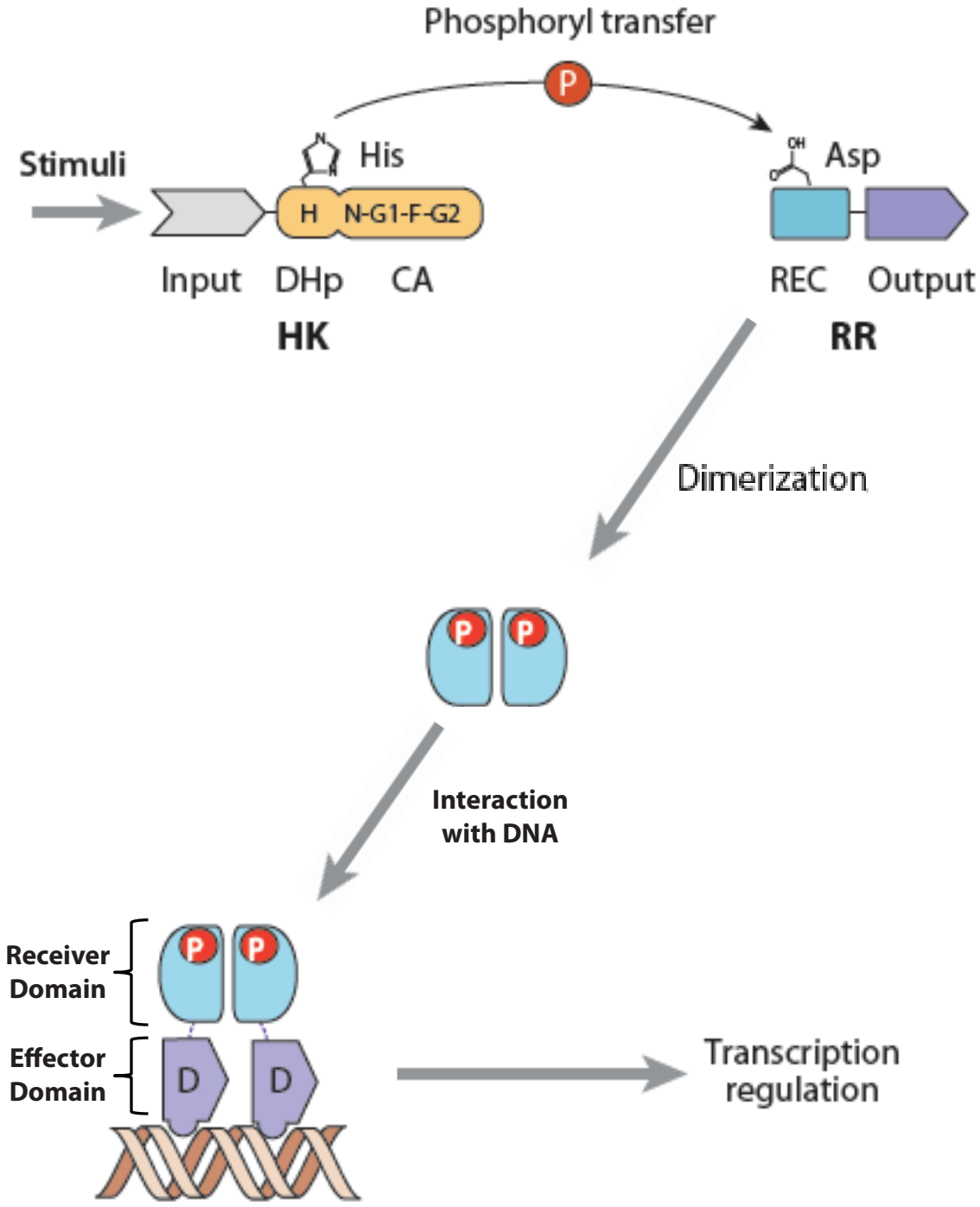
Phosphoryl transfer
P
Stimuli
His
Asp
H
N-G1-F-G2
Input
DHp
CA
REC
Output
HK
RR
Dimerization
P
P
Interaction
with DNA
Receiver
Domain
Effector
Domain
D
D
Transcription
regulation

Extensive research on members of the OmpR/PhoB subfamily has elucidated the conserved events that occur upon phosphorylation and result in their transcriptional regulatory activity (Gao and Stock 2009; Bourret 2010). Upon sensing stimuli, the cognate sensor kinase transfers the phosphoryl group to a conserved phospho-accepting Asp in the receiver domain of the response regulator. An essential Mg^{2+} ion and a conserved Lys assist in the transfer and retention of the phosphoryl group (Sola, Gomis-Ruth et al. 1999; Bachhawat, Swapna et al. 2005). The activation signal is then transduced to the dimer interface through the reorientation of two conformational switch residues (Thr or Ser and Tyr or Phe) towards the site of phosphorylation. The reorientation of these two residues dramatically enhances homodimer formation by properly aligning residues involved in ionic and hydrophobic interactions between protomers. Homodimer formation through the receiver domain enhances the ability of the effector domain to bind to DNA and regulate transcription (Mack, Gao et al. 2009).

Numerous structural studies with members of the OmpR/PhoB subfamily have determined the essential structural components and interfaces necessary for their activity. The structures of the receiver domain of 20 OmpR/PhoB subfamily members have been experimentally determined, among which four have been structurally characterized in their inactive (unphosphorylated) and active (phosphorylated) state (Sola, Gomis-Ruth et al. 1999; Bachhawat, Swapna et al. 2005; Toro-Roman, Mack et al. 2005; Toro-Roman, Wu et al. 2005; Bachhawat and Stock 2007). All 20 structures are very similar and share a common β1-α1-β2-α2-β3-α3-β4-α4-β5-α5 molecular topology (Fig. 1.3A). Additionally, the dimerization interface is generally conserved and consists of the α4-β5-α5 region of the receiver domain.

FIG. 1.3. Ribbon diagrams of a typical OmpR/PhoB receiver and effector domain. A) Receiver domains have a β1-α1-β2-α2-β3-α3-β4-α4-β5-α5 topology and form dimers through the α4-β5-α5 region (red). B) OmpR/PhoB effector domains share a common β6-β7-β8-β9-α6-α7-α8-β10-β11 topology. α8 and the β10-β11 loop (red) interact with DNA while the transactivation loop (blue) interacts with RNA polymerase. The PhoB receiver domain (PDB ID: 1ZES; (Bachhawat, Swapna et al. 2005)) and effector domain (PDB ID: 1GXP; (Blanco, Sola et al. 2002)) were used to generate this figure.

A

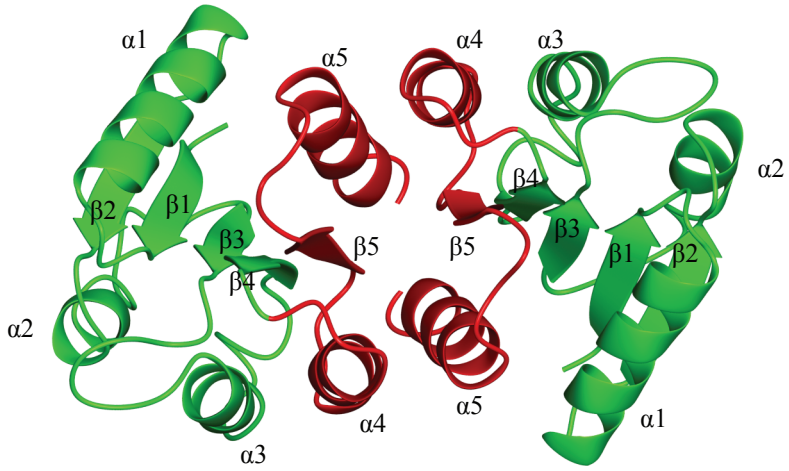
α1
α5
α4
α3
α2
β4
β2
β1
β3
β5
β5
β3
β1
β2
β4
α2
α4
α5
α1
α3

B

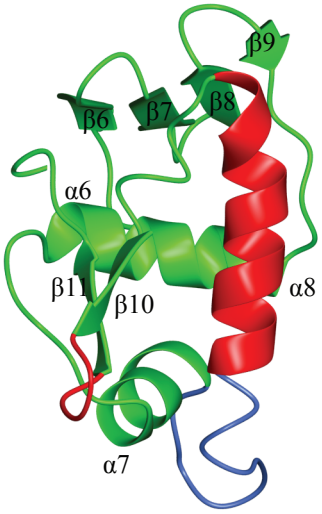
β9
β6
β7
β8
α6
β11
β10
α8
α7

Similar to the large number of receiver domain structures available, the structures of the effector domain of 16 OmpR/PhoB subfamily members have been elucidated. These effector domains consist of a β6-β7-β8-β9-α6-α7-α8-β10-β11 molecular topology (Fig. 1.3B). The typical effector domain is comprised of an N-terminal β-sheet (β6-β7-β8-β9), a winged helix-turn-helix DNA-binding motif (α7-α8), and a C-terminal β-sheet (β10-β11) (Kenney 2002). The α-helix 8 interacts with the major groove of DNA, while the wing (the loop region between β10-β11) interacts with the adjacent minor groove of the DNA. The loop between α7-α8 is the site of interaction with the σ factor or the α-subunit of RNA polymerase (Kondo, Nakagawa et al. 1997; Blanco, Sola et al. 2002).

Atypical Response Regulators

An increasing number of response regulators have been identified that do not appear to incorporate the canonical phosphorylation mechanism of activation and are termed atypical response regulators (Bourret 2010). Currently, six atypical response regulators from the OmpR/PhoB subfamily have been identified and shown to be functionally active in the absence of phosphorylation. The atypical regulators within the OmpR/PhoB subfamily consist of: ChxR from *Chlamydia trachomatis*, JadR1 from *Streptomyces venezuelae*, NblR from *Synechococcus elongates*, HP1021 and HP1043 from *Helicobacter pylori*, and FrzS from *Myxococcus xanthus* (Schar, Sickmann et al. 2005; Koo, Walthers et al. 2006; Fraser, Merlie et al. 2007; Ruiz, Salinas et al. 2008; Wang, Tian et al. 2009). These proteins are important factors in many different cellular processes including the general stress response, antibiotic-production, and cell motility (Schar, Sickmann et al. 2005; Fraser, Merlie et al. 2007; Ruiz, Salinas et al. 2008). Additionally,

deletions of the genes encoding two atypical response regulators result in severe growth defects, supporting their importance in their respective organisms (Schar, Sickmann et al. 2005; Salinas, Ruiz et al. 2007).

How these atypical transcription factors regulate gene expression in the absence of phosphorylation is poorly understood due to the paucity of structural and functional studies of these proteins. From the data currently available, these proteins are maintained in a constitutively active state that appears to mimic the phosphorylated (active) state of OmpR/PhoB response regulators. Atypical response regulators do not retain many of the residues critical to the canonical phosphorylation (activation) process. At least two of the six highly conserved residues critical to this process in phosphorylation-dependent OmpR/PhoB response regulators are absent in atypical subfamily members (Fig. 1.4).

The limited number of structures of atypical OmpR/PhoB response regulators has revealed that the overall structural compositions of the receiver and effector domain of the OmpR/PhoB subfamily are retained in these phosphorylation-independent response regulators. The receiver domains of HP1043 and FrzS have been experimentally determined and are composed of five α/β-folds, similar to other members of the OmpR/PhoB subfamily (Fraser, Merlie et al. 2007; Hong, Lee et al. 2007). Additionally, the effector domain of HP1043 has been solved and contains the subfamily-defining winged helix-turn-helix DNA-binding motif (Hong, Lee et al. 2007). Despite the structures of these proteins currently available, the intra- and intermolecular interactions that maintain the phosphorylation-independent activity of atypical OmpR/PhoB response regulators remain poorly understood.

FIG. 1.4. Primary sequence comparison of atypical and typical OmpR/PhoB response regulators. The primary sequence of the receiver domains of two typical OmpR/PhoB response regulators (OmpR and PhoB) and the currently identified atypical OmpR/PhoB response regulators (JadR1, NblR, HP1043, FrzS, HP1021, and ChxR) were aligned using the multiple sequence alignment program ClustalW (Larkin, Blackshields et al. 2007). The red box denotes the phospho-accepting Asp in typical OmpR/PhoB subfamily members. The black boxes represent the residues involved in coordinating the Mg^{2+} ion and the phosphoryl group. The blue boxes represent the two conformational switch residues. The secondary sequence elements correspond to PhoB (PDB ID: IZES). The proteins used for the primary sequence alignment are OmpR (*E. coli*; GenBank: CAQ33726.1), PhoB (*E. coli*; PDB ID: 1ZES), JadR1 (*S. venezuelae*; AAB36584.2), NblR (*S. elongates*; GenBank: AAC33849.1), HP1043 (*H. pylori*; PDB: 2PLN), FrzS (*M. xanthus*; GenBank: AAC98490.1), HP1021 (*H. pylori*; NP_207811.1), and ChxR (*C. trachomatis*; UniProt: B0B8K5).

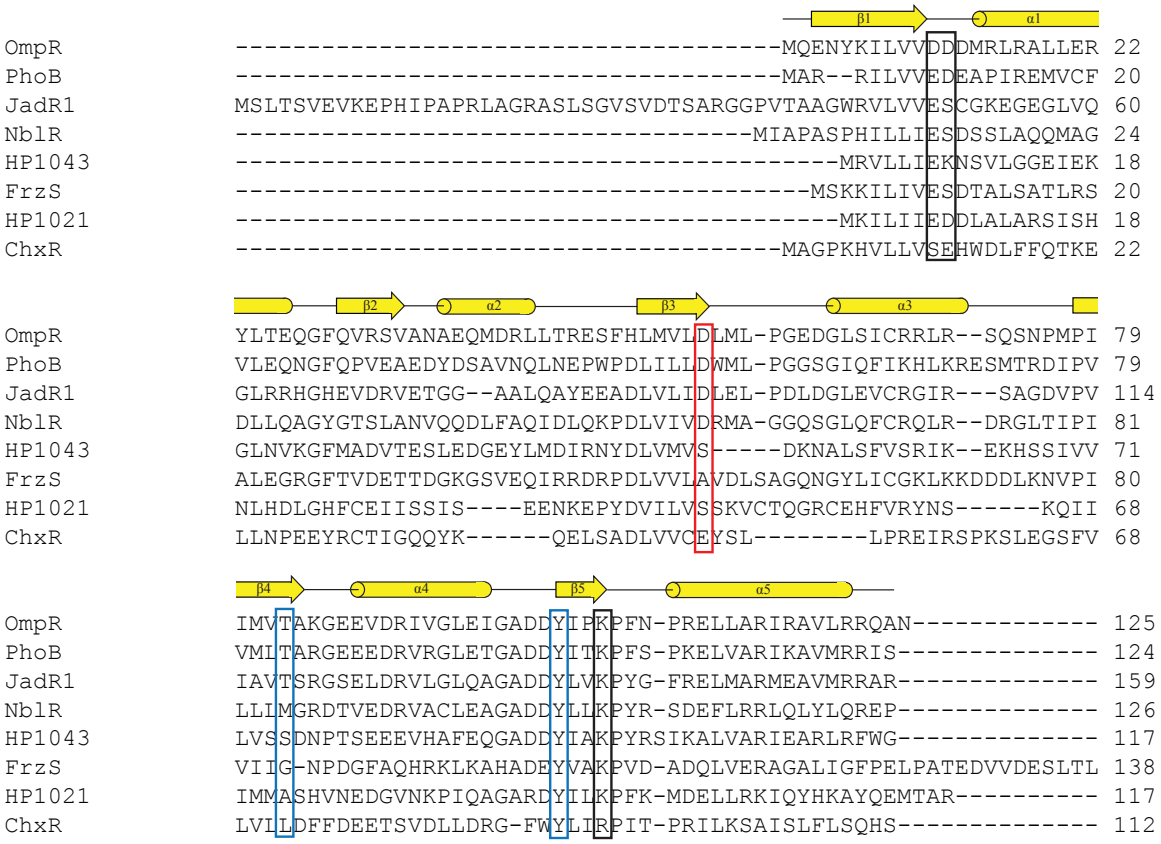
β1
α1
OmpR ----------MQENYKILVVDDDMRLRALLER 22
PhoB ----------MAR--RILVVEDEAPIREMVCF 20
JadR1 MSLTSVEVKEPHIPAPRLAGRASLSGVSVDTSARGGPVTAAGWRVLVVESCGKEGEGLVQ 60
NblR ----------MIAPASPHILLIESDSSLAQQMAG 24
HP1043 ----------MRVLLIEKNSVLGGEIEK 18
FrzS ----------MSKKILIVESDTALSATLRS 20
HP1021 ----------MKILIIEDDLALARSISH 18
ChxR ----------MAGPKHVLLVSEHWDLFFQTKE 22
β2
α2
β3
α3
OmpR YLTEQGFQVRSVANAEQMDRLLTRESFHLMVLDLML-PGEDGLSICRRLR--SQSNPMPI 79
PhoB VLEQNGFQPVEAEDYDSAVNQLNEPWPDLILLDWML-PGGSGIQFIKHLKRESMTRDIPV 79
JadR1 GLRRHGHEVDRVETGG--AALQAYEEADLVLIDLEL-PDLDGLEVCRGIR---SAGDVPV 114
NblR DLLQAGYGTSLANVQQDLFAQIDLQKPDLVIVDRMA-GGQSGLQFCRQLR--DRGLTIPI 81
HP1043 GLNVKGFMADVTESLEDGEYLMDIRNYDLVMVS-----DKNALSFVSRIK--EKHSSIVV 71
FrzS ALEGRGFTVDETTDGKGSVEQIRRDRPDLVVLAVDLSAGQNGYLICGKLKKDDDLKNVPI 80
HP1021 NLHDLGHFCEIISSIS----EENKEPYDVILVSSKVCTQGRCEHFVRYNS------KQII 68
ChxR LLNPEEYRCTIGQQYK------QELSADLVVCEYSL--------LPREIRSPKSLEGSFV 68
β4
α4
β5
α5
OmpR IMVTAKGEEVDRIVGLEIGADDYIPKPFN-PRELLARIRAVLRRQAN---------- 125
PhoB VMLTARGEEEDRVRGLETGADDYITKPFS-PKELVARIKAVMRRIS---------- 124
JadR1 IAVTSRGSELDRVLGLQAGADDYLVKPYG-FRELMARMEAVMRRAR---------- 159
NblR LLLMGRDTVEDRVACLEAGADDYLLKPYR-SDEFLRRLQLYLQREP---------- 126
HP1043 LVSSDNPTSEEEVHAFEQGADDYIAKPYRSIKALVARIEARLRFWG---------- 117
FrzS VIIG-NPDGFAQHRKLKAHADEYVAKPVD-ADQLVERAGALIGFPELPATEDVVDESLTL 138
HP1021 IMMASHVNEDGVNKPIQAGARDYILKPFK-MDELLRKIQYHKAYQEMTAR---------- 117
ChxR LVLLDFFDEETSVDLLDRG-FWYLIRPIT-PRILKSAISLFLSQHS---------- 112

Identification and Initial Characterization of ChxR

Transcriptional analysis indicates that *chxR*, a gene encoding the transcription factor ChxR, is upregulated during the middle and late stages of the developmental cycle (Fig. 1.5). Using a heterologous system (*E. coli*), ChxR was shown to regulate the expression of multiple genes from *Chlamydia*, including: the *omcAB* operon (outer membrane protein A and B) *tufA* (translation elongation factor), *infA* (translation initiation factor), *oppA* (oligopeptide transport protein) and *CT084* (hypothetical protein) (Koo, Walthers et al. 2006). Additional gene targets for ChxR were identified through a chromosomal-immunoprecipitation coupled with PCR (ChIP-PCR) analysis in which endogenous ChxR was found to be associated with the promoters of many chlamydial genes (*CT630*, *CT480*, *CT091*, *CT557*, *CT559*, *CT576*, *CT444*, *CT619/620*, and *CT733/734*) (Spedding 2009). *CT630* and *CT480* encode ChxR and OppA, respectively, which supports the previous finding that ChxR was found to be associated with these genes by ChIP-PCR. *CT091*, *CT557*, *CT559*, and *CT576* are the first genes of four operons (17 genes in total) encoding components of the chlamydial type III secretion system (Hefty and Stephens 2007). *CT444* is the first gene of the *omcAB* operon, which encodes the cystine-rich outer membrane proteins OmcA and OmcB. A limitation of the assay was that ChxR could not be directly linked with the *CT619* or *CT620* and *CT733* or *CT734* promoters, as the promoters of these genes overlap. *CT619*, *CT620*, *CT733*, and *CT734* encode hypothetical proteins. Additional experiments are clearly needed to confirm that ChxR regulates the expression of these genes but these findings, in combination with the previous study, demonstrate that ChxR is associated with

FIG. 1.5. *chxR* transcripts increase during the middle and late stages of the developmental cycle. RNA was isolated from *C. trachomatis* L2 infected L929 cells at 6 hour increments. *gyrB* and *hctB* were included for controls. *gyrB* is constitutively expressed while *hctB* is differentially expressed and has been previously demonstrated to be associated with events in the later stages of the conversion from RBs to EBs (Yu and Tan 2003). *chxR* is differentially expressed with increased transcription during 12 to 24 hpi, which overlaps with the conversion from RBs to EBs. The transcript ratio is of each transcript level (*chxR*, *gyrB*, or *hctB*) relative to the constitutively expressed *secY* transcript. (Figure courtesy of Scott Hefty)

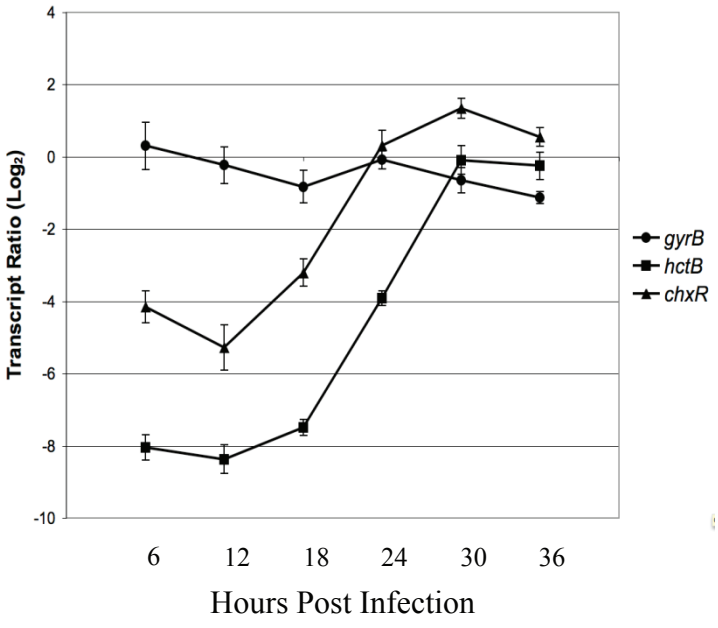
4
2
0
-2
-4
-6
-8
-10
Transcript Ratio (Log2)
6
12
18
24
30
36
Hours Post Infection
gyrB
hctB
chxR

many (26) genes in *Chlamydia* and indicate that ChxR is an important transcription factor in *Chlamydia*.

ChxR was annotated as a transcription factor as it shares primary sequence homology to the OmpR/PhoB subfamily of transcriptional regulators (Stephens, Kalman et al. 1998; Koo, Walthers et al. 2006). Despite primary sequence homology, some of the important characteristics of the OmpR/PhoB subfamily are not shared in ChxR. A cognate sensor kinase is not apparent in the chlamydial genome and a conserved phospho-accepting Asp, which is an important factor in controlling the functional activity of most OmpR/PhoB transcription factors, is absent in ChxR. Furthermore, ChxR has been shown to regulate transcription in the absence of phosphorylation *in vitro* and within a heterologous system (*E. coli*) (Koo, Walthers et al. 2006). The mechanism of ChxR transcriptional regulation is currently poorly understood, but defining this mechanism is important given the connection between ChxR and factors (i.e. components of the type III secretion system and outer membrane) that are critical for the progression of the developmental cycle and consequently pathogenesis.

The central hypothesis for this research is that the intra- and intermolecular interactions involved in forming a transcriptionally competent ChxR are distinct from the canonical phosphorylation (activation) paradigm in the OmpR/PhoB response regulator subfamily. The goal of this work is to identify the structural and functional characteristics of ChxR that are important for its ability to regulate transcription. Characterizing the ChxR mechanism of transcriptional regulation will likely facilitate the rational design of small molecule compounds that inhibit the function of ChxR and potentially prevent the bacteria from becoming infectious. Additionally, elucidating the ChxR *cis*-acting element could be used to identify additional gene targets and define the role of ChxR in *Chlamydia*.

Chapter II

Introduction

Response regulators are essential regulatory factors of two-component signal transduction systems. They predominantly function as phosphorylation-activated switches to control gene expression at the transcriptional level (Galperin 2005). The largest subfamily of response regulators is the OmpR/PhoB subfamily, in which the vast majority of homologs share a conserved phosphorylation-dependent transcriptional regulation mechanism (Galperin 2005; Gao, Mack et al. 2007). This subfamily of response regulators is structurally very similar and composed of two domains: a receiver domain and an effector domain (Stock, Robinson et al. 2000; West and Stock 2001; Gao, Mack et al. 2007; Gao and Stock 2009). Phosphorylation at an Asp within a highly conserved binding site in the receiver domain causes reorientation of two conformational-switch residues and relatively subtle overall changes to the receiver domain (Gao and Stock 2009). These changes promote homodimer formation between receiver domains, which allows the effector domain to bind to DNA and regulate transcription.

The effector domain of response regulators binds to either tandem, or more infrequently, inverted repeats of DNA through a subfamily-defining winged helix-turn-helix DNA binding motif to regulate transcription. The DNA recognition site generally ranges from 18–23 bp containing two 6–10-bp DNA-binding site separated by 2–5 bp of intervening sequence (Harlocker, Bergstrom et al. 1995; Blanco, Sola et al. 2002; Kenney 2002). The target promoters of OmpR/PhoB subfamily members often contain multiple binding sites that vary in their nucleotide sequence, promoter position, and relative binding affinities (Kenney 2002; Schaaf and

Bott 2007). As a result, cooperativity and differential binding are commonly incorporated as an important component of transcriptional regulation by OmpR/PhoB response regulators.

Atypical response regulators have recently been identified and described in phylogenetically diverse organisms, including *Chlamydia*, *Helicobacter*, *Myxococcus*, *Streptomyces*, and *Synechococcus* (Ainsa, Parry et al. 1999; Delany, Spohn et al. 2002; Schar, Sickmann et al. 2005; Koo, Walthers et al. 2006; Rotter, Muhlbacher et al. 2006; Fraser, Merlie et al. 2007; Kato, Chibazakura et al. 2008; Mittal and Kroos 2009). These atypical response regulators do not require phosphorylation to function as transcriptional regulators. In concert with these observations, the receiver domain binding site, frequently including the typically phosphorylated Asp, is not conserved. This and other observations support the finding that phosphorylation-dependent activation mechanisms are not utilized by atypical response regulators (Ainsa, Parry et al. 1999; Kato, Chibazakura et al. 2008; Ruiz, Salinas et al. 2008; Mittal and Kroos 2009). Highlighting the biological importance of these atypical response regulators to their respective organism, gene disruptions of many of these transcription factors cause severe phenotypic defects or are requisite for growth (Chater 1972; Beier and Frank 2000; Schar, Sickmann et al. 2005).

Despite the apparent importance of atypical response regulators, relatively little information exists regarding the transcriptional regulation mechanisms utilized by these regulators. Structural analysis of the atypical response regulator homolog HP1043 from *H. pylori* revealed that the two residues in the same position as the conformational-switch residues in a typical OmpR/PhoB subfamily member were oriented similar to those in the canonical phosphorylated (active) orientation (Hong, Lee et al. 2007). This study also reported that recombinant HP1043 forms stable homodimers and recognizes an inverted repeat of DNA

sequences. In contrast, analyses of the atypical response regulator homolog NblR in *Synechococcus* demonstrated that, unlike phosphorylated (active) response regulators, this essential regulator existed as a monomer both *in vitro* and *in vivo* (Ruiz, Salinas et al. 2008). These observations suggest that atypical OmpR/PhoB response regulator mechanisms (e.g., homodimerization) are most likely similar to, but distinct from, the canonical mechanisms.

Chlamydia are phylogenetically distant from other bacteria and encode an atypical response regulator named ChxR (Stephens, Kalman et al. 1998; Stephens 2002). ChxR is homologous to the OmpR/PhoB subfamily of response regulators; however, none of the binding site residues and only one of the conformational switch residues is conserved relative to other typical OmpR/PhoB subfamily members. Similar to other atypical response regulators, previous studies demonstrated that ChxR activated transcription both *in vitro* and within a heterologous *in vivo* system (*E. coli*) in the absence of phosphorylation (Koo, Walthers et al. 2006). These analyses also revealed that ChxR has a direct autoregulatory role because it recognizes multiple sites within its own promoter region and activates transcription, as do many other atypical response regulators (Ainsa, Parry et al. 1999; Delany, Spohn et al. 2002).

Chlamydia infections have an immense impact on public health and are associated with diverse disease manifestations including atherosclerosis, blindness, and sterility (Schachter 1999). The pathogenic mechanisms utilized by *Chlamydia* are still undefined; however, growth of these obligate intracellular bacteria and their ability to maintain the characteristic biphasic developmental cycle are intrinsically linked with the immune-mediated pathology associated with *Chlamydia* infections (Stephens 2003). Largely due to the current absence of a system for specific genetic manipulation in *Chlamydia*, relatively little is known regarding the signals and components that regulate the chlamydial developmental cycle; however, transcriptional

regulation has a governing role in the developmental cycle (Belland, Zhong et al. 2003; Nicholson, Olinger et al. 2003; Abdelrahman and Belland 2005).

ChxR is hypothesized to play an important role in regulating the chlamydial developmental cycle and incorporates mechanisms and exhibits properties similar to, but distinct from, the OmpR/PhoB response regulator subfamily. This study was designed to begin defining the fundamental mechanisms employed by and properties of ChxR. Included is the characterization of the *cis*-acting element recognized by ChxR, which is expected to facilitate the identification of additional ChxR gene targets and eventual assignment of a specific role for ChxR in the developmental cycle.

Chapter II

Methods and Materials

Purification of ChxR- chxR was PCR amplified using *Chlamydia trachomatis* LGV (L2/484/Bu) genomic DNA and primers specific for *chxR* (Table 2.1) (Integrated DNA Technologies, Coralville, IA). The resulting amplicon was digested with *NdeI/XhoI*, ligated into pET28b (Novagen, San Diego, CA), and transformed into *E. coli* TOP1 cells (Invitrogen, Carlsbad, CA). After sequence confirmation (DNA Sequencing Laboratory, University of Kansas, Lawrence, KS), the plasmids were transformed into *E. coli* BL21 (DE3) (Invitrogen) and grown to an OD_{600} of 0.7 in Luria broth containing 50 μg/mL kanamycin. Isopropyl-β-D-thiogalactopyranoside (IPTG) was added to a final concentration of 1 mM, and the cells were harvested by centrifugation after overnight incubation at 15°C. The ChxR-expressing *E. coli* cells were resuspended in 50 mM Tris (pH 7.0) and 400 mM NaCl, disrupted by sonication, and subjected to centrifugation (30 min at 14,000 × *g*; 4°C). Residual cell debris was removed by passing the supernatant through a 0.22-μm filter before protein purification. ChxR was purified by Co^{2+}-affinity chromatography (Clontech, Mountain View, CA). The hexahistidine-tagged proteins bound to the metal resin were washed with 5 mM imidazole, 50 mM Tris (pH 7.0), and 400 mM NaCl before elution from the resin with the wash buffer that contained 250 mM imidazole.

Elution fractions containing ChxR were pooled and applied to a Sephacryl S-200 16/60 size exclusion column (GE Healthcare, Pittsburgh, PA) equilibrated with 50 mM Tris (pH 7.0) and 400 mM NaCl. Fractions containing ChxR were pooled, and the protein was determined to be >95% pure, as determined by Coomassie staining after sodium dodecyl sulfate-

Table 2.1. Oligonucleotides used in this study

Name	Sequence[1, 2]
chxR Forward	5′-GGAATTCCATATGCAGGGCCTAAACATGTG-3′
chxR Reverse	5′-CCGCTCGAGCTAAGAAAGCTTTGTATCTTGTT-3′
chxR Promoter Forward	5′-CGATATCAACGGCTATAGAAG-3′
chxR Promoter Reverse	5′-TAG ATTACCTAATACAACAAAAATAG-3′
CT863 Promoter Forward	5′-GCGGCAATAGGTTAATCGTCT-3′
CT863 Promoter Reverse	5′-GCGCCTTAAGAGAAGCGTTT-3′
DR1 (-100-70)	5′-CACAGAACAAGTGTAGTCTAAACTTGAAAAA-3′
DR2 (-145-117)	5′-ATTTTTCGATCAAAAACTAGATAAAGCAG-3′
DR3 (-188-158)	5′-TCTGACGATGTTGTTATCAATTAACGTTTTC-3′
DR4 (-218-183)	5′-GTTTTAGAAATATTTTTGAATCTGAC-3′
DR5 (-241-215)	5′-TTAACTTGAAAATTAACGAAAATACCC-3′
DR6 (-286-255)	5′-AACGGCTATAGAAGCTGTAAAGGAAGCCCC-3′
NC (-120-95)	5′-GCAGAGAATGAGCTTTTATCACAG-3′
DR2-2 Mutant	5′-TCTCAAATTTTTC**CCC**CAAAAACTAGATAAAGCAG-3′
DR2-1 Mutant	5′-TCTCAAATTTTTCGATCAAAAACTA**CCC**AAAGCAG-3′
DR2-1/2 Double Mutant	5′-TCTCAAATTTTTC**CCC**CAAAAACTA**CCC**AAAGCAG-3′
140 G	5′-CAAATTTT**G**CGATCAAAAACTAGATAAAG-3′
139 A	5′-CAAATTTTT**A**GATCAAAAACTAGATAAAG-3′
138 T	5′-CAAATTTTTC**T**ATCAAAAACTAGATAAAG-3′
137 C	5′-CAAATTTTTCG**C**TCAAAAACTAGATAAAG-3′
136 G	5′-CAAATTTTTCGA**G**CAAAAACTAGATAAAG-3′
135 A	5′-CAAATTTTTCGAT**A**AAAAACTAGATAAAG-3′
134 C	5′-CAAATTTTTCGATC**C**AAAACTAGATAAAG-3′
133 C	5′-CAAATTTTTCGATCA**C**AAACTAGATAAAG-3′
132 C	5′-CAAATTTTTCGATCAA**C**AACTAGATAAAG-3′
131 C	5′-CAAATTTTTCGATCAAA**C**ACTAGATAAAG-3′
130 C	5′-CAAATTTTTCGATCAAAA**C**CTAGATAAAG-3′
129A	5′-CAAATTTTTCGATCAAAAA**A**TAGATAAAG-3′
128 G	5′-CAAATTTTTCGATCAAAAAC**G**AGATAAAG-3′
127 C	5′-CAAATTTTTCGATCAAAAACT**C**GATAAAG-3′
126 T	5′-CAAATTTTTCGATCAAAAACTA**T**ATAAAG-3′
125 C	5′-CAAATTTTTCGATCAAAAACTAG**C**TAAAG-3′
124 G	5′-CAAATTTTTCGATCAAAAACTAGA**G**AAAG-3′
123 C	5′-CAAATTTTTCGATCAAAAACTAGAT**C**AAG-3′
122 C	5′-CAAATTTTTCGATCAAAAACTAGATA**C**AG-3′
121 C	5′-CAAATTTTTCGATCAAAAACTAGATAA**C**G-3′
120 T	5′-CAAATTTTTCGATCAAAAACTAGATAAA**T**-3′

[1] All nucleotide numbers are relative to the transcriptional start site.
[2] Mutated nucleotides are in bold.

polyacrylamide gel electrophoresis (SDS-PAGE).

Analytical size exclusion chromatography- Fractions containing purified ChxR were concentrated to 100 μM using an Amicon Ultra centrifugal filter (3,000 MWCO, Millipore). Equal volumes of protein samples at 100 μM, 10 μM, or 1 μM were applied to a Superdex 75 10/300 GL analytical size exclusion column (GE Healthcare) equilibrated with 50 mM Tris-HCl (pH 7.5), 100 mM NaCl, and 250 mM KCl. In the same buffer, a protein standard containing bovine serum albumin (66 kDa), chicken ovalbumin (44 kDa), and horse myoglobin (17 kDa) (BIO-RAD, Hercules, CA) was used to generate a standard curve.

In vitro *chemical crosslinking*- Purified ChxR-His_6 was dialyzed in crosslinking buffer (30 mM sodium phosphate (pH 7.0) and 300 mM NaCl). ChxR was exposed to the primary amine chemical crosslinker disuccinimidyl suberate (DSS) (Pierce, Rockford, IL) at 500 μM. The reactions were incubated at 25°C for 2 min and quenched with 1 M Tris (pH 8.0). The samples were heat denatured in Laemmli buffer, separated by SDS-PAGE, and visualized by Coomassie staining.

Time course of expression of ChxR- Mouse L929 fibroblast cells (8×10^5 cells/ml) were propagated in RPMI medium (Mediatech, Manassas, VA) supplemented with 5% fetal bovine serum (Hyclone, Logan, UT) and 50 μg/mL vancomycin (MP Biomedicals, Solon, OH) as previously described (Scidmore 2005). L929 cells were infected with *C. trachomatis* LGV (L2/434/Bu) at a dilution that resulted in approximately 80% of the cells infected as visualized by immunofluorescence microscopy at 24 hours post-infection (hpi) (Microtrak, Trinity Biotech, Berkeley Heights, NJ). At 12, 24, and 36 hpi, 1 L, 500 mL, and 350 mL of cells, respectively, were harvested by centrifugation (10 min at 1,400 × *g*; 15°C). The resulting pellets were washed

twice with and resuspended in Hanks' Balanced Salt Solution (Mediatech) before transferring to 40-mL Oakridge tubes. *C. trachomatis* specimens were liberated from the host cells by gentle sonication. The lysate was layered over 30% renografin (Bracco Diagnostics, NJ) and subjected to ultracentrifugation (10 min at 16,000 × *g*; 15°C). The resulting chlamydial pellet was resuspended in PBS. The samples were subjected to SDS-PAGE, and an immunoblot assay was performed using monospecific-polyclonal antibodies against ChxR (Proteintech, Chicago, IL).

In vivo *chemical crosslinking*- Reticulate body (RB)-enriched pellets were resuspended in PBS and exposed to 10 mM DSS (Pierce). After 20 min incubation at 25°C, the reaction was quenched with the addition of 50 mM Tris (pH 8.0). The samples were subjected to SDS-PAGE, and immunoblot assays were performed using monospecific-polyclonal antibodies against ChxR.

Immunoprecipitation of ChxR- RB-enriched fractions from 36 hpi cells were obtained as described above. RBs were crosslinked with 1% formaldehyde, and the reaction quenched with 250 µM glycine. After crosslinking, cells were incubated in RIPA buffer (10 mM Tris-Cl (pH 8.0), 1 mM EDTA, 1% Triton X-100, 0.1% sodium deoxycholate, 0.1% SDS, 140 mM NaCl, and 5 mM DTT) with 15 µL of AEBSF (Thermofisher Scientific) for 45 min on ice. Samples were sonicated to shear DNA and centrifuged (14,000 × *g*, 15 min, 24°C), and supernatants were removed. For immunoprecipitation, protein G dynabeads (Invitrogen) were washed three times and resuspended in RIPA buffer. Ten micrograms of affinity-purified anti-ChxR polyclonal antibodies were added to beads and incubated at 4°C for 24 h with rotating. Beads were subsequently washed twice with RIPA buffer, and supernatants were added to the beads. Samples were incubated at 4°C for 24 h with rotating. Beads were washed twice with RIPA buffer before resuspension in RIPA buffer and incubated at 25°C for 2 h with rotating. Beads were again washed five times with RIPA buffer prior to 30 µL of TE (10 mM Tris-Cl (pH 7.4), 1

mM EDTA) being added. Samples were boiled 5 min to reverse the crosslinks and centrifuged (13,000 × *g*, 3 min, 25°C), and supernatants were collected. PCR was performed on supernatants by using primers to the *chxR* promoter region or the *CT863* promoter region (Table 2.1). PCR products were separated by agarose gel electrophoresis and detected by ethidium bromide staining.

Electrophoretic gel mobility shift assays (EMSAs) and quantitative binding analysis- Oligonucleotides were designed to contain each of the putative ChxR binding sites (direct repeat (DR) 1-6) and at least 3 bp of the flanking sequence (Table 2.1). Three or more base pairs of flanking sequence were shown to result in equal maximal binding (data not shown). IR800-labeled (Eurofins MWG Operon, Huntsville, AL) or unlabeled (Integrated DNA Technologies) oligonucleotides were hybridized prior to use in EMSAs. Binding reactions (20 μL) contained DNA and ChxR at their respective concentrations as listed in the results section and were performed in triplicate. EMSAs were performed as previously described (Koo, Walthers et al. 2006), except the reactions were incubated at 25°C for 20 min. After native PAGE, unlabeled-hybridized DNA fragments were visualized by SYBR Green (Invitrogen) staining by using an excitation wavelength of 488 nm and an emission filter of 520 nm on a Typhoon Trio imager (GE Healthcare). IR800-labeled DNA fragments were visualized using the Odyssey Infrared Imaging System (LI-COR Biosciences, Lincoln, NE). DNA was quantified using the software program ImageQuant (GE Healthcare). Percent DNA shifted was determined by the amount of photons emitted for the shifted DNA band relative to the total amount of photons emitted between the shifted and non-shifted DNA bands. To measure the ChxR binding affinity with the six DR sites, EMSAs were performed with 1 nM DR1-DR6 and increasing concentrations of ChxR (5 nM–5 μM). Dissociation constants (K_d) were calculated using non-linear regression

with GraphPad Prism software (GraphPad Software Inc., San Diego, CA). The dissociation constant is the calculated protein concentration that resulted in 50% ChxR-DNA interaction.

For the analysis of single site mutations in DR2 (Fig. 7), each individual gel included a ChxR binding reaction and wild-type DR2. Overall, the wild-type DR2 DNA sequence averaged 67% of ChxR shifted DNA through 18 independent reactions. Student's two-tailed t-test was used for statistical analysis of triplicate data sets.

ChxR^{E49D} site-directed mutagenesis- PCR was performed using the QuickChange II XL site-directed mutagenesis kit (Stratagene, Cedar Creek, TX) by following the manufacturer's instructions. The wild-type Glu at residue 49 of ChxR (E49) was replaced with an Asp by using *chxR* plasmid as the reaction template. ChxR^{E49D} was expressed and purified as described above for ChxR.

Chapter II

Results

ChxR forms homodimers in vitro *and* in vivo.

In response to phosphorylation, homodimer formation has been shown to be critical for OmpR/PhoB subfamily response regulators to bind cognate DNA and activate transcription (Gao, Mack et al. 2007). Only two studies have evaluated the ability of atypical OmpR/PhoB response regulators to form homodimers, and the observations were discordant (Hong, Lee et al. 2007; Ruiz, Salinas et al. 2008). Prior data indicated that ChxR is an atypical OmpR/PhoB response regulator, although the ability to form homodimers was not evaluated (Koo, Walthers et al. 2006). To begin understanding the mechanisms important for ChxR to activate transcription, studies were designed to determine if ChxR forms homodimers and mimics that of the active conformation of OmpR/PhoB subfamily response regulators.

During purification of recombinant ChxR protein, size exclusion chromatography indicated that ChxR forms stable homodimers. When a relatively high concentration of ChxR (~ 100 μM) was applied to the column, a single peak of protein eluted at the size expected (45 kDa) for a ChxR homodimer (Fig. 2.1). While the *in vivo* concentration of ChxR is unknown, OmpR in *E. coli* has been measured to be present at concentrations around 1–3 μM (Cai and Inouye 2002). To address the possibility that ChxR forms homodimers only at high concentrations and not at potentially physiologic concentrations, dilutions of ChxR were applied to size exclusion chromatography. As Fig. 2.1 demonstrates, when the lowest concentration (1 μM) of ChxR was

FIG. 2.1. Recombinant ChxR purifies as a stable homodimer. Purified recombinant ChxR at 1 μM, 10 μM, or 100 μM was subjected to analytical size exclusion chromatography to determine the *in vitro* oligomeric state of the protein. A molecular weight standard curve was generated using bovine serum albumin (66 kDa), chicken ovalbumin (44 kDa), and horse myoglobin (17 kDa).

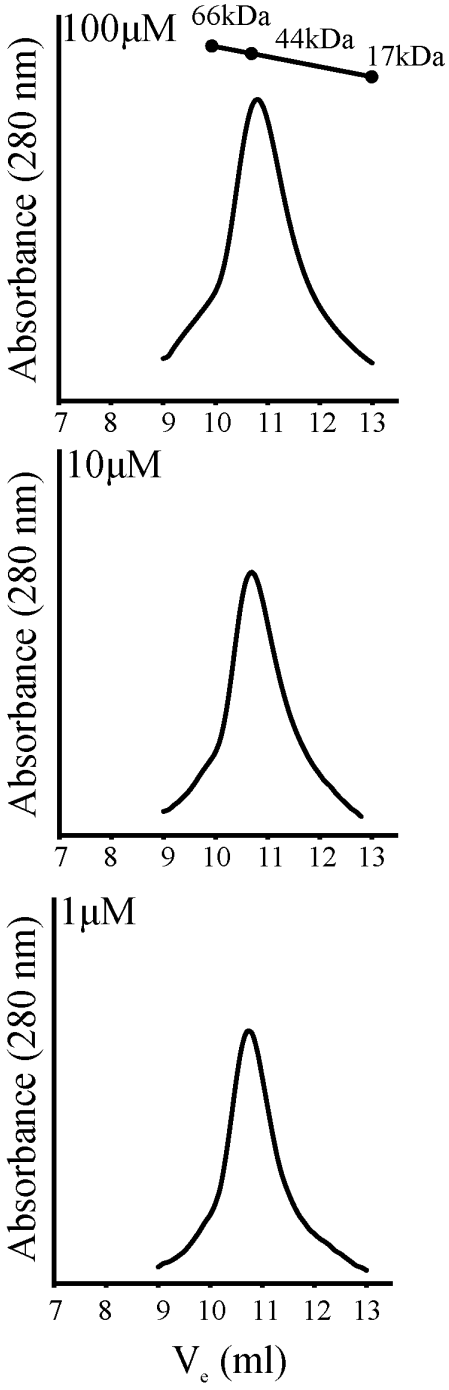
100µM
66kDa
44kDa
17kDa
Absorbance (280 nm)
7 8 9 10 11 12 13
10µM
Absorbance (280 nm)
7 8 9 10 11 12 13
1µM
Absorbance (280 nm)
7 8 9 10 11 12 13
V_e (ml)

applied to the column, protein was only detected at the expected size of the ChxR homodimer. These data support that ChxR forms stable homodimers and that the molecular interactions between the two protomers form a relatively strong association, albeit within the testing conditions described.

While the previous data supported that recombinant ChxR forms stable homodimers in the absence of phosphorylation, it was unknown whether ChxR homodimerization occurs *in vivo*. Given the inability to perform directed genetic studies in *Chlamydia*, membrane-permeant chemical crosslinkers were employed to obtain the most biologically relevant observations. Chemical crosslinkers have previously been utilized to capture homodimer formation by activated OmpR/PhoB subfamily response regulators, even if only within *in vitro* conditions (Delany, Spohn et al. 2002; Maris, Walthers et al. 2005). DSS is a crosslinker that was previously employed on the atypical response regulator HP1043 (Delany, Spohn et al. 2002). DSS is a membrane-permeant, primary amine homobifunctional crosslinker with a short spacer arm (11.4 Å). ChxR has 17 lysines in addition to the amino terminus (primary amines) that would be expected to serve as targets for DSS and form covalent intermolecular, as well as intramolecular, bonds.

The ability to capture ChxR homodimers through the use of DSS was first tested *in vitro*. After incubating recombinant ChxR with DSS, two bands of protein were evident following SDS-PAGE analysis (Fig. 2.2A). One band migrated at the expected size of a ChxR monomer (~26 kDa), and another migrated at a molecular mass of an expected ChxR homodimer (~50 kDa). To address the possibility that the detected protein dimerization was due to non-specific protein interactions, concentrations of ChxR were increased prior to adding DSS. While small amounts of higher-order species were present, after increasing the concentration of ChxR, the

FIG. 2.2. ChxR forms homodimers *in vivo*. Recombinant ChxR forms homodimers *in vitro*; however the *in vivo* oligomeric state of ChxR was unknown. (A) To determine if the primary amine chemical crosslinker DSS could capture ChxR homodimers, increasing concentrations (2.2 μM, 3.5 μM, 7 μM, 14 μM, 21 μM) of purified, recombinant ChxR was incubated with 500 μM DSS. As a control, 21 μM ChxR was not incubated with DSS. Denatured samples were separated by SDS-PAGE and observed by Coomassie staining. (B) At 12, 24, and 36 hpi, *C. trachomatis* were enriched from infected L929 cells and the relative amount of ChxR present was assayed by an immunoblot with polyclonal-monospecific antibodies against ChxR (αChxR). The alpha subunit of RNA polymerase (αRpoA) was used to normalize the amount of chlamydial protein (ChxR) each time point. (C) To test dimer formation *in vivo*, 10 mM DSS was added to uninfected host cells (Mock) or *C. trachomatis* enriched lysates at 30 hpi (Infected). The samples were separated by SDS-PAGE and an immunoblot was performed using antibodies against ChxR.

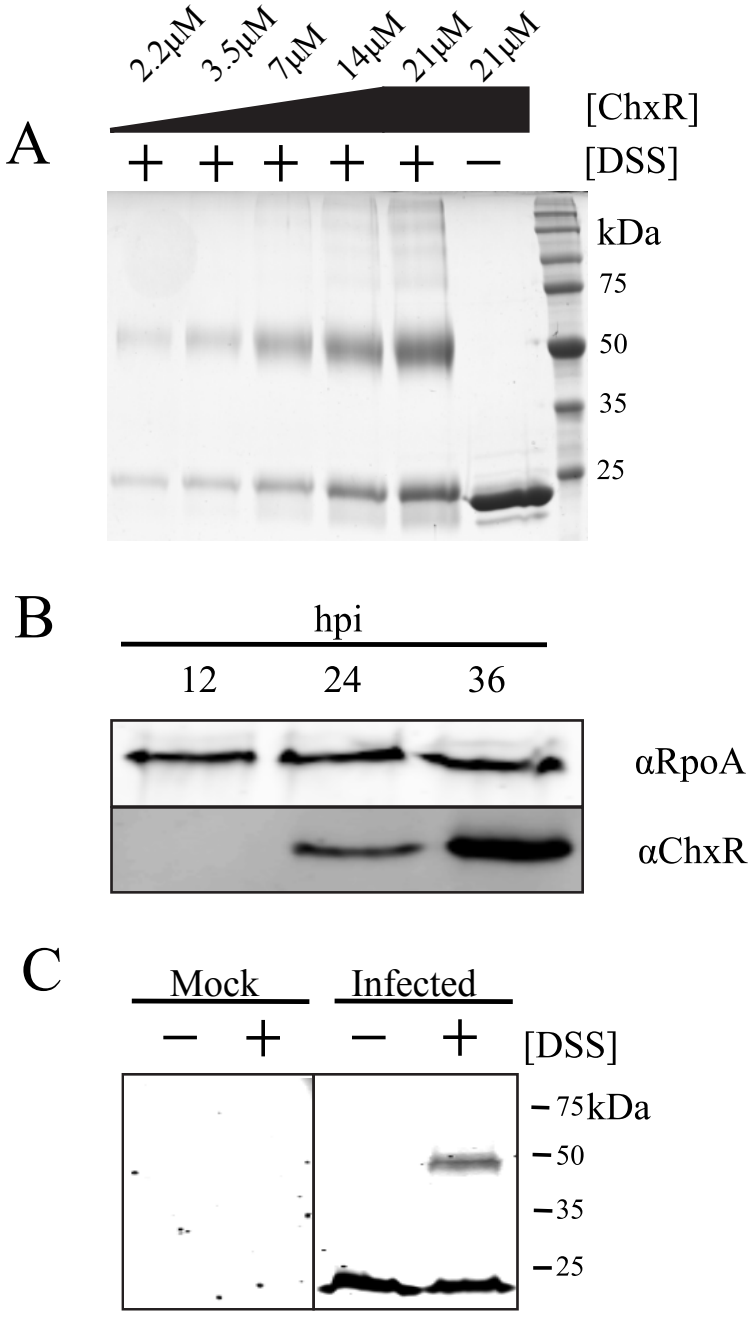
A
2.2μM
3.5μM
7μM
14μM
21μM
21μM
[ChxR]
+ + + + + −
[DSS]
kDa
75
50
35
25
B
hpi
12
24
36
αRpoA
αChxR
C
Mock
Infected
− + − +
[DSS]
75kDa
50
35
25

predominant species were still homodimers (Fig. 2.2A). As an additional control for protein-protein interaction specificity, increasing concentrations of a typically monomeric protein, bovine serum albumin, were incubated with DSS. Appreciable formation of higher complexes was not observed (data not shown). These data suggest that the primary amine chemical crosslinker DSS can capture ChxR homodimers *in vitro*.

Prior to applying DSS to *Chlamydia*-infected cells to determine if ChxR forms homodimers *in vivo*, it was necessary to determine when ChxR is present during the developmental cycle of *Chlamydia*. Simply described, the biphasic developmental cycle consists of a primarily extracellular, metabolically inactive, and infectious form termed elementary body (EB) converting intracellularly into the metabolically active, replicative, and non-infectious form RB. After numerous rounds of RB replication, asynchronous reciprocal conversion (RB into EB) occurs, and EBs are released to infect new cells (Hybiske and Stephens 2007).

Prior RT-PCR data indicate that *chxR* is expressed at 12 hpi and upregulated through 48 hpi (Koo, Walthers et al. 2006); however, protein expression has not been determined. To ascertain if the protein expression pattern complements these findings, the expression profile of ChxR in an RB-enriched fraction of infected cell lysates from 12, 24, and 36 hpi was determined. At 12 hpi, EBs have fully converted to RBs, and the RBs are replicating. At 18–24 hpi, some RBs have begun to convert to EBs. At 36 hpi, the inclusion occupies most of the host cell and is composed of RBs and EBs. Immunoblot analysis of these lysates indicated that no ChxR protein was detected at 12 hpi but that ChxR is evident at 24 hpi, and the protein levels dramatically increase by 36 hpi (Fig. 2.2B). In addition to providing the key times during the developmental cycle to apply DSS, these observations also support that ChxR is most likely exerting its

functional activity during the middle (~24 hpi) and late (>36 hpi) stages of the chlamydial developmental cycle.

Expression data indicated that studies designed to determine the homodimerization capability of ChxR should be performed after 24 hpi. A fraction of *C. trachomatis*-infected cells enriched for RBs was isolated at 30 hpi and incubated with DSS. Immunoblot analyses of lysates from RB-enriched fractions treated with DSS (Fig. 2.2C) revealed a protein profile very similar to that in the *in vitro* experiment (Fig. 2.2A). Immunoreactive bands were detected near the molecular mass of a ChxR monomer (26 kDa) and homodimer (~50 kDa). These data support the *in vitro* observations and indicate that ChxR is forming homodimers *in vivo*.

***ChxR recognizes its own promoter* in vivo.**

Prior *in vitro* analyses have demonstrated that ChxR is a transcriptional activator and recognizes its own promoter (Koo, Walthers et al. 2006). To provide evidence that ChxR is transcriptionally active *in vivo*, a commonly utilized immunoprecipitation approach combined with PCR was enlisted (Wade, Struhl et al. 2007). RB-enriched fractions were treated with formaldehyde to crosslink ChxR to DNA targets. Following immunoprecipitation with anti-ChxR antibodies and extensive washing, DNA was eluted and used in PCR reactions to determine if *chxR* promoter DNA was associated with ChxR. As Fig. 2.3 indicates, PCR analysis revealed that *chxR* promoter DNA was specifically associated with ChxR. The specificity of the immunoprecipitation reaction was indicated by the presence of *chxR* promoter amplicons only when anti-ChxR antibody and crosslinker were applied (Fig. 2.3).

To provide further support for the specificity of ChxR-*chxR* promoter DNA capture, the association of ChxR with the promoter region of the open reading frame 863 (*CT863*) was

FIG. 2.3. ChxR is associated with its own promoter *in vivo*. To determine if ChxR recognizes the *chxR* promoter during a chlamydial infection, ChxR was crosslinked to DNA using formaldehyde at 36 hpi and immunoprecipitated from the lysates using antibodies that recognize ChxR (αChxR). PCR was then performed using primers specific for the *chxR* promoter. The lack of a PCR product with primers to the *CT863* promoter supports that ChxR specifically recognizes the *chxR* promoter *in vivo*. The presence (+) or absence (-) of *C. trachomatis* genomic DNA (DNA) was used as PCR controls for both promoters. The presence (+) or absence (-) of αChxR was used as controls for the immunoprecipitation of ChxR.

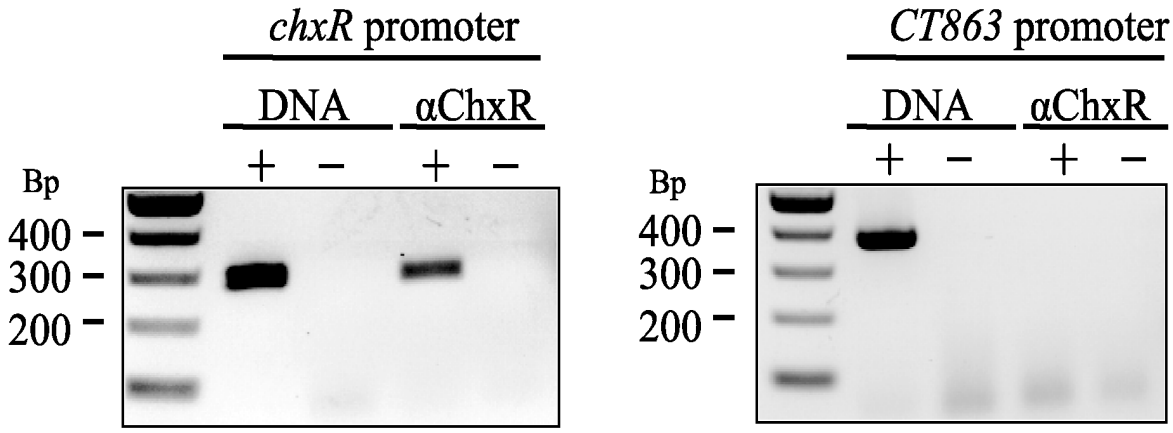
chxR promoter
DNA
αChxR
+ − + −
Bp
400
300
200
CT863 promoter
DNA
αChxR
+ − + −
Bp
400
300
200

similarly analyzed. *CT863* is a gene transcribed at 6 hpi, and transcription levels are constitutively maintained throughout the developmental cycle (Nicholson, Olinger et al. 2003; Hefty and Stephens 2007); (Belland, Zhong et al. 2003). Based on the expression patterns of ChxR (Fig. 2.2), it would not be expected that ChxR plays a role in regulating a constitutively expressed *CT863*. Using primers for this promoter region, a PCR product representative of *CT863* promoter was not detected in any of the immunoprecipitated ChxR-DNA samples (Fig. 2.3). While these are negative observations (lack of *CT863* promoter amplification) from a limited sample size, these observations provide additional support to the specificity of *chxR* promoter amplification from the immunoprecipitation samples. In combination, these data support that ChxR recognizes its own promoter *in vivo* and likely plays a key role in regulating its own expression.

Identification of a conserved direct-repeat DNA sequence in each of the ChxR binding sites.

Homodimers of OmpR/PhoB subfamily response regulators generally recognize a region of DNA that ranges from 18–23 bp and contains a direct repeat (DR) of DNA sequences that are critical for binding (Harlocker, Bergstrom et al. 1995; Blanco, Sola et al. 2002; Kenney 2002). Alternatively, examples of DNA binding motifs that consist of inverted repeats have been identified, including the atypical OmpR/PhoB response regulator HP1043 in *Helicobacter pylori* (Hong, Lee et al. 2007; Wang, Engohang-Ndong et al. 2007). Observations within this study support that ChxR exists as a homodimer and would be expected to bind to a similar DNA repeat motif; however, the critical DNA sequences and configuration are undetermined.

Previously, DNase protection assays indicated that ChxR binds to five regions within the *chxR* promoter, although a consensus recognition sequence was not reported (Koo, Walthers et al. 2006). To identify a shared DNA sequence and/or motif, the DNA sequences within these five ChxR binding sites were visually inspected. Within each of the five binding sites, direct repeat (DR) sequences (5′-T/A-T/A/C-G-A-T/A-N-T/A/C-3′) separated by 3–5 bp were identified (DR1–5; Fig. 2.4B), albeit with various degrees of conservation. Using this DNA sequence and arrangement as a guide, an additional sixth site (DR6) was identified upstream of DR5 (Fig. 2.4A and 2.4B) and was demonstrated to bind to this site (Fig. 2.5). A multiple sequence alignment of all 12 individual binding sites was used to establish a consensus ChxR recognition sequence. The frequency of nucleotides at each position in the DNA recognition sites was calculated, and the computational program Weblogo (Crooks, Hon et al. 2004) was utilized to generate a graphic that reflects the nucleotide frequencies (Fig. 2.4C). Using the nucleotide frequencies at each position, orientation of repeat DNA sequence, and the spacer distance, a ChxR DNA recognition motif was determined (Fig. 2.4D).

ChxR binds to and exhibits differential affinity for the six individual DR sites in the* chxR *promoter.

Differential affinity between individual binding sites within a single promoter has been observed for members of the OmpR/PhoB subfamily and is often a central component in the mechanism of regulation (Bergstrom, Qin et al. 1998; Barnard, Wolfe et al. 2004; Yoshida, Qin et al. 2006). Furthermore, it has been reported that binding of a transcription factor to one site can dramatically affect the capability of a neighboring site to become occupied (i.e., cooperativity) (Harlocker, Bergstrom et al. 1995). To determine the ability of ChxR to bind to

FIG. 2.4. *chxR* promoter region and putative ChxR binding motif. (A) The five putative binding sites (underlined and identified as DR5, DR4, DR3, DR2, and DR1) were derived from a previously reported DNase protection assay (Koo, Walthers et al. 2006). A sixth recognition site (DR6) was later identified within the *chxR* promoter. The arrows denote the orientation of each recognition site. Transcriptional start site and σ^{66} holoenzyme promoter element are indicated by +1 and -35/-10, respectively (Koo, Walthers et al. 2006) (B) Visual inspection of the six binding sites in the *chxR* promoter suggested a conserved direct repeat sequence. The two recognition motifs and intervening sequence within the six DR sites were aligned. (C) A consensus sequence was generated using Weblogo (Crooks, Hon et al. 2004) with each half site from the sequences in Fig. 4B. (D) The recognition sequence and linker length is listed (W=A/T, H=C/A/T, N=G/C/A/T).

A

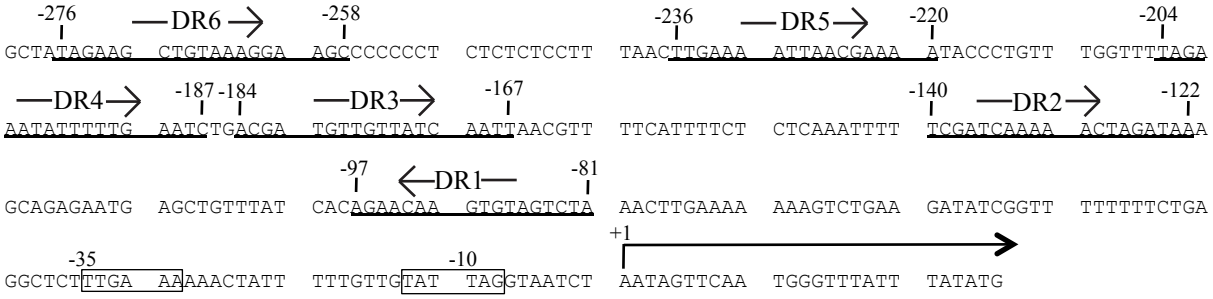

B

DR1 5′-TAGACTA--CAC--TTGTTCT-3′

DR2 5′-TCGATCA-AAAAC-TAGATAA-3′

DR3 5′-ACGATGT-TGTT--ATCAATT-3′

DR4 5′-TAGAAAT-ATTT--TTGAATC-3′

DR5 5′-TTGAAAA--TTA--ACGAAAA-3′

DR6 5′-TAGAAGC-TGTAA-AGGAAGC-3′

C

D

5’-WHGAWNH-N_{3-5}-WHGAWNH-3’

FIG. 2.5. Binding of ChxR to individual DR sites. (A) To determine if ChxR interacts with the six recognition sites within the *chxR* promoter individually, EMSAs were performed with 100 nM of each IR800-labeled binding site (DR1-DR6) with (+) or without (-) 1 μM ChxR. A DNA sequence corresponding to the -120 to -95 region of the *chxR* promoter was used as a nonspecific DNA control (NC). The K_d for each binding site is given in Table 2.2.

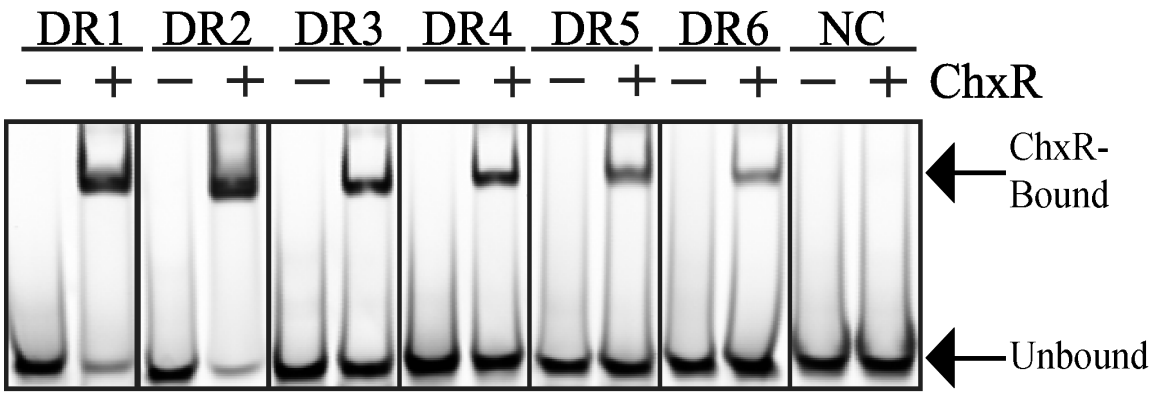
DR1
DR2
DR3
DR4
DR5
DR6
NC
− + − + − + − + − + − + − + ChxR
ChxR-
Bound
Unbound

each of the DR sites independently and whether a potential binding hierarchy exists, the binding capability of ChxR to each of the six DNA binding sites was analyzed and measured independently. EMSAs were performed with DNA representative to each of the binding sites and ChxR (Fig. 2.5A and Table 2.1). ChxR was able to interact with each site independently. In support of the specificity of ChxR to these binding sequences, ChxR did not interact with an oligonucleotide that did not contain a ChxR binding sequence (Fig. 2.5A; NC). The ability of ChxR to interact with DR6 affirms that the visually derived consensus sequence (Fig. 2.4D) is indeed recognized by ChxR. In addition, by using a static concentration of protein and DNA, it appeared that ChxR has a differential affinity for the individual DR sites.

To measure the differential affinity for the six DR sites, EMSAs were performed with each recognition site and increasing concentrations of ChxR (data not shown). K_d was then calculated for each site (Table 2.2). The K_d values listed are for a ChxR:DNA stoichiometric ratio of 2:1 given that recombinant ChxR is a homodimer *in vitro*. The quantitative analysis revealed that ChxR had the highest affinity (K_d = 44 ± 4 nM) for DR2 and the lowest affinity (K_d = 1500 ± 300 nM) for DR6. The affinity for DR2 is more than 33-fold higher than that for DR6. This suggests that there is a hierarchy of binding in the *chxR* promoter and that the order of binding is DR2>DR1-DR3>DR4-DR5>DR6.

Three highly conserved bases within the ChxR binding motif are critical to recognition.

As described previously, visual inspection of the six DR sites revealed a conserved recognition sequence (Fig. 2.4C). Based upon the nucleotide frequency in the deduced recognition site, it is expected that the nucleotides are critical for DNA binding. To the hypothesis that ChxR requires the conserved GAW nucleotides for binding, EMSAs were

Table 2.2 Dissociation constants for ChxR and each binding site

Binding Site	K_d (nM)[1]
DR1	140 ± 30
DR2	44 ± 4
DR3	120 ± 30
DR4	410 ± 30
DR5	480 ± 70
DR6	1500 ± 300

[1] The dissociation constant and standard error of the mean from three replicates

performed with wild-type or mutated DNA constructs from the site (DR2) in the *chxR* promoter that exhibited the highest affinity for ChxR (Fig. 2.6A). Increasing concentrations of ChxR were incubated with DR2 DNA containing triple cytosine mutations at either GAW position (DR2-2; −138 to −136 or DR2-1; −126 to −124) or the same mutations at both sites (DR2-1/2). Triple mutations at either GAW site dramatically reduced the ability of ChxR to bind to the DNA fragment relative to the wild-type sequence (Fig. 2.6B). Mutations in DR2-2 had dramatic negative effects on ChxR binding, although an interaction was still observed at the highest two concentrations of ChxR (25:1 and 100:1). Similarly, mutations in DR2-1 dramatically reduced the interaction between ChxR and the DNA (Fig. 2.6B). Mutations at both ChxR monomer-binding sites eliminated any observable ChxR-DNA interaction (Fig. 2.6B). These data support the hypothesis that the central GAW nucleotides in both sites are important to ChxR binding.

Single base pair contribution to ChxR binding to the DR2 sequence.

The prior analysis supports the conclusion that the central GAW in the DR2 sequence is critical to ChxR binding. It is expected that additional ChxR-nucleotide interactions are integral to stabilizing the ChxR-DNA complex. To identify these individual bases and measure the effect on ChxR binding, single transversion mutations that would result in a base pair change (A or T⇔C or G, respectively) were introduced throughout the DR2 binding site and the intervening sequence. The DR2 site was chosen for single base pair contribution analysis because it is the highest affinity binding site in the *chxR* promoter. The base pair transversions were expected to disrupt both major and minor groove interactions. As described previously in this report, EMSAs were performed with each of the mutated DR2 DNA sequences in triplicate, and the percent of DR2 DNA relative to wild-type DNA bound by ChxR was determined (Fig. 2.7).

FIG. 2.6. Mutations within the DNA recognition motif significantly reduce ChxR-DNA interaction. (A) The DR2 nucleotide sequence from the *chxR* promoter is shown. The two consensus recognition sequences are underlined and the bolded nucleotides indicate the sites of triple-cytosine mutations. EMSAs were performed with increasing concentrations of ChxR (39 nM-3.9 μM) and 39 nM of each DNA construct: (B) wild-type sequence (WT), DR2-2 mutant, DR2-1 mutant, and DR2-1/2 double mutant.

A

DR2-2 DR2-1

5'-TCTCAAATTTTTCGATCAAAAACTAGATAAAGCAG-3'

B

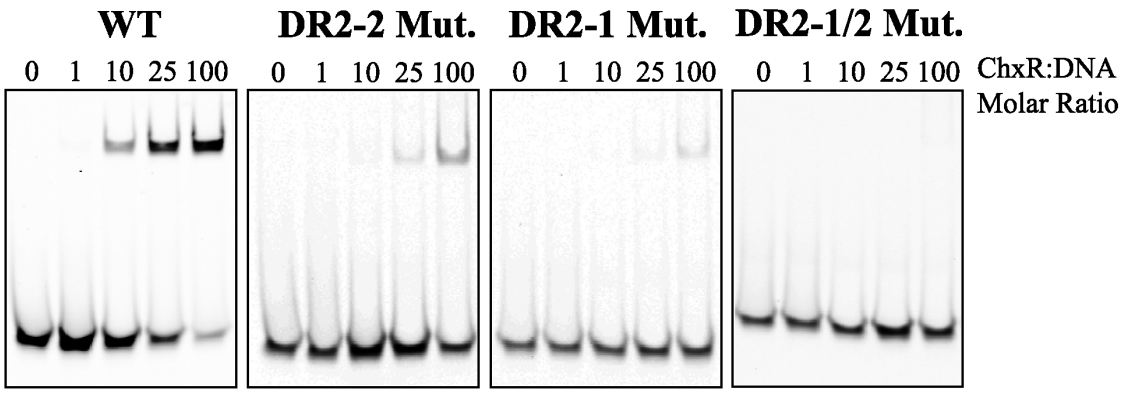

FIG. 2.7. Single base pair contributions to ChxR-DNA interactions within the DR2 binding site. EMSAs were performed with 5 μM ChxR and 50 nM DNA containing transversion mutations. The target DNA used in the experiment was the DR2 sequence from the *chxR* promoter, comprising the DR2 half sites (underlined). The percent of DNA shifted with each transversion mutation (n = 3) are shown in the graph relative to the DNA shifted with the wild-type sequence (n = 18). The amount of DNA shifted, was quantified using the photon emission of the SYBR Green at 520 nm. The mutations that resulted in a significant ($p < 0.05$) reduction of DNA-interaction are denoted by an asterisk.

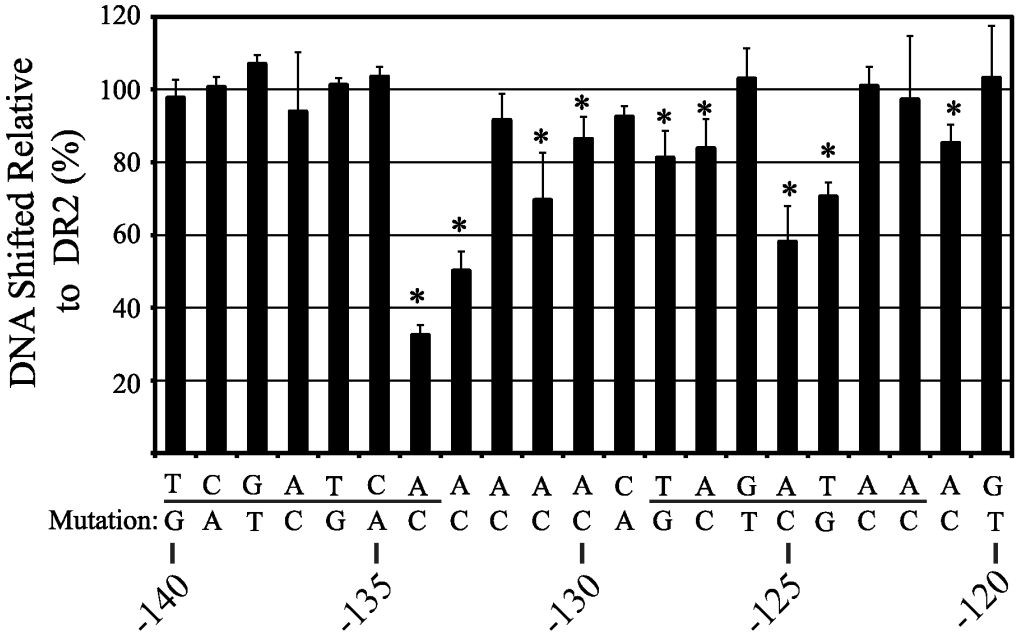
DNA Shifted Relative to DR2 (%)
120
100
80
60
40
20
T C G A T C A A A A A C T A G A T A A A G
Mutation: G A T C G A C C C C C A G C T C G C C C T
-140
-135
-130
-125
-120

Nine of the single base pair mutations resulted in a statistically significant decrease of percent DNA shifted relative to wild-type DR2 DNA. Out of the nine single base pair mutations that had a statistically significant decrease in DNA shifted, four mutations had dramatically (>20%) less DNA shifted than wild-type DR2 DNA. The most dramatic decrease in DNA shifting occurred when a transversion was introduced at position −134. Position −134 is located at the 3′ end of the DR2-2 ChxR binding site and resulted in a 70% reduction in DNA shifted relative to wild-type DR2 sequence. Within the predicted spacer region, at the base immediately 3′ of the DR2-2 site, a transversion caused an approximately 50% reduction of DNA binding by ChxR. In contrast to DR2-2, transversions at four separate locations in DR2-1 (−124, −125, −127, and −128) resulted in a statistically significant decrease in ChxR binding; however, only the mutations in the central GAW positions (−124 and −125) resulted in more than a 20% reduction in the percent of DNA shifted. Together, these data support that single base transversions can have a negative effect on ChxR binding to the DR2 region; however, no single mutation eliminated ChxR binding.

ChxR^{E49D} retains dimerization and DNA binding activity.

Typically, members of the OmpR/PhoB response regulator subfamily are phosphorylated through a highly conserved Asp residue in the receiver domain of these proteins (Friedland, Mack et al. 2007). This phosphorylation facilitates the reorientation of two switch residues and promotes homodimerization, DNA binding, and transcriptional regulation. ChxR is uncommon in this respect because the amino acid in the predicted position of the conserved Asp is a Glu residue (E49) (Koo, Walthers et al. 2006). Many transcription factors that are activated by a

phosphorylated Asp can be converted into a phosphoryl-independent constitutively active state via substitution with Glu (Klose, Weiss et al. 1993; Siam and Marczynski 2003; Gao, Mukhopadhyay et al. 2006; Arribas-Bosacoma, Kim et al. 2007). Based upon these observations, it was hypothesized that Glu 49 is critical to DNA binding and transcriptional activity of ChxR and that conversion to an Asp could render the molecule inactive. To begin testing this hypothesis, Glu 49 was substituted with an Asp (E49D), and the modified ChxR^{E49D} was assayed for homodimerization and DNA binding capability.

Similar to wild-type ChxR, recombinant ChxR^{E49D} migrated via size exclusion chromatography at a size expected for a homodimer (data not shown), indicating that this modification had a minimal effect on monomer-monomer interactions. To further test the capability of ChxR^{E49D} to dimerize, unmodified ChxR or ChxR^{E49D} was exposed to a chemical crosslinker (DSS) to capture homodimers prior to separation via SDS-PAGE. The resulting observations also support that ChxR^{E49D} retained the ability to form homodimers (Fig. 2.8A). The ability of ChxR^{E49D} to bind to DNA was tested via EMSA by using the DR2 site from the *chxR* promoter (Fig. 2.8B). The percent of DNA shifted with ChxR^{E49D} was quantified and found to be very similar to that with wild-type ChxR. These data indicate the Glu residue (E49) in the position of the conserved Asp in other OmpR family members does not solely account for the constitutive transcriptional activity of ChxR.

FIG. 2.8. $ChxR^{E49D}$ retains homodimer formation and DNA binding activity. (A) To test homodimerization, 5 μM ChxR or 6 μM $ChxR^{E49D}$ was incubated with 500 μM DSS. Proteins were separated by SDS-PAGE and visualized by Coomassie staining. (B) To determine the DNA binding activity of $ChxR^{E49D}$, EMSAs were performed in triplicate with 1.25 μM ChxR or 1.25 μM $ChxR^{E49D}$ and 50 nM DNA from the DR2 site. The percent of DNA shifted was quantified and normalized as described previously.

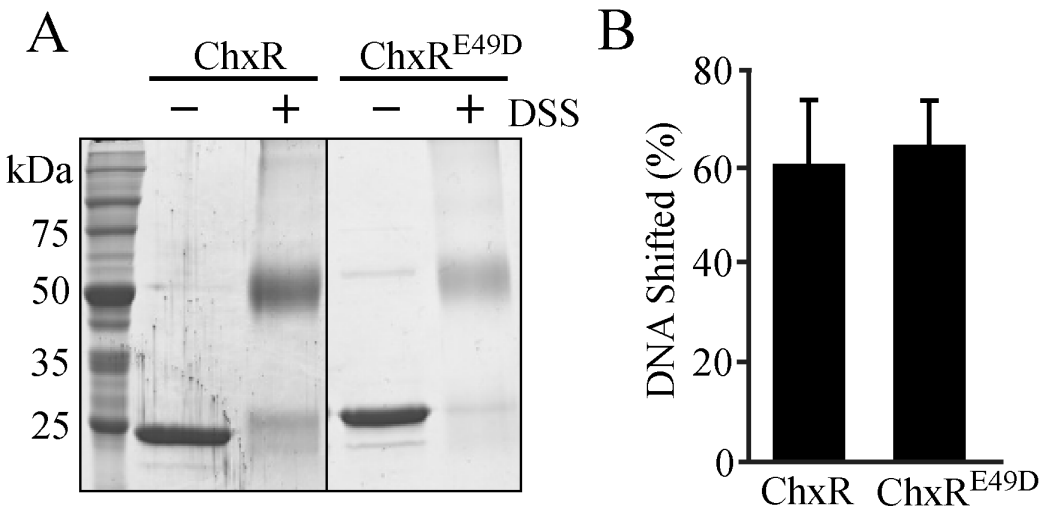
A
ChxR
ChxR^E49D
− + − + DSS
kDa
75
50
35
25
B
DNA Shifted (%)
80
60
40
20
0
ChxR
ChxR^E49D

Chapter II

Discussion

Homodimer formation, predominantly in response to phosphorylation, is a governing step for the regulation of transcription by a large majority of the OmpR/PhoB subfamily of response regulators (Bourret 2010). Homodimerization orients and stabilizes individual protomers that promote DNA binding and subsequent transcriptional regulation (Mack, Gao et al. 2009). While prior studies on atypical response regulators support phosphorylation-independent transcriptional activation, the importance of homodimer formation is still uncertain (Beier and Frank 2000; Ruiz, Salinas et al. 2008). Data presented here demonstrated that ChxR, in the absence of phosphorylation, forms stable homodimers *in vitro* at concentrations (1 μM) that are likely to be physiologically relevant (Figs. 2.1 and 2.2). This conclusion is further supported by the utility of the membrane-permeant crosslinker DSS, which allowed us to demonstrate that ChxR forms homodimers *in vivo* (Fig. 2.2). While it is possible that ChxR has an alternate site of phosphorylation or undetermined modification that promotes homodimerization within *Chlamydia*, prior analyses showed that unmodified ChxR activated transcription at its own promoter *in vitro* and within a heterologous *E. coli* system (Koo, Walthers et al. 2006). As such, it is unlikely that this unknown mechanism for phosphorylation at an alternate site or undetermined mechanism is present in *E. coli*. These observations and those described herein support that wild-type ChxR protein is in a conformation that likely mimics the phosphoryl-activated OmpR/PhoB response regulators, including homodimerization.

While the conformation of ChxR may mimic that of phosphorylated OmpR/PhoB members, ChxR exhibits unique characteristics. Substitution of the phosphorylated Asp with Glu

can render response regulators constitutively active (Klose, Weiss et al. 1993; Siam and Marczynski 2003; Gao, Mukhopadhyay et al. 2006; Arribas-Bosacoma, Kim et al. 2007). However, the ability of ChxR to maintain a homodimer conformation and interact with DNA is not the result of this single substitution (D49E). Supporting this result was the retention of the homodimer formation and DNA binding capability of ChxR after a Glu to Asp substitution ($ChxR^{E49D}$; Fig. 2.8). These data suggest that those residues (Ser/Thr in β4 and Phe/Tyr in β5) that are typically reoriented in response to Asp phosphorylation might be stabilized in an 'active' orientation in unphosphorylated ChxR. Notably, ChxR does not encode a Ser or Thr in the expected β4 strand but does encode a Tyr (Y90) in the predicted β5 strand. Structural studies on the receiver domain would be useful to identify the molecular orientations, such as that of Tyr90, and interactions that may be critical to forming stable homodimers and eventual transcriptional regulation by this atypical OmpR/PhoB response regulator.

Alternatively, it is possible that phosphorylation of recombinant $ChxR^{E49D}$ in *E. coli* facilitated the formation of an active ChxR molecule. This appears unlikely based upon a number of observations. First, the rate of unaided dephosphorylation in OmpR/PhoB subfamily response regulators typically occurs within seconds to an hour (Stock, Ninfa et al. 1989), which would suggest that the phosphoryl group would not have been retained throughout the purification process and storage of the protein before the assays were conducted. Secondly, a cognate sensor kinase that could phosphorylate ChxR is likely not present given the phylogenetic distance between *Chlamydia* and *E. coli*. Response regulator phosphorylation by cognate sensor kinases is relatively specific, and crosstalk between sensor kinases and response regulators is limited, even within bacteria of the same species. Thirdly, the three-dimensional structure of the ChxR

response regulator has been solved (manuscript in preparation), and structural analysis does not indicate the presence of a phosphoryl group.

The affinities for ChxR to each of the six DR sites are lower than those of typical OmpR/PhoB subfamily response regulators. Studies with phosphorylated OmpR have determined that, of the protein-DNA interactions measured, the DNA affinity ranged from ~7–300 nM (Head, Tardy et al. 1998). Furthermore, DNA interaction is greatly enhanced when multiple repeat sequences are present. In the current study, the affinity for ChxR with the individual six DR sites was measured and ranged from ~44 nM–1.5 μM (Table 2.2), which is about 5-fold lower than that of OmpR. It may be possible that cooperativity plays a key role in enhancing affinity to the promoter region. As such, it is currently unclear how the presence of multiple binding sites influences the affinity of ChxR for DNA but is a focus of ongoing studies.

Several individual base pair mutations were demonstrated to have significant effects on ChxR binding to the DR2 DNA binding site (Fig. 2.7). Interestingly, only one of these mutations (−134) resulted in a greater than 50% reduction in ChxR binding to DNA. The overall tolerance to single base transversions is likely indicative of relatively strong ChxR affinity to this particular binding site. This is supported by the observation that ChxR has the highest binding to a DR2 DNA fragment as compared to the other five sites (Table 2.2). Furthermore, no single mutation completely eliminated ChxR binding to the DR2 DNA sequence. This is in contrast to the triple base pair mutation introduced into either conserved ChxR binding sequence that had a large impact on all DNA binding by ChxR (Fig. 2.6). Moreover, no single mutation caused a significant increase in ChxR binding efficiency.

Single base mutations appeared to have more negative influence on DR2-1 ChxR binding site than DR2-2. Four base mutations (−128, −127, −125, and −124) all caused statistically

significant reductions in ChxR binding to DR2-1. In contrast, only a mutation at −134 caused a decline in DR2-2 binding, albeit the largest effect by a single mutation. These observations indicate that affinity of ChxR to the DR2-1 wild-type sequence is weaker, as individual base changes are not tolerated well. This is in congruence with the apparent requirement for both ChxR recognition sites for a stable protein-DNA interaction (Fig. 2.6). Furthermore, the dramatic negative affect at −134 also supports that, in the context of the surrounding sequencing, this residue is critical for ChxR binding. Interestingly, single mutations that resulted in a negative effect were not constrained to the seven bases within a conserved binding site. Three intervening base mutations (−133, −131, and −130) resulted in significant reductions in ChxR binding. This suggests that protein contacts are likely occurring within this region and playing a role in the affinity of ChxR to DNA. Of note, the wing of the OmpR/PhoB subfamily winged-helix motif typically interacts with an adjacent DNA minor groove in a non-base-specific fashion. Additionally, these mutations could be affecting the topology of the relatively small fragment of DNA and disrupting ChxR interactions in the conserved sequences. A comparison of the intervening sequence between binding sites does not reveal any conserved nucleotide frequencies, which suggests that the latter (DNA topology) is more likely; however, sequence-specific interactions may be involved in only a few of the binding sites, such as DR2. Along these lines, a recent report has emphasized the role of DNA topology on gene regulation in *Chlamydia* (Case, Peterson et al.).

Based upon the ChxR DNA binding sequence (WHGAWNH; Fig. 2.4), it may be expected that ChxR has a relatively low level of DNA binding specificity. This may be insightful in regards to the overall role of ChxR in *Chlamydia*. Bacterial transcription factors that exhibit relatively low levels of specificity are consistently global regulators which are transcription

factors that regulate relatively large number of genes and incorporate different response conditions, co-regulators, or different sigma factors (Lozada-Chavez, Angarica et al. 2008). For example, OmpR has been reported to regulate the transcription of at least 125 genes (Rhee, Sheng et al. 2008). In contrast, local regulators, transcription factors that regulate a relatively small number of genes associated with a specific stimulus/physiologic response, have high levels of specificity. The ChxR direct repeat binding sequence with a 3–5 base spacer occurs at 3203 and 3303 sites in the *C. trachomatis* serovar D and serovar L2 genomes, respectively (data not shown). However, when the two genomes are searched with a consensus sequence (WHGAWNW) from the three highest affinity sites (DR1-3), the number of binding sites decreased to 1826 and 1902 for the D and L2 genomes, respectively. Further analyses are clearly needed to correlate the ability of ChxR to recognize any of these sites for transcriptional regulation. Characterizing other ChxR binding sites may refine the ChxR recognition motif. However, the low nucleotide conservation in the binding sequence supports the hypothesis that ChxR is a global regulator in *Chlamydia*, in contrast to a local, more restricted transcriptional regulator.

The presence of *chxR* transcripts during the early stages of the developmental cycle, albeit at a relatively low level, indicates that the previously determined σ^{66} promoter (Koo, Walthers et al. 2006) is active but weakly initiating transcription or that post-transcriptional repression mechanisms are employed. Based upon the ability of ChxR to bind to the six sites present in the *chxR* promoter, we speculate that full expression of *chxR* may rely on a threshold of ChxR molecules being attained. This threshold would require occupancy of 12 ChxR proteins (6 homodimers) to all six binding sites within the *chxR* promoter. This potential mechanism is intriguing, as the signal for the asynchronous conversion of RB to EB is unknown. As RBs

replicate, it may be expected that the cytosolic contents, including ChxR, are diluted and distributed randomly to the daughter cells. This possibility, combined with differential replication rates of individual organisms, could permit ChxR to accumulate and reach a threshold for full *chxR* expression in subpopulations of *Chlamydia*. Many other factors are expected to play a role in the stability of ChxR that would also affect this proposed mechanism. While this mechanism is largely speculative, future studies regarding the mechanism of ChxR activation and identifying global ChxR gene targets are expected to address the validity of the proposed model.

Chapter III

Introduction

Two-component signal transduction systems are important mechanisms that mediate many physiological functions within an organism. The output response of these systems is generally an alteration of gene expression (Stock, Robinson et al. 2000; Wang, Engohang-Ndong et al. 2007). The prototypical two-component system consists of a membrane bound sensor histidine kinase that transfers a phosphoryl group to a cognate response regulator (For review (Gao and Stock 2009)). Phosphorylation of the response regulator induces relatively subtle conformational changes within the protein that promote oligomerization through a receiver domain. Oligomerization facilitates an effector domain to interact with DNA and the transcriptional machinery.

While the genes regulated by these transcription factors vary, a highly conserved protein architecture and residue composition (i.e. structure and sequence) appear to be critical for a canonical mechanism of activation. Currently, ~200 receiver domain structures have been elucidated for response regulators and almost all share a common β1-α1-β2-α2-β3-α3-β4-α4-β5-α5 topology (Gao and Stock 2009; Bourret 2010). Within these 200 structures, 20 belong to the OmpR/PhoB subfamily, which is the largest subfamily of response regulators (Galperin 2006). Members of this subfamily are composed of a receiver domain that contains the site of phosphorylation and is involved in homodimerization, and an effector domain that interacts with DNA through a subfamily-defining winged helix-turn-helix motif.

In addition to the conserved domain architecture of the OmpR/PhoB subfamily, current understanding of the mechanism of activation within these proteins is derived from comparisons

of multiple structures of these proteins in both the inactive (unphosphorylated) and active (phosphorylated) state (Sola, Gomis-Ruth et al. 1999; Bachhawat, Swapna et al. 2005; Toro-Roman, Mack et al. 2005; Toro-Roman, Wu et al. 2005; Bachhawat and Stock 2007). The cognate sensor kinase transfers a phosphoryl group to a conserved phospho-accepting Asp in the receiver domain of the response regulator. An essential Mg^{2+} ion and a Lys residue assist in the transfer and retention of the phosphoryl group within the binding site (Sola, Gomis-Ruth et al. 1999; Bachhawat, Swapna et al. 2005). The activation signal is then transduced to the dimer interface (α4-β5-α5) through the reorientation of two conformational switch residues (Thr/Ser and Tyr/Phe) towards the phosphoryl group. The reorientation of these two residues dramatically enhances homodimer formation by properly aligning residues within the dimer interface that are involved in ionic and hydrophobic interactions between protomers. Homodimer formation through the receiver domain enhances the ability of the effector domain to bind to DNA and regulate transcription (Mack, Gao et al. 2009).

An increasing number of response regulators have been identified that appear to not rely on a sensor kinase or a phosphorylation event for activation. These atypical response regulators do not retain many of the residues critical to the canonical phosphorylation (activation) process (Bourret 2010). For example, HP1043, from *Helicobacter pylori*, lacks the phospho-accepting Asp but is still capable of forming homodimers and interacting with DNA in the absence of phosphorylation (Delany, Spohn et al. 2002; Schar, Sickmann et al. 2005; Hong, Lee et al. 2007). Two experimentally determined structures of atypical receiver domains have shown that the conserved structural topology of the OmpR/PhoB subfamily is largely retained in these atypical response regulators (Fraser, Merlie et al. 2007; Hong, Lee et al. 2007). Functional studies of these proteins, albeit limited, have determined that the propensity to form homodimers is also

generally retained (O'Connor and Nodwell 2005; Fraser, Merlie et al. 2007; Hong, Lee et al. 2007; Hickey, Weldon et al. 2011). The structural elements that maintain their phosphorylation-independent activity, however, are poorly understood due to the paucity of functional and structural studies of these proteins.

The medically important bacteria *Chlamydia* encodes an atypical transcriptional regulator termed ChxR. Transcriptional regulation has been determined to be a key factor in the development and pathogenesis of *Chlamydia* (Belland, Zhong et al. 2003; Nicholson, Olinger et al. 2003). ChxR was identified from primary sequence homology to be a member of the OmpR/PhoB subfamily of response regulators (Stephens, Kalman et al. 1998). Computational analysis indicated that ChxR lacks the phospho-accepting Asp and a cognate sensor kinase was not identified within the chlamydial genome, suggesting that the function of ChxR is not directly controlled by phosphorylation (Koo, Walthers et al. 2006). Functional studies have reported that ChxR exists as a stable homodimer and could activate transcription in the absence of phosphorylation (Koo, Walthers et al. 2006; Hickey, Weldon et al. 2011 (Chapter 2)). While these results support the conclusion that ChxR is an atypical OmpR/PhoB transcriptional regulator, the critical structural features that permit the protein to be maintained in an active state, and thereby mimic the mechanism of phosphorylated response regulators, have yet to be identified. We hypothesize that the intra- and intermolecular interactions involved in activation and dimerization of ChxR are distinct from the canonical phosphorylation (activation) paradigm in the OmpR/PhoB response regulator subfamily. To test this hypothesis, structural and functional studies were performed with the receiver domain of ChxR to identify the residues and structural features necessary for dimerization.

Chapter III

Methods

Cloning, Expression, and Purification of $ChxR_{Rec}$. DNA encoding the receiver domain of ChxR ($ChxR_{Rec}$, residues 2-113) was PCR amplified using *Chlamydia trachomatis* LGV (L2/434/Bu) genomic DNA and primers for $ChxR_{Rec}$ (5'-GGAATTCCATATGCAGGGCCTAAACATGTG-3' and 5'-CCGCTCGAGATGTAGCGAATGCTGAGAAAG-3') (Integrated DNA Technologies, Coralville, IA). The PCR product was digested with *NdeI/XhoI* and inserted into the N-terminal polyhistidine tag encoding pET28b vector (Novagen, San Diego, CA). $ChxR_{Rec}$ was expressed and purified as described for full-length ChxR ($ChxR_{FL}$) (Hickey, Weldon et al. 2011 (Chapter 2)). Briefly, the protein was initially purified using Co^{2+} affinity chromatography (Clontech, MountainView, CA) equilibrated with 50 mM Tris-HCl pH 8.0, 400 mM NaCl. $ChxR_{Rec}$ was further purified by size exclusion chromatography using a Sephacryl S-200 16/60 column (GE Healthcare Biosciences, Pittsburg, PA) equilibrated with 50 mM Tris-HCl pH 8.0, 400 mM NaCl.

Crystallization of $ChxR_{Rec}$. Purified $ChxR_{Rec}$, concentrated to 10 mg/ml in 20 mM NaH_2PO_4/K_2HPO_4 pH 7.0, 400 mM NaCl, was screened for crystallization in Compact Jr. (Emerald BioSystems, Bainbridge Island, WA) sitting drop vapor diffusion plates by mixing 1 μL of protein and 1 μL of crystallization solution equilibrated against 100 μL of the latter. Prismatic $ChxR_{Rec}$ crystals were obtained from two crystallization conditions. $ChxR_{Rec}$ crystals, belonging to a *C*-centered monoclinic lattice (space group *C*2) grew in approximately 2 days at 4°C from the Wizard 3 screen (Emerald Biosystems) condition #10 (20% (w/v) PEG 3350, 0.2

M sodium thiocyanate). A tetragonal crystal form (space group $I4_1$) grew in approximately 2 days at 4°C from the Precipitant Synergy screen (Emerald Biosystems) condition #7 and pHat screen (Emerald Biosystems) condition #42 (4 M NaCl, 5% Isopropanol, and 100 mM NaH_2PO_4/K_2HPO_4 pH 7.0). Single crystals were transferred to a cryoprotectant solution containing 80% crystallization solution and 20% ethylene glycol before flash cooling in liquid nitrogen for data collection. For SIRAS phasing, a crystal belonging to the *C*2 form was soaked for 5 minutes in 50 mM 5-Amino-2,4,6-triiodoisophthalic acid (I3C, Hampton Research, Aliso Viejo, CA) (Beck, Krasauskas et al. 2008) dissolved in crystallization solution prior to the transfer to the cryoprotectant solution.

Data Collection and Processing. Diffraction data for structure solution using the SIRAS phasing method were collected at 93 K at the University of Kansas Protein Structure Laboratory using a Rigaku RU-H3R rotating anode generator (Cu-Kα) equipped with an R-axis IV^{++} image plate detector and osmic blue focusing mirrors. The exposure time for each 1° oscillation image was 8 minutes at a detector distance of 150 mm. Intensities were integrated and scaled using the *HKL2000* package (Otwinowski and Minor 1997). Structure solution was carried out using the SIRAS phasing method with the *SHELX C/D/E* software package (Sheldrick 2008) via the CCP4 interface (1994). Iodine positions corresponding to three I3C sites were identified using *SHELXC* and *SHELXD* that yielded correlation coefficient all/weak of 38.80/27.17. Calculation of initial phase angles and density modification were conducted with *SHELXE* and yielded a pseudo-free correlation coefficient of 69.28% and an estimated mean figure of merit of 0.653 for the inverted substructure. *BUCCANNER* (Cowtan 2006) was used to generate a C_α trace of the model for future molecular replacement against the high-resolution native data. High-resolution native $ChxR_{Rec}$ (*C*2 space group) data were collected at 100K at the IMCA-CAT beamline 17BM

at the Advanced Photon Source using an ADSC Quantum 210r CCD detector at a wavelength of 1.0 Å. The exposure time for each 1° oscillation image was 5 seconds. Intensities were integrated and scaled using *D*TREK* (Pflugrath 1999). High-resolution native $ChxR_{Rec}$ ($I4_1$ space group) data were collected at 100K at Stanford Synchrotron Radiation Laboratory (SSRL) beamline 9-2 using an MAR325 detector at a distance of 170 mm, wavelength of 1.54 Å, an exposure time of 5 seconds, and a 1° oscillation per image. Intensities were integrated and scaled using *MOSFLM* and *SCALA* (Evans 2006), respectively. The model obtained from SIRAS phasing was used as the search model for molecular replacement with *PHASER* (McCoy, Grosse-Kunstleve et al. 2007) against the high-resolution synchrotron data. Initial automated model building was carried out using *ARP/wARP* (Langer, Cohen et al. 2008). Anisotropic atomic displacement parameters were modeled by TLS refinement 7 groups as generated by the TLSMD server (http://skuld.bmsc.washington.edu/~tlsmd/)(Painter and Merritt 2006). Final model building and structure refinement were performed with *COOT* (Emsley and Cowtan 2004) and *PHENIX* (Adams, Afonine et al. 2010) respectively. Data collection and processing statistics are listed in Table 3.1. Figures were created using CCP4 Molecular Graphics Program (http://www.ysbl.york.ac.uk/~ccp4mg/) (Potterton, McNicholas et al. 2004).

For the 1.6 Å resolution model, monomer A comprises residues 2-111 and monomer B comprises residues 4-37, 43-60, and 68-110. The model contained two ethylene glycol molecules and 106 water molecules. For the 2.15 Å resolution model, monomer A comprises residues 4-54 and 66-110, and monomer B comprises residues 4-60 and 67-109. The model contained two sodium ions and 39 water molecules. For the 2.1 Å resolution structure, monomer A comprises residues 3-111 and monomer B comprises residues 4-37, 43-60, and 68-109. The model contained three I3C molecules and 75 water molecules. A Ramachandran plot with *PHENIX*

(Adams, Afonine et al. 2010) determined that 99.5% of the residues for all three models were in a favored position and 0.5% of the residues in the 1.6 Å and 2.15 Å resolution models were in an allowed position. Residue 55 (Arg55) of monomer B of the 2.1 Å resolution model was in a disallowed position due to poor electron density in the region of the amide.

Far-UV CD Spectroscopy. CD analysis was performed with a Chirascan-plus Circular Dichroism spectrometer equipped with a Peltier temperature controller and a 4-position cuvette holder (Applied Photophysics Ltd, Leatherhead UK). Far UV spectra of YycF and ChxR at 0.1 mg/ml in CD buffer (20 mM NaH_2PO_4 pH 7.5, 20 mM NaCl) were collected in the range of 190-260 nm using a 0.1 cm path length cuvette sealed with a Teflon stopper. A sampling time-per-point of 2 s and a bandwidth of 1 nm were used. The secondary structure components were estimated by the CDNN CD spectra deconvolution software (Bohm, Muhr et al. 1992). CDNN is a neural networks method based program, which can be used to analyze data to determine the content of α-helix, parallel and anti-parallel β-structure, turns and random coil. The results from the CDNN analysis were sorted automatically in five regions (190-260nm, 195-260nm, 200-260nm, 205-260nm and 210-260nm) for each secondary structure component. For each secondary component, results of five regions were averaged and standard deviations were calculated.

Site-Directed Mutagenesis. Mutations were introduced into the $ChxR_{FL}$ plasmid using the QuikChange II XL Site-Directed Mutagenesis kit and following the manufacturers protocol (Agilent Technologies, La Jolla, CA). All clones were verified by DNA sequencing analysis (ACGT, Inc., Wheeling, Il). The proteins were over-expressed in pET28b and purified as described previously (Hickey, Weldon et al. 2011 (Chapter 2)).

Analytical Size Exclusion Chromatography. Following purification, $ChxR_{Rec}$, $ChxR_{Rec}^{W89E}$, $ChxR_{FL}$, and $ChxR_{FL}^{W89E}$ were concentrated to 100 μM using an Amicon Ultra centrifugal filter (Millipore, Billerica, MA). $ChxR_{Rec}$ was then diluted to 10 μM and 1 μM in 50 mM Tris-HCl pH 8.0, 400 mM NaCl. The proteins were applied to a Superdex 75 10/300 GL analytical size exclusion column (GE Healthcare Biosciences) equilibrated with 50 mM Tris-HCl pH 8.0, 400 mM NaCl for $ChxR_{Rec}$ and $ChxR_{Rec}^{W89E}$, and 50 mM Tris-HCl pH 7.5, 100 mM NaCl, and 250 mM KCl for $ChxR_{FL}$ and $ChxR_{FL}^{W89E}$. A protein standard solution containing bovine serum albumin (66kDa), chicken ovalbumin (44kDa), horse myoglobin (17kDa), and vitamin B12 (1.35kDa) (BIO-RAD, Hercules, CA) was used to generate a standard curve.

Electrophoretic Mobility Shift Assay. An electrophoretic mobility shift assay to test DNA binding by ChxR was performed as previously described (Hickey, Weldon et al. 2011 (Chapter 2)) with IR800-labeled DNA corresponding to the high-affinity (DR2) binding site within the *chxR* promoter. The binding reactions contained 1 nM DNA and either 44 nM wild-type or variant $ChxR_{FL}$. The DNA was visualized and quantified using an Odyssey Infrared Imaging System (LI-COR Biosciences, Lincoln, NE). The effector domain of ChxR ($ChxR_{Eff}$) used in this assay was purified as described previously (Hickey, Hefty et al. 2009 (Chapter 4)).

Chapter III

Results

Primary sequence comparison of ChxR and other OmpR/PhoB subfamily members.

Prior studies have reported that ChxR can activate transcription despite the absence of a phospho-accepting Asp (Koo, Walthers et al. 2006; Hickey, Weldon et al. 2011 (Chapter 2)); however, a comprehensive analysis of residues that may be important to its function has not been performed. Six conserved residues within the receiver domain of phospho-accepting OmpR/PhoB subfamily members have been demonstrated to be important for activation. Three carboxyl-containing residues (Glu9, Asp10, and Asp53; using PhoB numeration (PBD ID: 1ZES)) are involved in the binding of the essential Mg^{2+} ion (Fig. 1). The Mg^{2+} ion and two residues (Asp53 and Lys105) interact with the phosphoryl group (Sola, Gomis-Ruth et al. 1999; Bachhawat, Swapna et al. 2005). Following the phosphoryl-transfer, the two conformational switch residues (Thr83 and Tyr102) reorient towards the site of phosphorylation, which dramatically enhances the interaction between protomers. To determine if these six residues are conserved in ChxR, the primary sequence of $ChxR_{Rec}$ from *C. trachomatis* L2/434/Bu was aligned with an atypical (HP1043) and three well characterized phospho-accepting (PhoB, OmpR, and YycF) subfamily members using the multiple sequence alignment program ClustalW (Fig. 3.1)(Larkin, Blackshields et al. 2007). Only one (Tyr90) of the six highly conserved residues important for activation in phosphorylation-dependent homologs is retained in ChxR. This suggests that the six conserved residues found in other OmpR/PhoB subfamily members may not contribute to the function of ChxR in *Chlamydia*.

FIG. 3.1. Primary sequence alignment of ChxR and other OmpR/PhoB subfamily members. The primary sequence of $ChxR_{Rec}$ was aligned with an atypical OmpR/PhoB subfamily member (HP1043) and three well-characterized phosphorylation-dependent OmpR/PhoB subfamily members (YycF, OmpR, and PhoB). The secondary structure elements correspond to PhoB (PDB ID: 1ZES). The catalytic and conformational switch residues important for activation are highlighted in blue and orange, respectively. The percent sequence identity and similarity for $ChxR_{Rec}$ with each homolog is listed. The proteins used for the primary sequence alignment are ChxR from *C. trachomatis* (UniProt: B0B8K5), HP1043 from *H. pylori* (PDB ID: 2PLN), YycF from *B. subtilis* (PDB ID: 3F6P), OmpR from *E. coli* (GenBank: CAQ33726.1), and PhoB from *E. coli* (PDB ID: 1ZES).

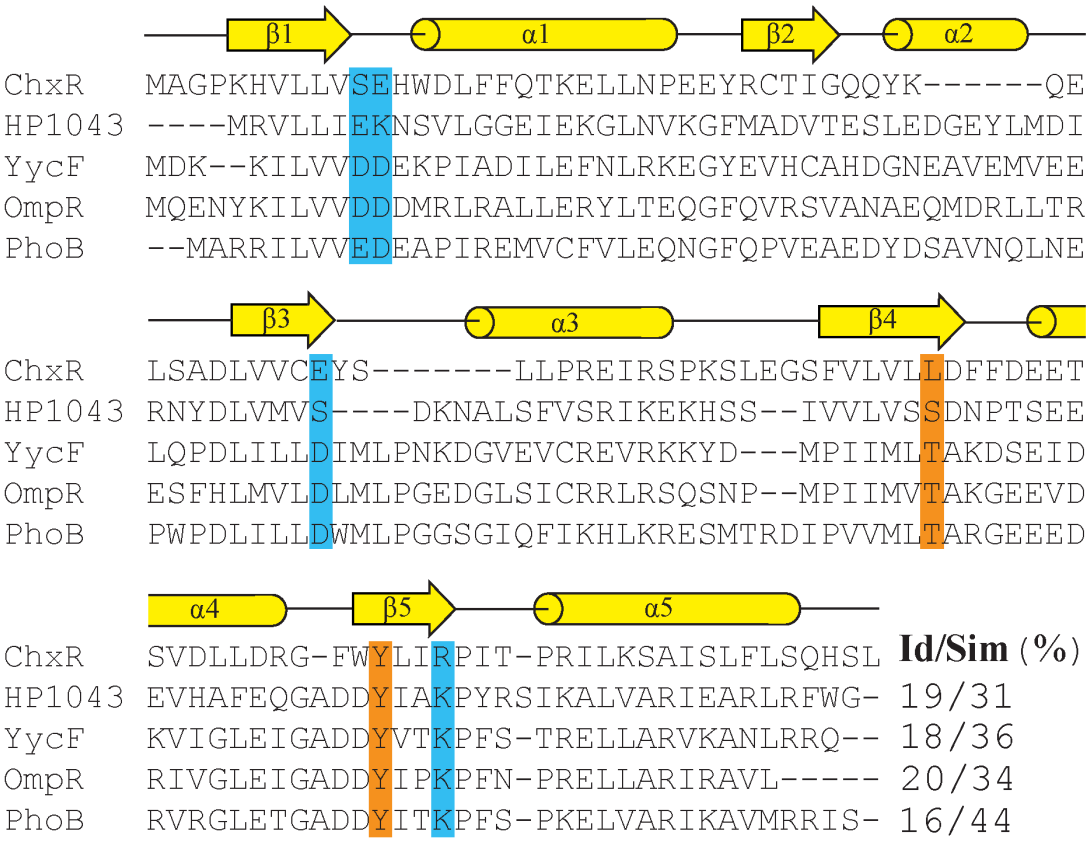
β1 α1 β2 α2
ChxR MAGPKHVLLVSEHWDLFFQTKELLNPEEYRCTIGQQYK------QE
HP1043 ----MRVLLIEKNSVLGGEIEKGLNVKGFMADVTESLEDGEYLMDI
YycF MDK--KILVVDDEKPIADILEFNLRKEGYEVHCAHDGNEAVEMVEE
OmpR MQENYKILVVDDDMRLRALLERYLTEQGFQVRSVANAEQMDRLLTR
PhoB --MARRILVVEDEAPIREMVCFVLEQNGFQPVEAEDYDSAVNQLNE
β3 α3 β4
ChxR LSADLVVCEYS-------LLPREIRSPKSLEGSFVLVLLDFFDEET
HP1043 RNYDLVMVS----DKNALSFVSRIKEKHSS--IVVLVSSDNPTSEE
YycF LQPDLILLDIMLPNKDGVEVCREVRKKYD---MPIIMLTAKDSEID
OmpR ESFHLMVLDLMLPGEDGLSICRRLRSQSNP--MPIIMVTAKGEEVD
PhoB PWPDLILLDWMLPGGSGIQFIKHLKRESMTRDIPVVMLTARGEEED
α4 β5 α5
ChxR SVDLLDRG-FWYLIRPIT-PRILKSAISLFLSQHSL Id/Sim (%)
HP1043 EVHAFEQGADDYIAKPYRSIKALVARIEARLRFWG- 19/31
YycF KVIGLEIGADDYVTKPFS-TRELLARVKANLRRQ-- 18/36
OmpR RIVGLEIGADDYIPKPFN-PRELLARIRAVL----- 20/34
PhoB RVRGLETGADDYITKPFS-PKELVARIKAVMRRIS- 16/44

Another observation from this comparison was that 13 residues are absent in ChxR in two regions corresponding to α2 and part of α3 in other OmpR/PhoB subfamily members (Fig. 3.1). Additionally, a primary sequence comparison using $ChxR_{Rec}$ from other serovars of *C. trachomatis* (A and D) and another species of *Chlamydia* (*C. pneumoniae*) with the OmpR/PhoB subfamily members listed above gave similar results (data not shown). The absence of these 13 residues in ChxR may have a large impact on number and length of secondary structure elements in $ChxR_{Rec}$. Interestingly, a previous sequence alignment with HP1043 and typical OmpR/PhoB subfamily members indicated a 4-residue deletion in the β3-α3 loop, which was supported by the structure of HP1043 (Hong, Lee et al. 2007). This finding provides further support for the conclusion that the secondary structure of ChxR may be unique within the OmpR/PhoB subfamily.

Secondary Structure Analysis.

The absence of the 13 residues in ChxR relative to other OmpR/PhoB subfamily members could affect the number and length of secondary structure elements in $ChxR_{Rec}$. Therefore CD was employed to determine the relative secondary structure content of $ChxR_{Rec}$ (Fig. 3.2). The receiver domain of YycF, an OmpR/PhoB homolog from *Bacillus subtilis*, was used as a reference protein for the analysis since its structure has been determined and is very similar to the 5 α/β-fold topology of the OmpR/PhoB subfamily (Zhao, Heroux et al. 2009). YycF is also one of the closest homologs of ChxR based upon primary sequence homology (Fig. 1). The CD analysis using the CDDN software indicated that a majority (37.6%) of $ChxR_{Rec}$ is

FIG. 3.2. Comparative CD spectra of $ChxR_{Rec}$ and a closely related response regulator (YycF). An estimation of the secondary structure elements was determined from a CD analysis of $ChxR_{Rec}$ (solid line). The receiver domain of YycF ($YycF_{Rec}$), one of the closest homologs of $ChxR_{Rec}$ based upon primary sequence comparison, was used as a reference protein (dotted line).

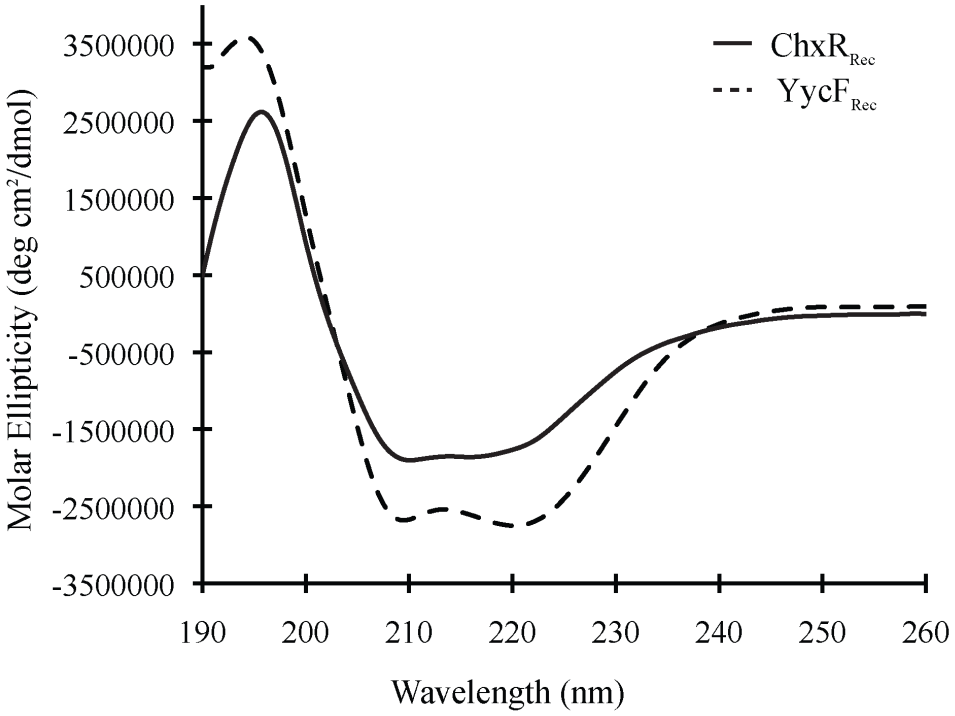
3500000
2500000
1500000
500000
-500000
-1500000
-2500000
-3500000
Molar Ellipticity (deg cm²/dmol)
190
200
210
220
230
240
250
260
Wavelength (nm)
ChxR Rec
YycF Rec

random coil and that 26.4%, 23.0%, and 18.2% of the protein is α-helical, β-sheet, and β-turn, respectively. In contrast, CD analysis of YycF indicated that the protein is 32.1% random coil, 32.5% α-helical, 16.9% β-sheet, and 16.6% β-turn. Comparing the relative estimated percentages of the secondary structures in the two proteins indicates that the α-helical content of $ChxR_{Rec}$ is reduced relative to YycF.

$ChxR_{Rec}$ is a stable homodimer.

The physiological concentrations of some members of the OmpR/PhoB subfamily have been reported to be ~1-15 μM (Cai and Inouye 2002; Lejona, Castelli et al. 2004). While we do not know the physiological concentration of ChxR in *Chlamydia*, our prior studies with full-length ChxR indicated that it is a stable homodimer at 1 μM (Hickey, Weldon et al. 2011 (Chapter 2)). Since dimerization occurs through the receiver domain, we determined the oligomeric state of the ChxR receiver domain at a relatively high concentration (100 μM) and at two concentrations (10 μM and 1 μM) within the reported physiological concentrations of OmpR/PhoB subfamily members (Fig. 3.3). The calculated molecular weight of a monomer of $ChxR_{Rec}$ is 13.8 kDa. $ChxR_{Rec}$ eluted from the analytical size exclusion column as a single population with an approximate molecular weight of 21 kDa, independent of concentration, corresponding to a compact homodimer. These results indicate that $ChxR_{Rec}$ is a stable homodimer, even at the physiological concentrations of other members of the OmpR/PhoB subfamily.

FIG. 3.3. Influence of protein concentration on the stability of $ChxR_{Rec}$. To determine the oligomeric state of the receiver domain of ChxR, recombinant $ChxR_{Rec}$ was subjected to analytical size exclusion chromatography at 100 μM, 10 μM, and 1 μM. The calculated molecular weight of monomeric and dimeric ChxR is 13.8 kDa and 27.6 kDa, respectively. Chicken ovalbumin (44 kDa), horse myoglobin (17 kDa), and vitamin B12 (1.35kDa) were used to generate the standard curve.

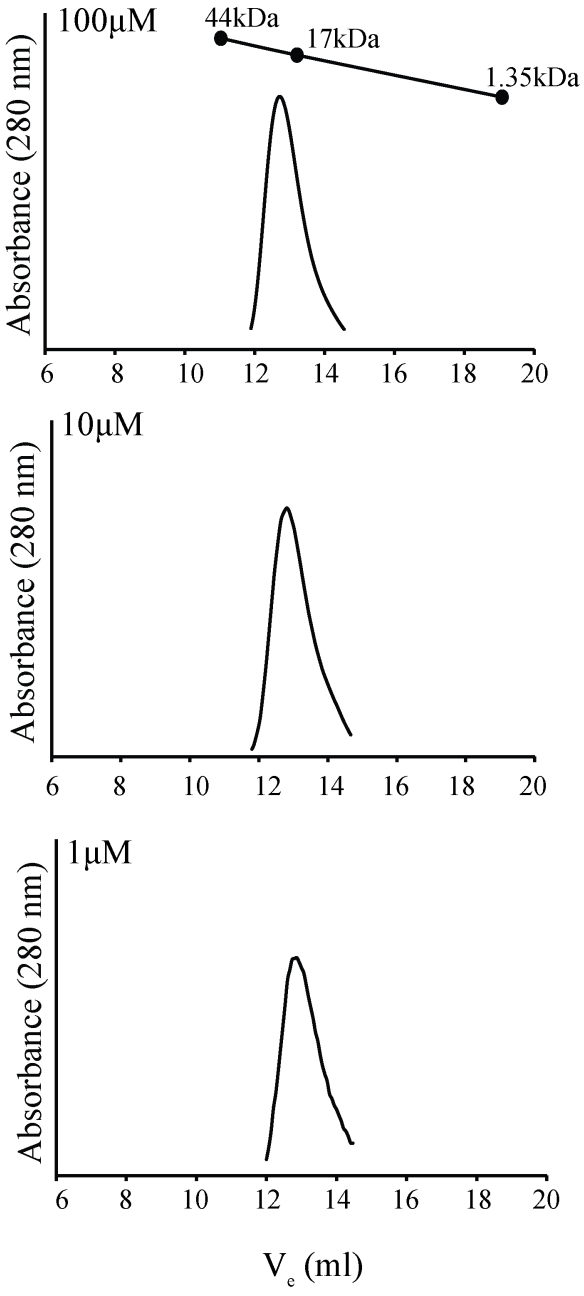
100µM
44kDa
17kDa
1.35kDa
Absorbance (280 nm)
6
8
10
12
14
16
18
20
10µM
Absorbance (280 nm)
1µM
Absorbance (280 nm)
V_e (ml)

$ChxR_{Rec}$ structure.

Structural studies were performed with $ChxR_{Rec}$ to elucidate the residues and structural elements that contribute to the protein's constitutive activity. Crystallization screening with recombinant $ChxR_{Rec}$ and commercially available sparse matrix screens resulted in multiple crystal forms from which two high-resolution data sets were obtained (Table 3.1). The space groups of these two crystals were monoclinic *C*2 and tetragonal $I4_1$. Molecular replacement with the current collection of known receiver domain structures of OmpR/PhoB subfamily members was unsuccessful. Therefore, the structure of $ChxR_{Rec}$ was solved using SIRAS phasing with the recently developed compound 5-Amino-2,4,6-triiodoisophthalic acid (I3C). I3C has proven to be a remarkable compound for phasing because it gives a strong anomalous signal using in-house X-ray instrumentation (Cu-Kα) from its three iodine atoms, and its carboxylic acid and amino groups facilitate hydrogen bonding with a protein (Beck, Krasauskas et al. 2008; Sippel, Robbins et al. 2008). Protein crystals were soaked in the crystallant supplemented with I3C. Using the I3C for initial phasing, the final $ChxR_{Rec}$ models of the two crystal forms were refined using data to 2.15Å and 1.6Å resolution for the $I4_1$ and *C*2 crystal forms, respectively.

The molecular topology of the two $ChxR_{Rec}$ models is β1-α1-β2-β3-β4-α2-β5-α3 with two large random coils between β2-β3 and β3-β4 (Fig. 3.4). The r.m.s. deviations between the C_α of the two models was 0.95Å, indicating a high degree of structural similarity. The asymmetric unit of both crystal lattices consisted of two $ChxR_{Rec}$ monomers, which formed a dimer with a similar interface (α2-β5-α3). The dimer interface surface area of each protomer is approximately 1095 $Å^2$.

Table 3.1

Data Collection and Refinement Statistics

	Apo	SIRAS (I3C)	Apo
Data Collection			
Unit-cell parameters (Å, °)	a = 149.9 b =41.3 c = 45.2, α = γ = 90 β = 105.5	a = 149.8 b = 41.1 c = 45.1, α = γ = 90 β = 106.1	a = 53.7 b = 53.7 c = 190.1, α = β = γ =90
Space group	$C2$	$C2$	$I4_1$
Resolution (Å)[1]	23.66-1.6 (1.66-1.6)	30.0-2.1 (2.18-2.1)	30.0-2.15 (2.27-2.15)
Wavelength (Å)	1.0	1.54	1.54
Observed reflections	128193	52247	54653
Unique reflections	35320	15613	14580
$\langle I/\sigma I \rangle$[1]	13.5 (3.1)	13.1 (2.9)	9.5 (2.7)
Completeness (%)[1]	99.8 (100)	98.8 (96.2)	99.9 (100)
Redundancy[1]	3.63 (3.63)	3.3 (3.2)	3.7 (3.7)
R_{merge} (%)[1, 2]	3.9 (29.6)	12.2 (46.7)	8.1 (45.6)
Refinement			
Resolution (Å)	23.66-1.60	28.14-2.09	29.67-2.15
R_{factor} / R_{free} (%)[3]	18.83/21.02	19.60/25.51	20.50/24.69
No. of atoms (protein / water)	1802/108	1700/77	1631/41
Model Quality			
R.m.s deviations			
Bond lengths (Å)	0.015	0.018	0.008
Bond angles (°)	1.513	1.698	1.079
Average B factor (Å^2)			
Protein	29.5	37.6	40.1
Water	30.9	35.6	39.4
I3C	-	43.4	-
Coordinate error based on Maximum Likelihood (Å)	0.21	0.30	0.25
Ramachandran Plot			
Favored (%)	99.5	99.5	99.5
Allowed (%)	0.5	0.0	0.5
Disallowed (%)	0.0	0.5	0.0
PDB ID	3Q7R	3Q7S	3Q7T

[1] Values in parenthesis are for the highest resolution shell.

[2] $R_{merge} = \Sigma_{hkl}\Sigma_i |I_i(hkl) - \langle I(hkl)\rangle| / \Sigma_{hkl}\Sigma_i I_i(hkl)$, where $I_i(hkl)$ is the intensity measured for the ith reflection and $\langle I(hkl)\rangle$ is the average intensity of all reflections with indices hkl.

[3] $R_{factor} = \Sigma_{hkl} ||F_{obs}(hkl)| - |F_{calc}(hkl)|| / \Sigma_{hkl} |F_{obs}(hkl)|$; Rfree is calculated in an identical manner using 5% of randomly selected reflections that were not included in the refinement

FIG. 3.4. Stereoviews of ribbon diagrams of $ChxR_{Rec}$. $ChxR_{Rec}$ crystallized in two distinct crystal forms. High-resolution data sets from each crystal form were refined to 2.15Å ($I4_1$ space group) and 1.6Å (*C*2 space group). The asymmetric unit of both crystals contained a dimer. A) The two monomers from the *C*2 data set are shown in yellow and blue, respectively. The molecular topology of each monomer is β1-α1-β2-β3-β4-α2-β5-α3. The dimer interface is comprised of the α2-β5-α3 region within each monomer. B) A side view of the two molecules from the *C*2 data set.

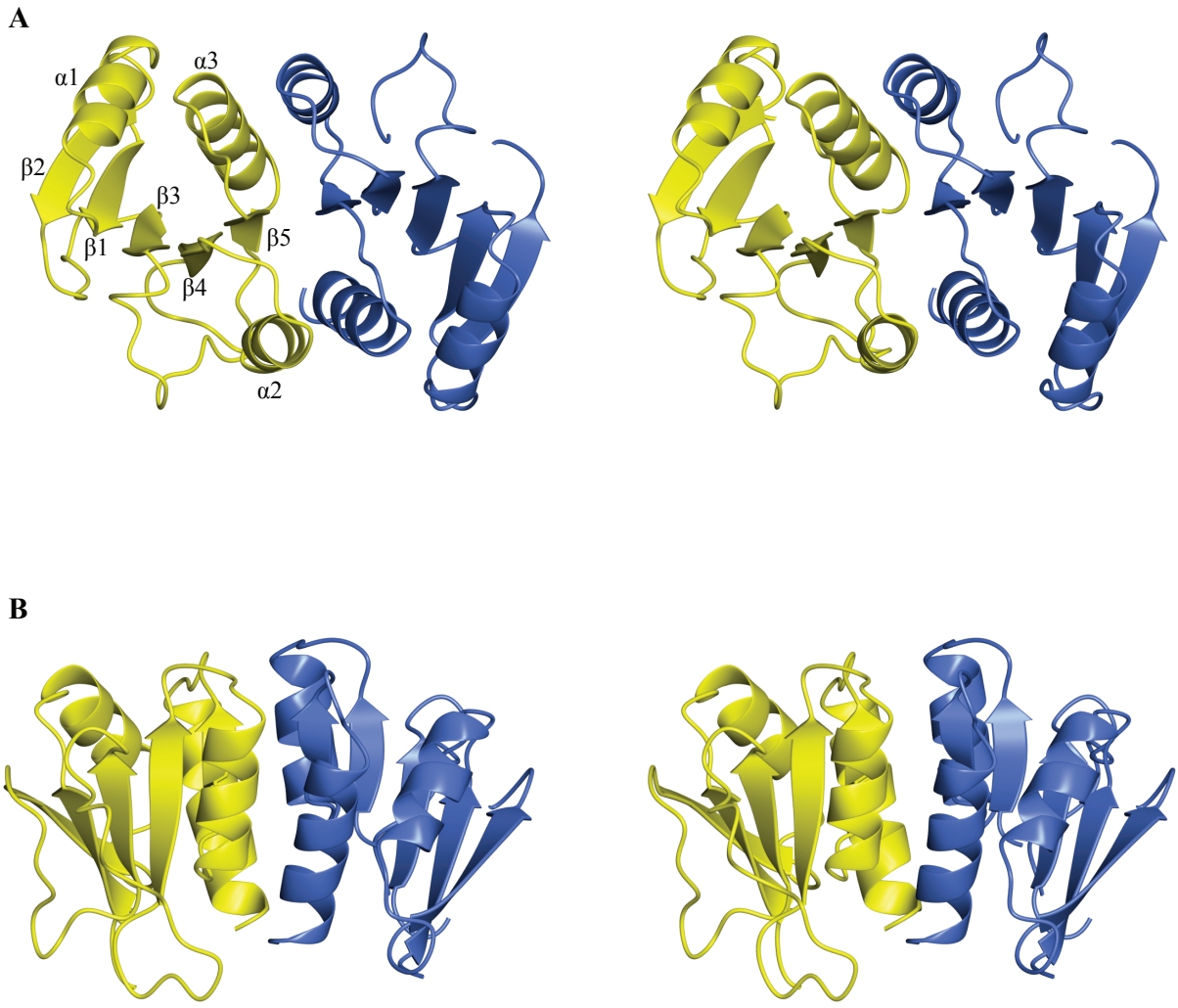
A
α1
α3
β2
β3
β1
β5
β4
α2
B

Structural comparison of $ChxR_{Rec}$ with other OmpR/PhoB subfamily members.

The structure of $ChxR_{Rec}$ is distinct from other subfamily members. Based on primary sequence, one of the closest homologs to $ChxR_{Rec}$ with a known structure is YycF (Fig. 3.1). A superimposition of the receiver domains of ChxR and YycF indicated that the r.m.s. deviations between the C_α of 94 residues in each structure was 2.05Å (Fig. 3.5A). Despite the overall structural conservation, the α2 and α3 of YycF correspond to random coils in $ChxR_{Rec}$ (Fig. 3.5B). The absence of these helices in the $ChxR_{Rec}$ structure may suggest that these two regions are random coils in endogenous ChxR.

In addition to the distinct molecular topology of $ChxR_{Rec}$, the structure also revealed that the architecture and residue composition of canonical site of phosphorylation is unique. As mentioned previously (Fig. 3.1), none of the residues that coordinate the divalent cation and phosphoryl group in phospho-accepting homologs are retained in ChxR. In $ChxR_{Rec}$, Glu49 and Arg93 replace the phospho-accepting Asp and coordinating Lys, respectively (Fig. 3.5C). Interestingly, Arg93 forms a salt bridge with Glu49, therefore these residues mimic the positions of the Asp and Lys in phosphorylated OmpR/PhoB homologs. This interaction could be important in maintaining ChxR in a constitutively active state.

The rotomeric state of the two conformational switch residues reflects the activation state of OmpR/PhoB response regulators (Gao and Stock 2009). In unphosphorylated OmpR/PhoB subfamily members, the Ser/Thr in β4 and the Phe/Tyr in β5 are oriented away from the site of phosphorylation (Bachhawat and Stock 2007). Phosphorylation induces a conformational change of these two conserved residues to reorient them towards the site of phosphorylation, which results in minor structural reorientations that dramatically enhance dimerization.

FIG. 3.5. Comparison of $ChxR_{Rec}$ structural features to other OmpR/PhoB subfamily members. A) A stereoview of the structure of $ChxR_{Rec}$ (yellow) superimposed on the receiver domain of the OmpR/PhoB subfamily member YycF (red) (PDB: 3F6P). Two α-helices that are present in YycF are absent in $ChxR_{Rec}$ (black circles). B) An electron density map (blue) of the two random coil regions (residues 35-43 and 53-64 (green)) contoured at 1σ. C) The conserved phospho-accepting Asp and coordinating Lys in other OmpR/PhoB subfamily members is a Glu (Glu49) and Arg (Arg93), respectively, in ChxR. Arg93 forms a salt bridge with Glu49 and Asp73. D) Two key conformational switch residues, typically a Ser/Thr and Phe/Tyr, reorient towards the site of phosphorylation following phosphoryl transfer from the cognate sensor kinase (blue; PhoP (PDB ID: 2PL1)). These two residues in an atypical OmpR/PhoB homolog (green; HP1043 (PDB ID: 2PLN)) have a similar orientation as an activated subfamily member. E) The conformational switch residues in $ChxR_{Rec}$ (red; Leu72 and Tyr90) are oriented similar to an inactive homolog (grey; PhoP (PDB ID: 2PKX)).

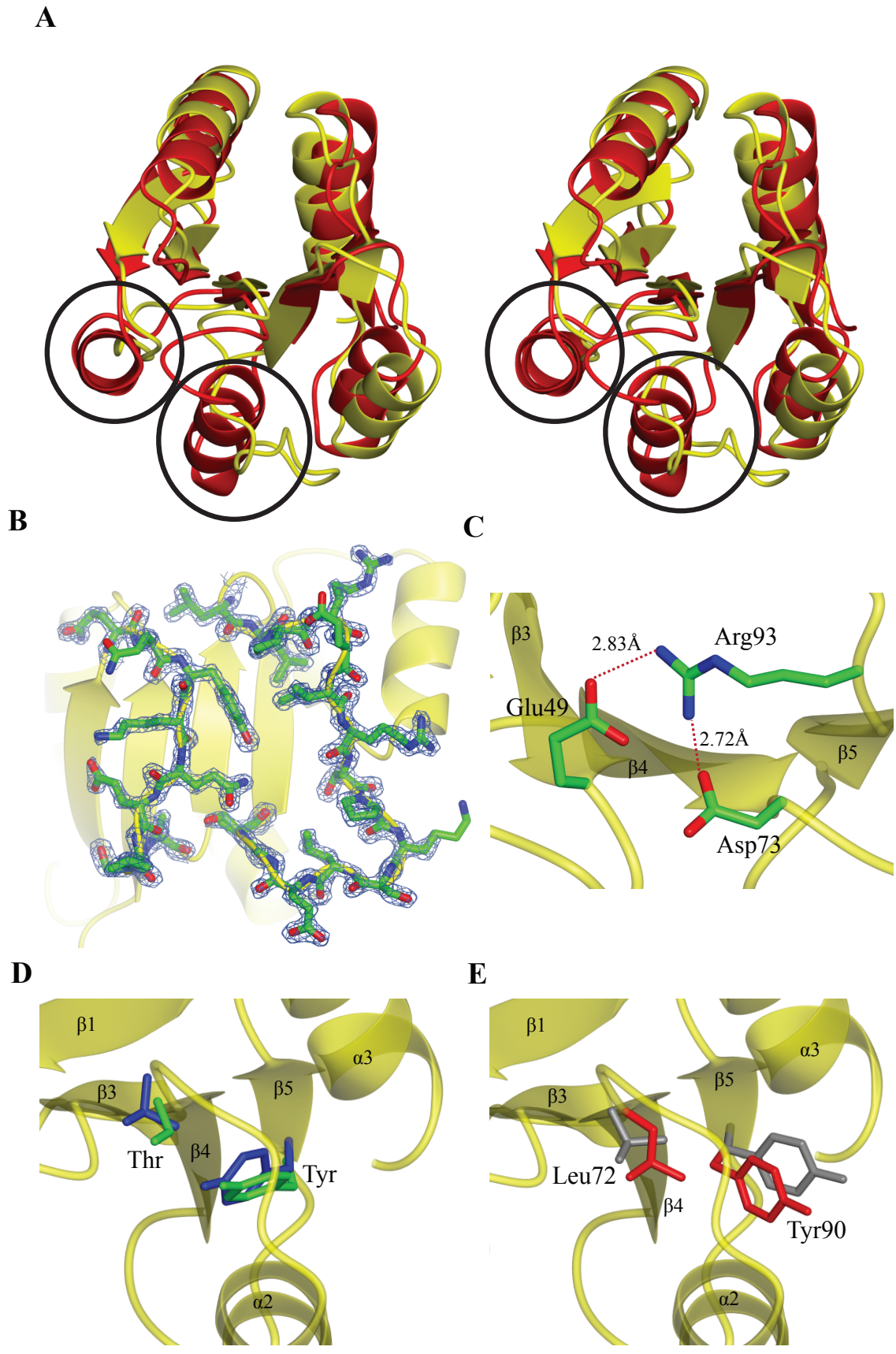
A
B
C
β3
2.83Å
Arg93
Glu49
2.72Å
β4
β5
Asp73
D
E
β1
α3
β3
β5
Thr
β4
Tyr
α2
β1
α3
β3
β5
Leu72
β4
Tyr90
α2

As indicated in Fig. 3.1, Leu72 and Tyr90 in ChxR correspond to the two conformation switch residues in other subfamily members. Because recombinant $ChxR_{Rec}$ was shown to exist as a stable homodimer (Fig. 3.3), we hypothesized that the orientation of Leu72 and Tyr90 would be in a similar conformation to that of an activated homolog (i.e. towards the site of phosphorylation) (Fig. 3.5D). In fact, the ChxR receiver domain structure revealed the exact opposite. These two residues had similar orientations to those in inactive subfamily members (Fig. 3.5E). This suggests that these two residues possibly contribute to the oligomeric state of ChxR in a different fashion than they do in other subfamily members.

$ChxR_{Rec}$ Dimer Interface.

The structure of $ChxR_{Rec}$ revealed that hydrophobic and ionic interactions appear to be the primary forces of interaction between $ChxR_{Rec}$ monomers. Based on a sequence alignment of residues comprising the dimer interface of ChxR, HP1043, and PhoB (Fig. 3.6A), two out of the three hydrophobic residues in PhoB (Val91, Leu94, and Ala112) are retained in ChxR (Val81 and Leu84). Additionally, four of the residues involved in hydrophobic interaction in an HP1043 dimer are retained in ChxR (Val81, Leu84, Iso99, and Leu106). The structure of $ChxR_{Rec}$ also revealed that Phe75 and Trp89 contribute to the hydrophobic core of the interface (Fig. 3.6B).

In contrast to the relative conservation of hydrophobic residues between ChxR and other subfamily members, the locations of the residues involved in ionic interactions between the two ChxR receiver domains are distinct from the subfamily. The residues involved in these ionic interactions in other subfamily members are positioned within the interior and periphery of the dimer interface (Fig. 3.6C). However, the structure of $ChxR_{Rec}$ revealed only two salt bridges, which occur through Glu78 and Arg98 of each monomer. These residues are located within the

FIG. 3.6. Comparison of the hydrophobic and charged residues at the dimer interface of OmpR/PhoB subfamily members. A) Sequence alignment of the residues comprising the dimer interface of ChxR, HP1043 (atypical; PDB ID: 2PLN), and PhoB (typical; PDB ID: 1ZES). The secondary structures of $ChxR_{Rec}$ and PhoB are indicated above and below the alignment, respectively. Blue and orange highlights represent residues involved in hydrophobic and ionic interactions, respectively. B) Hydrophobic interaction between $ChxR_{Rec}$ protomers occurs through Phe75, Val81, Leu84, Trp89, Ile99, and Leu106 in each monomer, while ionic interactions occur through Glu78 and Arg98, and potentially through Asp85 and Lys101 between each monomer. C) The electrostatic potential surface of the dimer interface of ChxR, HP1043, and PhoB.

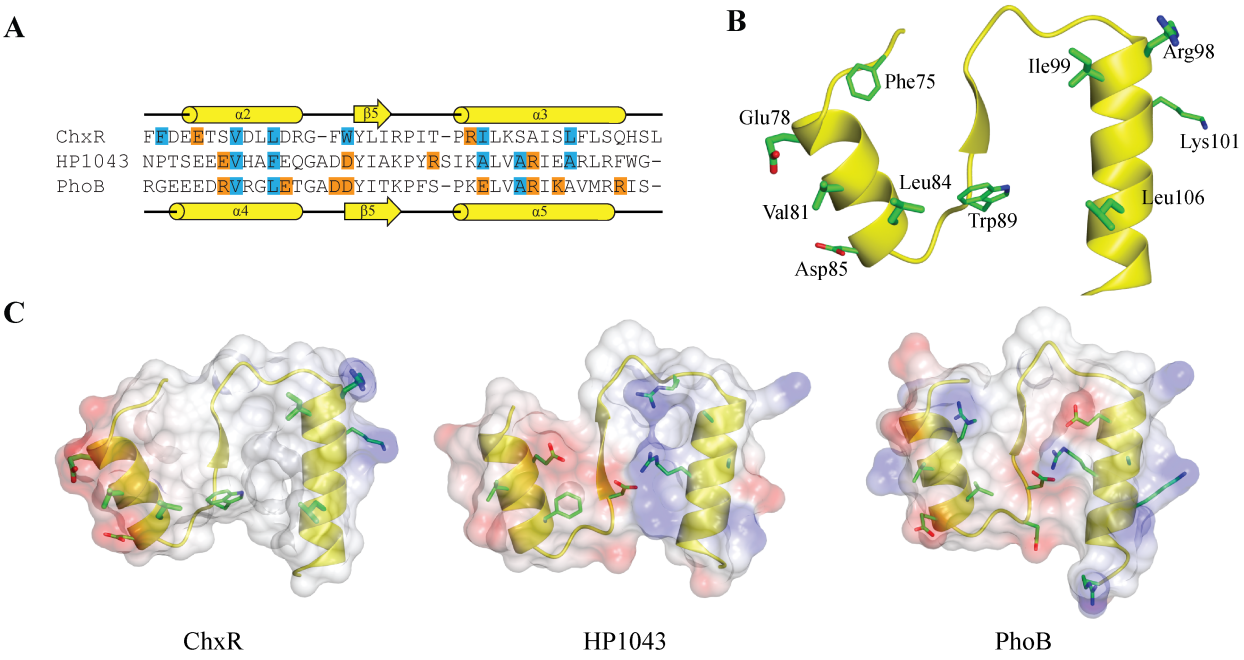
A
α2
β5
α3
ChxR FFDEETSVDLLDRG-FWYLIRPIT-PRTLKSAISLFLSQHSL
HP1043 NPTSEEEEVHAFEQGADDYIAKPYRSIKALVARIEARLRFWG-
PhoB RGEEEDRVRGLETGADDYITKPFS-PKELVARIKAVMRRIS-
α4
β5
α5
B
Phe75
Glu78
Ile99
Arg98
Lys101
Leu84
Val81
Trp89
Leu106
Asp85
C
ChxR
HP1043
PhoB

α2 and α3, respectively (Fig 3.6B). The $ChxR_{Rec}$ structure also suggested a potential second intermolecular salt bridge between Lys101 and Asp85 (Fig. 3.6B). These two residues are ~5Å apart in the crystal structure. While the distance between the two residues is slightly outside the limit of a salt bridge (4Å) (Jelesarov and Karshikoff 2008), the position of these two residues could be closer in solution. Unlike homologous structures, no salt bridges appeared to be located within the interior of the interface in $ChxR_{Rec}$, suggesting that hydrophobic interactions are the primary source of dimer stability in $ChxR_{Rec}$.

A comparison of the surface area and the residue composition of the dimer interface from many members of the OmpR/PhoB subfamily support that the dimer interface of ChxR is unique within the subfamily. As Table 3.2 indicates, the interface surface area of activated or inactivated phosphorylation-dependent OmpR/PhoB response regulators generally ranges from 1090-807 $Å^2$. Furthermore, the residues that comprise their intermolecular interface are 27-39% non-polar, 8-32% polar, and 36-56% charged. Despite the activity of HP1043 in the absence of phosphorylation, the dimer interface surface area and the residue composition of the protein are similar to typical OmpR/PhoB response regulators. In contrast, the intermolecular surface area of ChxR (1095$Å^2$) and the percentage of non-polar (52%), polar (26%), and charged residues (22%). The relatively large surface area and percentage of hydrophobic residues within the interface of ChxR provide further support that intermolecular interactions between ChxR monomers are distinct from both typical and atypical OmpR/PhoB response regulators.

Table 3.2 Surface area and residue composition of the OmpR/PhoB dimer interface

Protein	PDB ID	Interface Surface Area (Å^2) [1]	Interface Residues (%)[1]		
			Non-Polar	Polar	Charged
ChxR	3Q7R	1095	52	26	22
YycF	3F6P	1087	36	11	53
PhoP (BeF_3-activated)	2PL1	1027	32	32	36
TorR	1ZGZ	981	28	24	48
DrrD	3NNN	978	39	13	48
PhoB (BeF_3-activated)	1ZES	977	36	08	56
PhoP (Inactive)	2PKX	936	35	26	39
ArcA (BeF_3-activated)	1XHF	887	27	23	50
ArcA (Inactive)	1XHE	876	30	22	48
HP1043	2PLN	837	38	17	45
DrrB	3NNS	802	38	19	43

[1] The dimer interface surface area and residue composition were calculated using *PROTORP* (Reynolds, Damerell et al. 2009)

cc

FIG. 3.7. Dimerization analysis of the W89E substitution. Analytical size exclusion chromatography was utilized to determine the oligomeric state of the W89E substitution. A) The calculated molecular weight of a $ChxR_{FL}$ monomer or dimer is 25.8 kDa or 51.6 kDa, respectively. Wild-type $ChxR_{FL}$ (solid line) eluted from a size exclusion column as a dimer with an approximate molecular weight of 45 kDa, while $ChxR_{FL}^{W89E}$ (dashed line) eluted from the column as a compact monomer with an approximate molecular weight of 16 kDa. B) The calculated molecular weight of a $ChxR_{Rec}$ monomer or dimer is 13.8 kDa or 27.6 kDa, respectively. Wild-type $ChxR_{Rec}$ (solid line) eluted from a size exclusion column as a dimer with an approximate molecular weight of 21 kDa, while $ChxR_{Rec}^{W89E}$ (dashed line) eluted from the column as a compact monomer with an approximate molecular weight of 9.8 kDa.

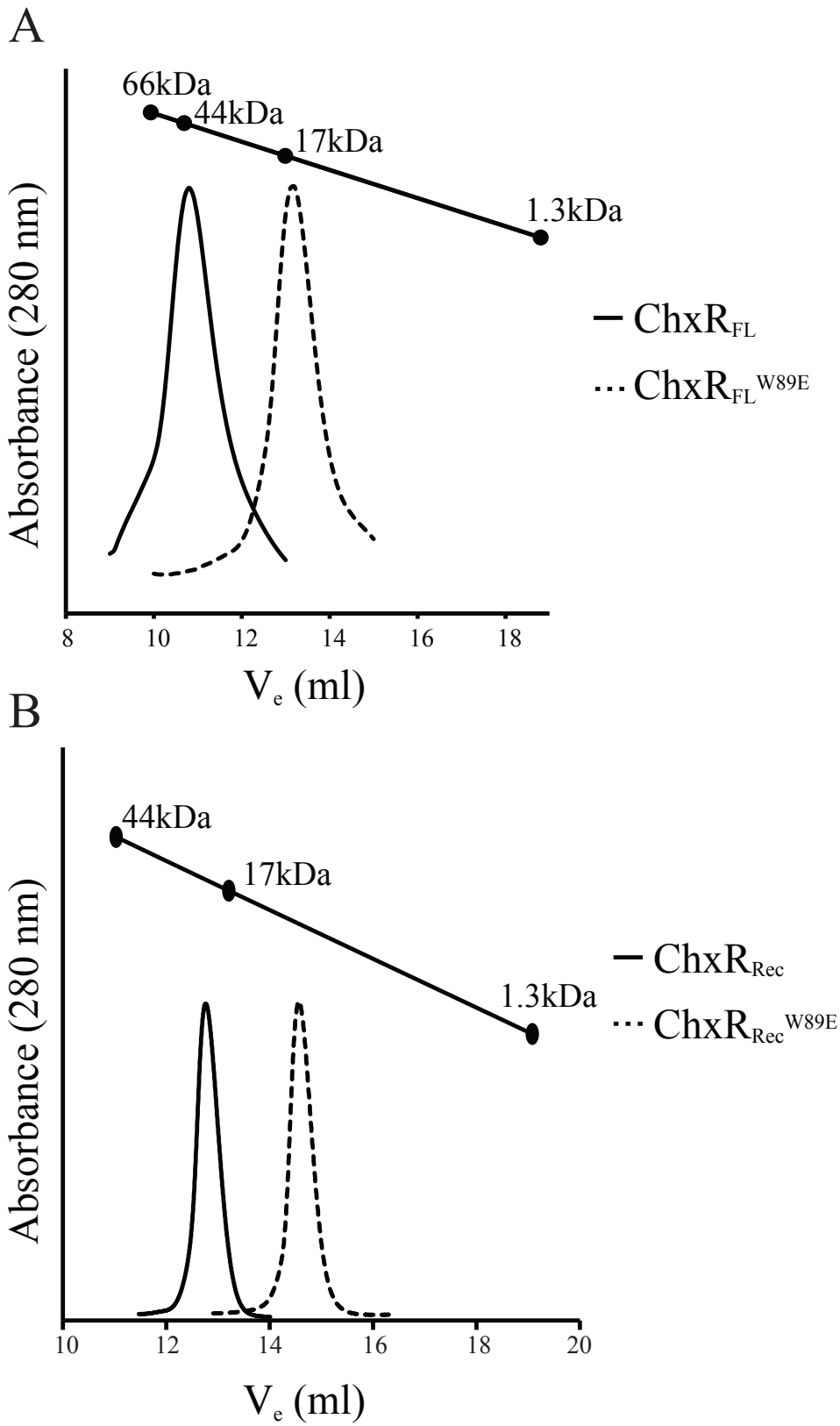
A
66kDa
44kDa
17kDa
1.3kDa
Absorbance (280 nm)
8
10
12
14
16
18
Ve (ml)
ChxRFL
ChxRFL W89E
B
44kDa
17kDa
1.3kDa
Absorbance (280 nm)
10
12
14
16
18
20
Ve (ml)
ChxRRec
ChxRRec W89E

(Chen, Birck et al. 2003). We therefore hypothesized that the monomeric $ChxR_{FL}$ protein (W89E) would have a reduced affinity for its target DNA. To test this hypothesis, electrophoretic mobility shift assays (EMSAs) were performed with W89E and the previously reported high-affinity binding site (DR2) in the *chxR* promoter (Fig. 3.8)(Hickey, Weldon et al. 2011 (Chapter 2)). Although the other substitutions (W89A, E49A, D73A, E49A/D73A, E78A, K101A, and E78A/K101A) did not affect dimer stability, their ability to interact with DNA was also quantified to determine if they influence overall protein conformation and/or an interaction between the receiver and effector domain. The assays were performed at a protein concentration of 44 nM, which is the approximate dissociation constant for this binding site and would thus permit maximal variation in the amount of DNA bound with the substitutions (Hickey, Weldon et al. 2011 (Chapter 2)). The effector domain of ChxR ($ChxR_{Eff}$) was included in the assay as a control for DNA interaction in the absence of the receiver domain.

As evident in Fig. 3.8, disrupting the hydrophobic interaction within the dimer interface had a significant impact on ChxR-DNA interaction. The amount of DNA shifted by the dimer mutants W89A, E49A, D73A, and E49A/D73A was found to not be statistically significant from wild-type ChxR. Similarly, the substitutions of potential residues involved in salt bridging between monomers (dimer mutants E78A, K101A, E78A/K101A) did not significantly effect DNA interaction. Interestingly, the W89E substitution, which was determined to exist as a monomer in solution (Fig. 3.7), had the lowest affinity (3%) for DNA, relative to wild-type $ChxR_{FL}$ from $ChxR_{Eff}$. The dramatic reduction in DNA affinity with the W89E substitution suggests that dimerization through the receiver domain is critical for stable ChxR-DNA interaction, albeit within the given *in vitro* experimental conditions.

FIG. 3.8. DNA binding analysis of canonical phosphoryl-coordinating and dimer interface residue substitutions in ChxR. To determine the effect of the substitutions on the proteins ability to bind DNA, EMSAs were performed with 1 nM of the high-affinity DR2 site from the *chxR* promoter and 44 nM of each protein. The percent of DNA shifted was calculated for each substitution relative to wild-type $ChxR_{FL}$. Substitutions that had a significant ($P < 0.001$) effect on DNA interaction are denoted by an asterisk (***). Error bars represent the standard deviation from triplicate experiments.

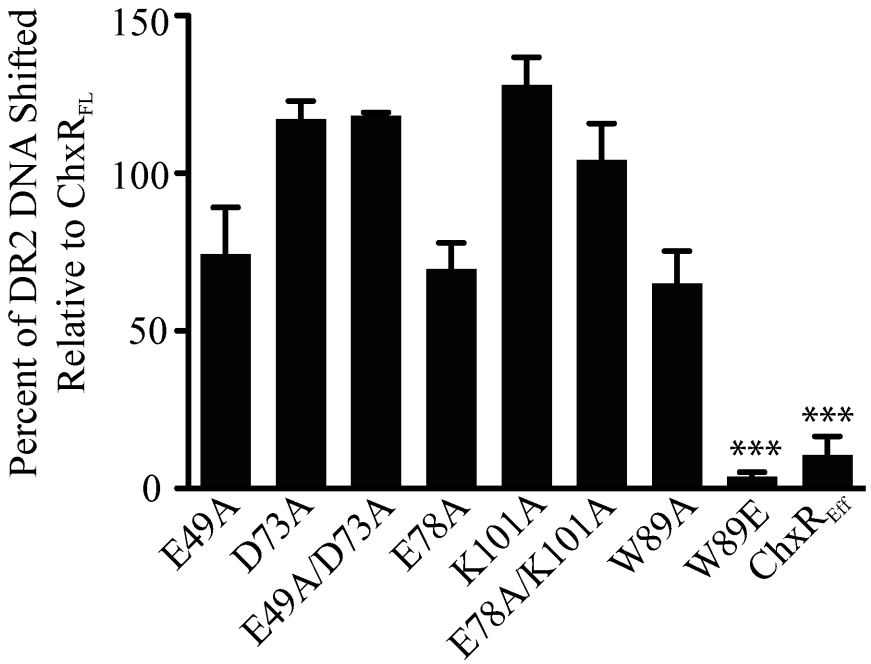
Percent of DR2 DNA Shifted Relative to ChxR$_{FL}$
150
100
50
0
***
***
E49A
D73A
E49A/D73A
E78A
K101A
E78A/K101A
W89A
W89E
ChxR$_{Eff}$

Chapter III

Discussion

The propagation of a activation signal from the site of phosphorylation to the dimer interface of response regulators is becoming better understood through numerous structural and functional studies (Appleby and Bourret 1998; Toro-Roman, Mack et al. 2005; Bachhawat and Stock 2007). The residues involved in this process have been identified and are highly conserved. However, atypical response regulators diverge from this canonical activation mechanism. These proteins do not retain all of the residues critical to this process, particularly those residues comprising the canonical site of phosphorylation, but do generally retain overall structural topology and a propensity to form homodimers. The structure of the receiver domain of ChxR revealed that this atypical transcriptional regulator does not share many of the conserved structural characteristics of either the phosphorylation-dependent and -independent OmpR/PhoB response regulators. Structural studies of the receiver domain of ChxR revealed numerous contrasting features to both the typical and atypical OmpR/PhoB response regulators including: the absence of two helices (α2/α3), the unique architecture and composition of the canonical site of phosphorylation, the inactive orientation of the conformational switch residues, and the relatively large number of hydrophobic residues at the dimer interface. Because of these unique features, the receiver domain of ChxR exists as a very stable homodimer, which is essential for DNA interaction.

The structure of $ChxR_{Rec}$ supported our hypothesis that the intra- and intermolecular interactions in ChxR are distinct from its phosphorylation-dependent homologs. The $ChxR_{Rec}$ structure revealed that the canonical site of phosphorylation is comprised of three resides (Glu49, Asp73, and Arg93; Fig. 3.5C). When Glu49 was substituted to an Ala, the protein was still able

to form a homodimer and the amount of DNA electrophoretically shifted with this substitution was not statistically significant from that of wild-type ChxR (Fig. 3.8). Similar to the Glu49 substitution, the Asp73 and Glu49/Asp73 substitutions resulted in proteins that formed homodimers and interacted with DNA in a manner similar to wild-type ChxR. These results were expected since the two conformational switch residues in ChxR are oriented away from the canonical site of phosphorylation (Fig. 3.5E) and therefore, modifications to this region would likely not be transduced to the dimer interface. These results also indicate that the residues in ChxR in the same positions as the residues critical to the coordination of the phosphoryl group in other OmpR/PhoB subfamily members do not significantly influence overall protein stability, homodimerization, or interaction with DNA.

Receiver domains from phosphorylation-dependent OmpR/PhoB subfamily members primarily exist in a monomeric state in the absence of phosphorylation (Toro-Roman, Mack et al. 2005; Bachhawat and Stock 2007). Analytical size exclusion chromatography indicated that $ChxR_{Rec}$ is a dimer, even at a concentration (1 μM; Fig. 3.3) similar to the physiological concentration of other OmpR/PhoB subfamily members (Lejona, Castelli et al. 2004). This observation implies that ChxR receiver domains have a higher propensity to form dimers than typical OmpR/PhoB subfamily members. The structure of the receiver domain supports this observation since six residues appear to contribute to the hydrophobic interaction between protomers. This is twice the number of hydrophobic residues found in the dimer interface of homologs (Toro-Roman, Mack et al. 2005). Furthermore, the surface area of the ChxR dimer interface is larger than other OmpR/PhoB response regulators (Table 3.2), and is composed primarily of hydrophobic residues, which is distinct from other subfamily members. Additionally, the only substitution that rendered ChxR monomeric was to a residue (W89E)

within this hydrophobic region of the dimer interface (Fig. 3.7A & 3.7B). In combination, these results strongly support the conclusion that ChxR is a stable homodimer in solution and that this interaction is accomplished largely through hydrophobic interactions.

Dimerization through the receiver domain of ChxR is essential for stable interaction with DNA. ChxR was previously reported to interact with tandem repeat sequences but mutations to either recognition site greatly reduced ChxR-DNA interaction (Hickey, Weldon et al. 2011 (Chapter 2)). These results suggested that optimal ChxR-DNA interaction requires that ChxR bind to DNA as a homodimer. EMSAs with a dimer deficient ChxR support this observation since the amount of DNA shifted with the W89E substitution was reduced >95% compared to wild-type ChxR (Fig. 3.8). In support of this observation, the effector domain of ChxR alone binds to DNA with approximately 10-fold less affinity than full-length ChxR (Chapter 4). Currently, it is unknown whether the ChxR receiver domain is responsible for positioning the effector domain for optimal interaction with DNA through a direct interaction but these data strongly support that dimerization increases DNA affinity by binding cooperatively to adjacent binding sites.

Interestingly, the significant reduction in DNA-binding by monomeric ChxR is in stark contrast to other atypical OmpR/PhoB response regulators, which may be a result of the DNA sequences recognized by these proteins. NblR was reported to exist as a monomer *in vivo* and likely binds to DNA as a monomer (Ruiz, Salinas et al. 2008). A dimer deficient HP1043 protein was reported to bind to DNA with an apparent similar affinity as dimeric HP1043 (Hong, Lee et al. 2007). This suggests that dimerization of these atypical response regulators is not essential for DNA interaction. These differing DNA-binding characteristics between ChxR, HP1043, and NblR are likely a result of their affinity and specificity for DNA. While the DNA sequence

recognized by NblR is currently unknown, HP1043 was determined to bind to relatively conserved DNA sequence (Delany, Spohn et al. 2002). In contrast, the nucleotide frequency in the DNA sequence recognized by ChxR is relatively low (Hickey, Weldon et al. 2011 (Chapter 2)). This suggests that HP1043 forms dimers primarily to increase DNA specificity while ChxR forms dimers to increase both DNA affinity and specificity.

The molecular topology of $ChxR_{Rec}$ is very unique within the OmpR/PhoB subfamily. The 20 receiver domains of both phosphorylation-dependent and -independent OmpR/PhoB response regulators are very similar and are comprised of 5 α/β-folds (Kenney 2002; Bourret 2010). The structure of $ChxR_{Rec}$ is distinct from these 20 structures since the α2 and α3 helices found in homologous structures are random coils in $ChxR_{Rec}$ (Fig. 3.5A). The CD analysis supports that these two regions are random coils and that this is not due to crystal packing since the α-helical content of ChxR is reduced compared to other OmpR/PhoB subfamily members (Fig. 3.2). The purpose of these random coils is not directly apparent since this region in other OmpR/PhoB response regulators is not known to be directly involved in the function of the protein. These two helices, however, probably provide structural support for optimal conformations of the residues that coordinate the phosphoryl group. The presence of these two helices in $ChxR_{Rec}$ would not be necessary for orienting these residues, because the residues comprising the canonical site of phosphorylation of ChxR were found to not have a significant influence on dimerization or interaction with DNA.

Recent studies have begun to identify potential mechanisms that regulate atypical response regulators, which include ligand and protein-protein interaction based mechanisms. NarB, a nitrogen reductase from *Synechococcus elongatus* PCC 7942, has been shown to interact with NblR and possibly inhibit its transcriptional regulatory activity (Kato, Chibazakura et al.

2008). Additionally, a recent study reported that the DNA binding activity of an atypical response regulator, JadR1 from *Streptomyces venezuelae*, is severely reduced in the presence of a compound (Jadomycin B), which led the authors to speculate that small ligands might regulate the activity of many atypical response regulators (Wang, Tian et al. 2009). Our structural and functional studies argue that ChxR exists in a constitutively active state; however these alternative mechanisms of regulation in atypical response regulators provide the possibility that the function of ChxR is regulated post-translationally in *Chlamydia*.

Chapter IV

Introduction

Bacteria use two-component signal transduction systems as a primary means of responding to stimuli within their environment and adjusting gene expression accordingly (Hoch 2000). These systems regulate a wide variety of processes, including bacterial development, virulence and physiology (Stock, Robinson et al. 2000; Jones 2005). Two-component signal transduction systems are predominantly comprised of a membrane-bound histidine (sensor) kinase and an associated response regulator. Frequently, the sensor kinase undergoes an autophosphorylation event in response to environmental stimuli. The phosphate group is then transferred to a highly conserved site within a cognate response regulator. Phosphorylation of the response regulator controls the activity of the response regulator, which is frequently transcriptional regulation.

OmpR/PhoB is one of the largest subfamilies of response regulators (Baikalov, Schroder et al. 1996). The function of the OmpR/PhoB subfamily of response regulators appears to be controlled by interactions between the two domains: the receiver domain and the effector domain. The receiver domain typically becomes phosphorylated at a highly conserved site that promotes homodimerization through a conserved receiver-domain interface. As a result of the receiver domain becoming phosphorylated, the affinity of the effector domain for DNA becomes enhanced (Kenney 2002). It is the winged helix–turn–helix motif in the effector domain that largely defines the OmpR/PhoB subfamily of response regulators (Brennan 1993).

Despite a relatively conserved three-dimensional structure of the OmpR/PhoB effector domain, the residues involved in interaction with DNA vary due to the distinct DNA sequences recognized by these transcription factors (Martinez-Hackert and Stock 1997). Currently, 16

effector domain structures from members of the subfamily have been experimentally determined and all share a common tertiary structure. The typical OmpR/PhoB effector domain is comprised of an N-terminal β-sheet (β1-β4), a winged helix-turn-helix DNA-binding motif (α1-α2), and a C-terminal β-hairpin (β5-β6) (Kenney 2002). Residues in the α2 and α3 helices interact with the major groove of DNA, while residues in the wing (the loop region between β5-β6) interact with the adjacent minor groove of the DNA. The loop between α2-α3 is the site of interaction with the σ factor or the α-subunit of RNA polymerase.

Chlamydia is a medically important obligate intracellular bacterial pathogen that encodes an OmpR/PhoB-subfamily homolog termed ChxR. It has previously been demonstrated that ChxR is an atypical OmpR/PhoB response regulator that does not require phosphorylation for transcriptional activity (Koo, Walthers et al. 2006). Despite this fundamental difference from OmpR/PhoB response regulators, we hypothesize that the DNA-binding effector domain of ChxR ($ChxR_{Eff}$) is in a structural conformation similar to the effector domains of other OmpR/PhoB response regulators. This is similar to the results of a structural analysis of another atypical response regulator, HP1043 (Hong, Lee et al. 2007). In addition to demonstrating overall structural similarity, determination of the three-dimensional structure of $ChxR_{Eff}$ is expected to reveal the residues within and the orientation of the functional regions (β5–β6 loop, α3 DNA binding helix, and α2–α3 transactivation loop). In this study, we report a crystal and NMR structure of $ChxR_{Eff}$, which were not structurally similar. Through a chemical shift mapping experiment and electrophoretic mobility shift assays, we identified residues in the functional regions of ChxR that interact with DNA. Additionally, ChxR was shown to interact with the α-subunit of RNA polymerase.

Chapter IV

Methods and Materials

Cloning, Expression, and Purification of $ChxR_{Eff}$

The coding region for $ChxR_{Eff}$, residues 115-227, was PCR amplified using genomic DNA from *Chlamydia trachomatis* serovar L2/434/Bu. The primers used for amplification were 5'-GGAATTCCATATGCATTCTGTTCCGGAAAGTT-3' (forward, containing the 5' *Nde*I site) and 5'-CCGCTCGAGCTAAGAAAGCTTTGTATCTTGTTG-3' (reverse, containing the *Xho*I site) (Integrated DNA Technologies). The PCR product was digested with NdeI/XhoI and ligated into a similarly digested pET29b vector (Novagen). The resultant plasmid encodes $ChxR_{Eff}$ with a C-terminal histidine tag. The $chxR_{Eff}$ plasmid was transformed into *E. coli* BL21(DE3) (Invitrogen). Protein was expressed in cells grown in LB medium containing 50 µg ml^{-1} kanamycin at 37°C with shaking at 250 rpm. Protein expression was induced by the addition isopropyl-β-D-thiogalactopyranoside to a final concentration of 1 mM at an optical density of 0.7. The cells were harvested by centrifugation (4,000 x g, 20 min, 4°C) after an overnight incubation at 15° C and 250 rpm.

E. coli cells were resuspended in 50 mM Tris pH 7, 400 mM NaCl, disrupted by sonication, and subjected to centrifugation (14,000 x g, 30 min, 4°C) to remove cell debris. The lysate was further clarified by passing the supernatant through a 0.22-µm filter before protein purification. The cell extract was applied to Talon Metal (Co^{2+}) Affinity Column (Clontech) according to the manufacturer's instructions. The column was washed with 5 mM imidazole, 50 mM Tris pH 7, 400 mM NaCl. $ChxR_{Eff}$ was eluted with the above buffer supplemented with 250 mM imidazole.

Peak fractions were pooled and further purified by gel filtration chromatography. The pooled protein mixture was applied to a Sephacryl S-300 16/60 gel filtration column (GE Healthcare) pre-equilibrated in 50 mM Tris pH 7, 400 mM NaCl. Fractions containing $ChxR_{Eff}$ were pooled and concentrated, using an Amicon (Millipore) 3,000 molecular weight cut-off centrifugal filtration devise, to 8.4 mg ml^{-1}. The purified protein was determined to be >95% pure by Coomassie staining after SDS-PAGE.

Crystallization of $ChxR_{Eff}$

Crystallization was carried out at room temperature by the hanging-drop vapor-diffusion method with 1 µl of 8.4 mg ml^{-1} $ChxR_{Eff}$ mixed with 1 µl of commercially available sparse matrix screens (Hampton Research). The protein crystallized in a variety of conditions with multiple morphologies after approximately three months incubation. One of the crystallization conditions was optimized and consisted of 0.2M Ammonium Sulfate, 0.1M Bis-Tris pH 6.5, 25% w/v PEG3350. $ChxR_{Eff}$ apo crystals were soaked for approximately 20 s in mother liquor supplemented with 10% ethylene glycol, and flash cooled by immersion in liquid nitrogen.

To obtain a heavy atom data set, purified $ChxR_{Eff}$ was concentrated to 8 mg/mL in 400 mM NaCl, 10 mM Tris-HCl pH 7. Crystals were obtained in 2 days at 20^{o}C in sitting drop vapor diffusion plates (Emerald biosystems) using 1uL of crystallization solution (0.1 M Hepes pH 7.5, 1 M KCl, 1 M ammonium sulfate) and 1 uL of protein equilibrated against 100uL of reservoir solution. Single crystals were transferred to a solution containing 30% Glycerol, 0.1 M Hepes pH 7.5, 0.5 M KBr, 1 M ammonium sulfate for 1 minute before flash cooling in liquid nitrogen for data collection.

Data Collection, Structure Solution, and Refinement

For the $ChxR_{Eff}$ apo crystal, data collection was carried out at 100K at Stanford Synchrotron Radiation Laboratory (SSRL) beamline 9-2. The exposure time for each 0.5° oscillation image was 5 s using an MAR325 detector and a wavelength of 0.1 nm. The resulting data sets were processed and scaled using *MOSFLM* and *SCALA* from the CCP4 suite (Collaborative Computational Project 1994). The data collection statistics are summarized in Table 4.1.

For $ChxR_{Eff}$ Br soaked crystal, data were collected at 100K at the Advanced Photon Source (APS) IMCA-CAT, sector 17BM using an ADSC Quantum 210 CCD detector and a wavelength of 0.91983 Å. The exposure time for each 1° oscillation image was 15 s at a detector distance of 170 mm. Intensities were integrated and scaled using the *HKL2000* package (Z. Otwinowski and Minor 1997). Structure solution was carried out using the SAD phasing method with the *SHELX C/D/E* software package (Sheldrick 2008) via the CCP4 interface (Collaborative Computational Project 1994). Bromine positions were identified using *SHELXC* and *SHELXD*, which yielded correlation coefficient all/weak of 47.63 / 29.34. Calculation of initial phase angles and density modification were conducted with *SHELXE*. The highest correlation coefficient (77.2%) and electron density map quality was observed for the original enantiomorph in the space group $P4_32_12$. Automated model building was carried out using the fast build feature in *BUCCANEER* (Cowtan 2006) which produced a nearly complete C_a trace for the expected non-crystallographic dimer and refined to an initial R_{factor} of 38.8%. Side chains were excluded from the model and the dimer was used for molecular replacement search model against higher resolution native data using *PHASER* (McCoy, Grosse-Kunstleve et al. 2007). The solution was refined with *REFMAC* (Murshudov, Vagin et al. 1997) and the model improved using automated

model building with *ARP/WARP*. Initial refinement of the resulting model converged at R = 27.5%, R_{free} = 30.1%. The final model was obtained from iterative rounds of manual model building and refinement with *COOT* (Emsley and Cowtan 2004) and *REFMAC* (Murshudov, Vagin et al. 1997) respectively. Relevant crystallographic data are listed in Table 4.1.

Monomer A comprises residues 118-213 and monomer B comprises residues 117-213. The model includes 28 waters and two sulfate ions. A Ramachandran plot with *PHENIX* (Adams, Afonine et al. 2010) determined that 96.3% of the residues were in a favored position and 3.7% of the residues were in an allowed position.

Analytical Size Exclusion Chromatography

$ChxR_{Eff}$ was expressed and purified as described above. During size exclusion chromatography, the protein was exchanged into buffer comprised of 20 mM Na_2HPO_4, 20 mM KH_2PO_4 pH 7, 400 mM NaCl, and 1 mM DTT. The purified protein was concentrated to 27 mg/ml using an Amicon (Millipore) 3,000 molecular weight cut-off centrifugal devise. The protein was then diluted to 1 mM, 100 μM, 10 μM, and 1 μM with the buffer listed above and subjected to analytical size exclusion chromatography using a Superdex 75 10/300 GL gel filtration column (GE Healthcare). A protein standard solution containing bovine serum albumin (66 kDa), chicken ovalbumin (44 kDa), horse myoglobin (17 kDa), and vitamin B12 (1.35 kDa) (BIO-RAD, Hercules, CA) was used to generate a standard curve.

The fractions containing each oligomer population were applied to a Bio-Dot microfiltration apparatus (Bio-Rad) as per the manufacturers instructions. The subsequent nitrocellulose membrane was initially probed with rabbit anti-ChxR antibodies, followed by IR700 goat anti-rabbit antibodies.

Table 4.1

Data Collection and Refinement Statistics

	Apo	SAD (Br)
Data Collection		
Unit-cell parameters (Å)	$a = b = 109.3$ $c = 95.7$	$a = b = 109.9$ $c = 95.2$
Space group	$P4_32_12$	$P4_32_12$
Resolution (Å)[1]	45.0-2.5 (2.56-2.50)	50.0-3.5 (3.63-3.50)
Wavelength (Å)	1.0	0.919
Observed reflections	164342	162330
Unique reflections	20605	14015
$<I/\sigma I>$[1]	22.2 (4.2)	13.3 (5.3)
Completeness (%)[1]	98.1 (99.3)	99.8 (100.0)
Redundancy[1]	8.1 (8.2)	11.6 (11.7)
R_{merge} (%)[1, 2]	38.0 (40.0)	19.9 (42.6)
Refinement		
Resolution (Å)	43.5-2.5	-
R_{factor} / R_{free} (%)[3]	25.9 / 30.5	-
No. of atoms (protein / water)	1515 / 27	-
Model Quality		
R.m.s deviations		
Bond lengths (Å)	0.011	-
Bond angles (^{o})	1.33	-
Average B factor (Å^2)		
Protein	41.7	-
Water	33.9	-
Coordinate error based on Maximum Likelihood (Å)	0.177	-
Ramachandran Plot		
Favored (%)	96.3	-
Allowed (%)	3.7	-
Disallowed (%)	0.0	-

[1] Values in parenthesis are for the highest resolution shell.

[2] $R_{merge} = \Sigma_{hkl}\Sigma_i |I_i(hkl) - <I(hkl)>| / \Sigma_{hkl}\Sigma_i I_i(hkl)$, where $I_i(hkl)$ is the intensity measured for the ith reflection and $<I(hkl)>$ is the average intensity of all reflections with indices hkl.

[3] $R_{factor} = \Sigma_{hkl} ||F_{obs}(hkl)| - |F_{calc}(hkl)|| / \Sigma_{hkl} |F_{obs}(hkl)|$; Rfree is calculated in an identical manner using 5% of randomly selected reflections that were not included in the refinement

Electrophoretic Mobility Shift Assay

Electrophoretic mobility shift assays were performed as described for ChxR with DNA corresponding to the high-affinity (DR2) binding site within the *chxR* promoter (Hickey, Weldon et al. 2011 (Chapter 2)). The binding reactions contained 1 nM DNA and 50 nM, 100 nM, 500 nM, 1 μM, 5 μM, 10 μM, or 50 μM $ChxR_{Eff}$. The assay was performed in triplicate and the amount of DNA shifted was visualized and quantified using the Odyssey Infrared Imaging System (LI-COR Biosciences, Lincoln, NE).

NMR Spectroscopy

$ChxR_{Eff}$ was overexpressed *E. coli* BL21(DE3) cells and $^{13}C/^{15}N$ labeled using a previously established method (Marley, Lu et al. 2001). Following overexpression, $ChxR_{Eff}$ was purified as described above. The purified protein was equilibrated in 20 mM Na_2HPO_4 pH 6.5, 20 mM KH_2PO_4, 400 mM NaCl, and 1 mM DTT and then concentrated to ~1.5 mM using an Amicon (Millipore) 3,000 molecular weight cut-off centrifugal device.

The sample for NMR spectroscopy experiments was comprised of ~1.5 mM $ChxR_{Eff}$ in 20 mM Na_2HPO_4 pH 6.5, 20 mM KH_2PO_4, 400 mM NaCl, 1 mM DTT, and 10% D_2O. All NMR spectra were recorded on Varian Inova 600 MHz NMR instrument equipped with room temperature triple resonance probe with XYZ pulse field gradients. All NMR experiments were recorded at 25°C. The backbone resonance assignments of ^{1}H, ^{13}C, and ^{15}N for $^{13}C/^{15}N$ labeled $ChxR_{Eff}$ were completed from the suites of heteronuclear 2D and 3D- triple resonance experiments: 2D-^{1}H-^{15}N-HSQC, HNCA, HNCO, HNCACB, CBCA (CO) NH, HBHA (CBCACO) NH, HCCH-COSY, HCCH-TOCSY, ^{1}H-^{13}C-HSQC, ^{15}N and ^{13}C edited NOESY.

All NMR spectra were processed using NMRDraw and NMRPipe (Delaglio, Grzesiek et al. 1995) and analyzed with SPARKY (Goddard & Kneller).

For the $ChxR_{Eff}$-DNA chemical shift titration experiment, $ChxR_{Eff}$ was ^{15}N labeled and purified as described above. After an initial 2D-^{1}H-^{15}N-HSQC was taken of the native protein, double-stranded DNA corresponding to the DR2 binding site in the *chxR* promoter (5'-CTTATCTAGTTTTTGATCGAAAAATTTC) was titrated into the protein sample. 2D-^{1}H-^{15}N-HSQCs were taken at DNA concentrations of 0.13 mM, 0.26 mM, 0.52 mM, and 1.04 mM.

Co-Immunoprecipitation

Samples containing 12.5µl bed volume of Dynabead Protein G beads (Invitrogen) were incubated overnight at 4°C with 1µg polyclonal rabbit anti-ChxR antibodies in binding buffer (100 mM Na_2HPO_4, 0.01% TWEEN-20 pH 8.2). Beads were separated on a magnetic rack and washed 3X with blocking buffer (PBS, 0.1% TWEEN-20, 10% BSA), and incubated overnight at 4°C. The samples were washed 3X with NP-40 buffer (1% NP-40 substitute, 150 mM NaCl, 50 mM Tris pH 7.0), and incubated with 4µg ChxR at 25°C for 2 hours. Once washed 3X with NP-40 buffer, 4µg of αCTD was added and the samples were incubated at RT for 1 hour. The samples were washed with 3X NP-40 buffer and subjected to SDS-PAGE and an immunoblot assay was performed using anti-ChxR or anti-RNA polymerase antibodies.

Chapter IV

Results and Discussion

$ChxR_{Eff}$ forms homodimers

During recombinant protein purification, size exclusion chromatography indicated that $ChxR_{Eff}$ was a mixed population of monomers and dimers (data not shown). To determine if this observation was a result of a high concentration (~1 mM) of protein during purification, $ChxR_{Eff}$ was subjected to analytical size exclusion chromatography at 1 mM, 100 μM, 10 μM, or 1 μM. The calculated molecular weight of a $ChxR_{Eff}$ monomer or dimer is 13.5 kDa or 27 kDa, respectively. At 1 mM, 100 μM, or 10 μM, $ChxR_{Eff}$ eluted as both a monomer and a dimer (Fig. 4.1A). The absorbance of 1 μM $ChxR_{Eff}$ was too low to detect, therefore we performed a dot blot using the fractions corresponding the elution of the $ChxR_{Eff}$ monomer (14.1 kDa) and dimer (29.9 kDa) from the higher protein concentrations (Fig. 4.1B). The amount of monomer and dimer from each protein concentration was quantified from the dot blot and indicated that the oligomeric state of recombinant $ChxR_{Eff}$ is approximately 30% dimer and 70% monomer (Fig. 4.1C). The detection of the $ChxR_{Eff}$ dimer at 1 μM suggests that the higher oligomeric state of the protein was not a result of a high concentration of protein. Furthermore, the $ChxR_{Eff}$ dimer does not appear to be an artifact of protein misfolding as size exclusion fractions containing monomeric or dimeric $ChxR_{Eff}$ each eluted as ~30% dimer and ~70% monomer when subjected again to size exclusion chromatography (data not shown), indicating that the $ChxR_{Eff}$ dimer is not a result of protein misfolding.

Intermolecular interactions between effector domains have been detected, albeit in relatively small amounts, in other OmpR/PhoB response regulators. Dimers of the PhoP effector

FIG 4.1. Concentration-dependent stability of $ChxR_{Eff}$. A) To determine the oligomeric state of recombinant $ChxR_{Eff}$, the protein was subjected to analytical size exclusion chromatography at 1 mM, 100 μM, and 10 μM. $ChxR_{Eff}$ eluted from the column as a mixed population of ~30% dimer (29.9 kDa) and ~70% monomer (14.1 kDa). B) The 280 nm absorbance at 1 μM was too weak to detect. Therefore, a dot blot was performed with each 0.5 ml elution fractions comprising the dimer/monomer molecular weight range and antibodies against ChxR. C) The amounts of dimeric and monomeric $ChxR_{Eff}$ were quantified using the photon emission of an IR700-labeled secondary antibody.

A

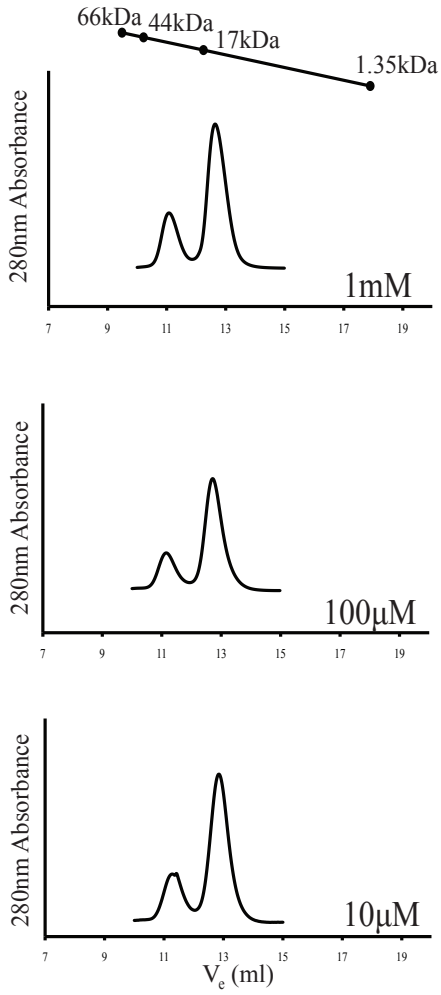

B

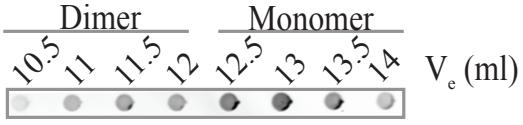

C

	Dimer	Monomer
1mM	40%	60%
100µM	30%	70%
10µM	30%	70%
1µM	30%	70%

domain have been observed but are only detected at a high protein concentration (>10 mg/ml) (Wang, Engohang-Ndong et al. 2007). Additionally, dimers of both OmpR and PhoB effector domains have been detected in the presence of DNA (Blanco, Sola et al. 2002; Rhee, Sheng et al. 2008), although, the interactions between these effector domains are weak and do not appear to contribute to DNA-binding. In contrast to these previous observations, the effector domain of ChxR was shown to form a homodimer at a relatively low concentration (1 μM), although, this interaction may not occur in the context of the full-length protein due to conformational restraints imposed by the receiver domain, as we have previously shown that the receiver domain forms a very stable homodimer (Fig. 3.3).

$ChxR_{Eff}$ can bind DNA

We have previously shown that full-length ChxR interacts with DNA corresponding to the DR2 binding site in the *chxR* promoter with a dissociation constant (K_d) of approximately 44 nM (Hickey, Weldon et al. 2011 (Chapter 2)). To determine if $ChxR_{Eff}$ alone can to bind to DNA, an electrophoretic mobility shift assay was performed with the DR2 DNA sequence. As figure 4.2 demonstrates, $ChxR_{Eff}$ can bind to DNA; although its affinity for DNA appeared to be less than that of full-length ChxR dimers. Therefore, the amount of DNA shifted with increasing concentrations of $ChxR_{Eff}$ (50 nM-50 μM) was quantified and a K_d was calculated (446 ± 74.7 nM). The calculated K_d assumes that two $ChxR_{Eff}$ molecules are bound to the DNA as the DR2 DNA sequence contains two binding sites. The approximate 10-fold decrease in DNA affinity for $ChxR_{Eff}$ relative to full-length ChxR indicates that the interaction between $ChxR_{Eff}$ and DNA is relatively weak and stable DNA interaction requires dimerization through the receiver domain. Furthermore, in addition to increasing DNA affinity by binding cooperatively to adjacent binding

FIG 4.2. DNA-binding analysis of $ChxR_{Eff}$. To determine if $ChxR_{Eff}$ can interact with DNA in the absence of the receiver domain, EMSAs were performed with IR800-labeled DNA corresponding to the DR2 site from the *chxR* promoter and increasing concentrations (50 nM, 100 nM, 500 nM, 1 μM, 5 μM, or 10 μM) of recombinant $ChxR_{Eff}$. The first lane (left) contains DNA in the absence of $ChxR_{Eff}$.

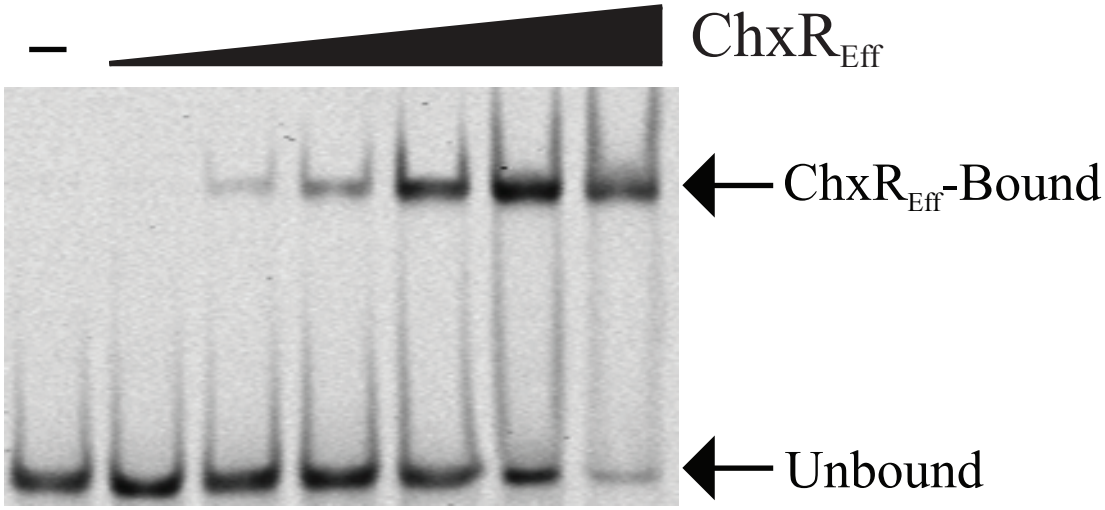
–
ChxR$_{Eff}$
ChxR$_{Eff}$-Bound
Unbound

sites through the protein-protein interaction of the receiver domain, the receiver domain may also properly orient the effector domain onto DNA.

Crystal structure of $ChxR_{Eff}$

A structure of $ChxR_{Eff}$ was experimentally determined to help elucidate the regions and residues that may be important for interaction with DNA and RNA polymerase machinery. A high-resolution data set was obtained from a $ChxR_{Eff}$ crystal. The space group of the crystal was $P4_32_12$ with 2 molecules comprising the asymmetric unit. Using SAD phasing, the final model of $ChxR_{Eff}$ was refined to 2.5Å (Fig. 4.3A). $ChxR_{Eff}$ is composed of a four-stranded antiparallel β-sheet (β1-β2-β3-β4, residues 119-122, 125-128, 133-136, and 139-142, respectively), followed by an α-helix (α1, residues 145-157), a short β-strand (β5, residues 162-163), two α-helices (α2-α3, residues 164-181 and 184-194, respectively), and a β-hairpin (β6-β7, residues 201-204 and 208-211, respectively). The overall topology of $ChxR_{Eff}$ is β1-β2-β3-β4-α1-β5-α2-α3-β6-β7 (Fig. 4.3B).

This crystal structure of $ChxR_{Eff}$ is unique within the OmpR/PhoB subfamily. All other OmpR/PhoB effector domain structures are monomers that share a highly conserved tertiary structure. In contrast, $ChxR_{Eff}$ crystallized as a sub-domain swap dimer. The β1-β2-β3-β4-α1-β5-α2 region of monomer A and the α3-β6-β7 region of monomer B reconstitute the typical effector domain tertiary structure (Fig. 4.4). Domain and sub-domain swapping has been observed in many other proteins (Liu and Eisenberg 2002), including a member of the OmpR/PhoB subfamily. The full-length structure of RegX3 from *Mycobacterium tuberculosis* crystallized as a dimer in which the receiver domains were swapped (King-Scott, Nowak et al. 2007). Despite the observation of domain or sub-domain swapping in proteins, it is currently

FIG 4.3. Crystal structure of $ChxR_{Eff}$. A) A Stereo representation of the electron density map (blue) of residues 125-131 (green) of monomer A. The electron density map is contoured at 1σ. B) Stereoviews of a ribbon diagram of $ChxR_{Eff}$. Monomer A and monomer B are colored yellow and blue, respectively. The molecular topology of each monomer is β1-β2-β3-β4-α1-β5-α2-α3-β6-β7.

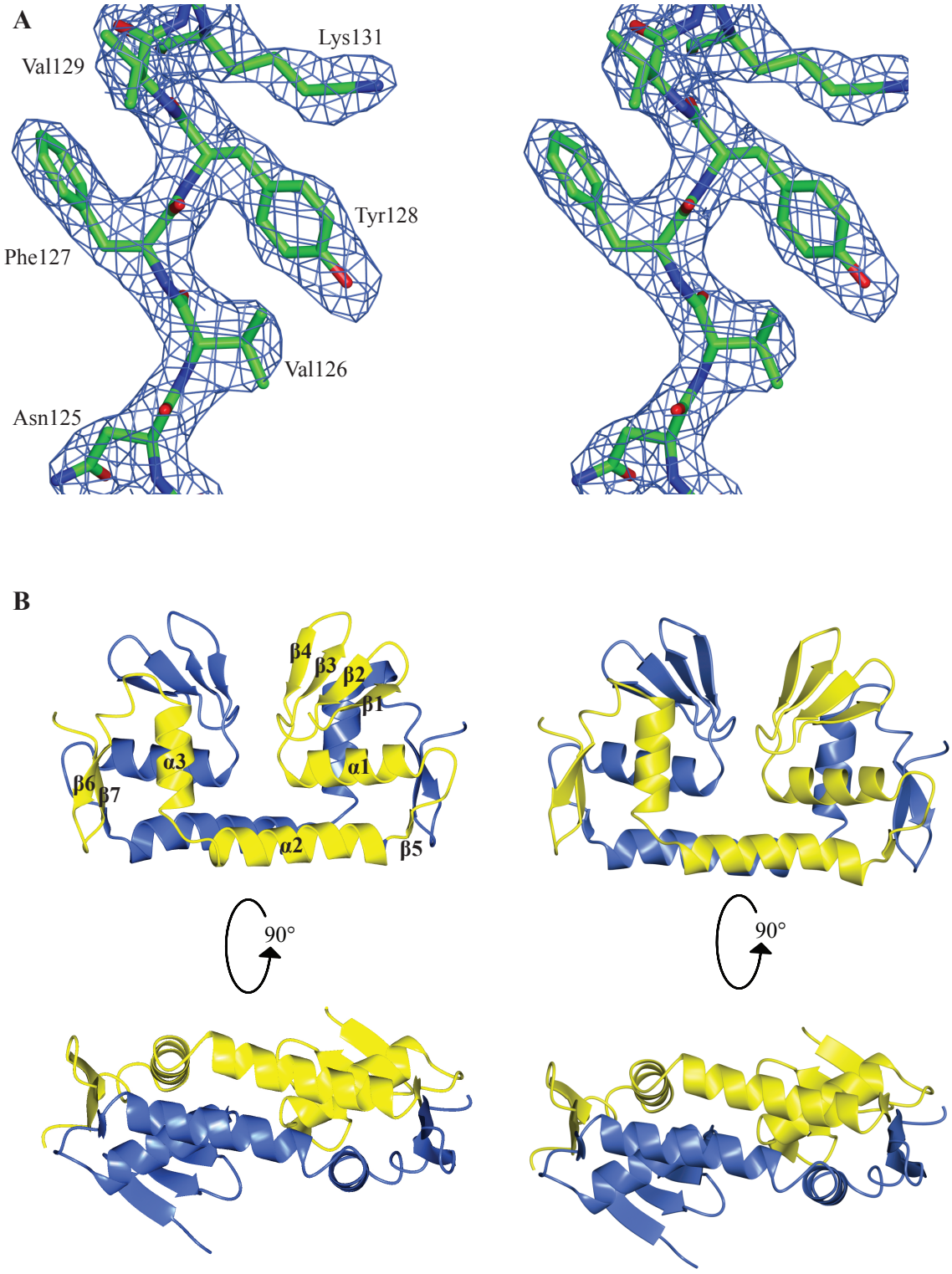
A
Lys131
Val129
Tyr128
Phe127
Val126
Asn125
B
β4
β3
β2
β1
α3
α1
β6
β7
α2
β5
90°
90°

FIG. 4.4. $ChxR_{Eff}$ crystallized as a sub-domain swap dimer. Stereoviews of a superimposition of $ChxR_{Eff}$ and the effector domain of YycF from *B. subtilis* (red; PDB ID: 2D1V). The β1-β2-β3-β4-α1-β5-α2 region of YycF superimposes with one $ChxR_{Eff}$ monomer (blue), while α3-β6-β7 of YycF aligns with the second $ChxR_{Eff}$ monomer (yellow).

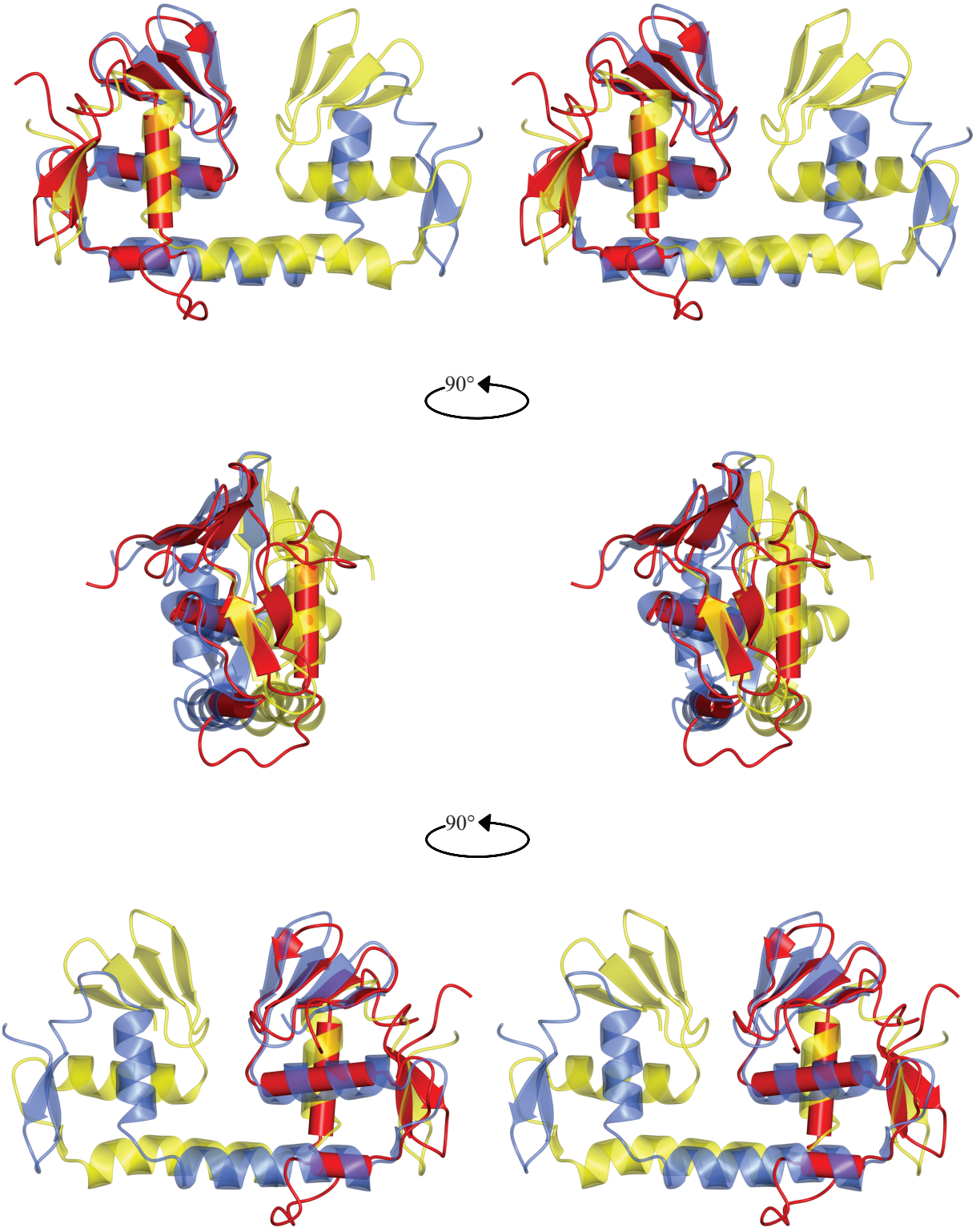
90°
90°

unknown how this swapping affects the functional activity of a protein but is thought to increase binding surfaces, introduce new active sites at domain/sub-domain interfaces, and allow for allosteric control (Liu and Eisenberg 2002).

For $ChxR_{Eff}$, sub-domain swapping could be a mechanism to control DNA interaction. Similar to previous studies with effector domain structures from other OmpR/PhoB subfamily members, we attempted to model the $ChxR_{Eff}$ dimer onto DNA (Wang, Engohang-Ndong et al. 2007; Gupta, Borin et al. 2009). Using the structure of PhoB from *E. coli* in a complex with DNA as a starting model (PDB ID: 1GXP)(Blanco, Sola et al. 2002), we superimposed the $ChxR_{Eff}$ dimer onto PhoB such that the α3 of $ChxR_{Eff}$ is in a similar position within the major groove of the DNA. However, the dimer structure could not be modeled onto the DNA without steric hindrance from either the β6-β7 loop or the extended α2, indicating that the $ChxR_{Eff}$ dimer cannot interact with the DNA in a similar manner as other OmpR/PhoB response regulators but this does not preclude the dimer from interacting with DNA in an alternative manner.

It is currently unclear if the $ChxR_{Eff}$ dimer structure is biologically relevant. The $ChxR_{Eff}$ dimer could represent an inactive state of the protein in which DNA interaction is inhibited possibly through an interaction with another protein or ligand. Such inactive states have been reported for other OmpR/PhoB subfamily members (Kato, Chibazakura et al. 2008; Wang, Tian et al. 2009). Alternatively, the $ChxR_{Eff}$ dimer could be an artifact of crystal packing, although our analytical size exclusion studies support the conclusion that $ChxR_{Eff}$ can form homodimers in solution at a relatively low (1 μM) concentration.

NMR Secondary structure of $ChxR_{Eff}$

The model of $ChxR_{Eff}$ obtained through crystallography is of a $ChxR_{Eff}$ sub-domain swapped dimer but the predominant oligomeric species of recombinant $ChxR_{Eff}$ was monomeric. Since the NMR resonance signal is proportional to the molar concentration of the sample, the more abundant $ChxR_{Eff}$ monomer should be more intense than the dimer and therefore NMR was used to elucidate the secondary structure of the monomer (Fig. 4.5).

As figure 4.6 indicates, the secondary structure of $ChxR_{Eff}$ determined through NMR is similar to, but distinct from the crystal structure. The topology of the $ChxR_{Eff}$ NMR structure is β1-β2-β3-β4-α1-α2-α3-α4-β6-β7. The positions of the four-stranded antiparallel β-sheet and the β-hairpin are similar to the crystal structure. The positions of the α-helices, however, are different from the crystal structure. α1 and α2 are 5 and 12 residues shorter in the NMR structure, respectively. The start of α3 is 6 residues before the α3 in the crystal structure, and is 4 residues longer.

This comparison indicates that the $ChxR_{Eff}$ secondary structure determined through NMR is different from the crystal structure, potentially indicating that the tertiary structure is also different. The secondary structure of the monomeric form of $ChxR_{Eff}$ appears to resemble the typical OmpR/PhoB subfamily effector domain structure. While the primary sequence similarity between effector domains of the OmpR/PhoB subfamily varies from 20-65% (Martinez-Hackert and Stock 1997), the secondary and tertiary structure of this domain is highly conserved throughout the subfamily. Likewise, the primary sequence similarity between $ChxR_{Eff}$ and OmpR or PhoB is 41% or 30%, respectively, and the secondary structure of $ChxR_{Eff}$ determined through NMR is similar to OmpR and PhoB (Fig. 4.6). The biggest regions of dissimilarity between $ChxR_{Eff}$ and OmpR or PhoB are in the lengths of the helices, which was not unexpected as the lengths of these secondary structural elements vary between OmpR/PhoB effector domains

FIG. 4.5. ^{1}H-^{15}N HSQC spectrum of $ChxR_{Eff}$. To begin to determine the structure of $ChxR_{Eff}$, an initial ^{1}H-^{15}N Heteronuclear Single Quantum Coherence (HSQC) was performed. The amide resonance signals for 100 residues are present in the HSQC. The spectrum is well dispersed on both dimensions indicating a well-folded protein.

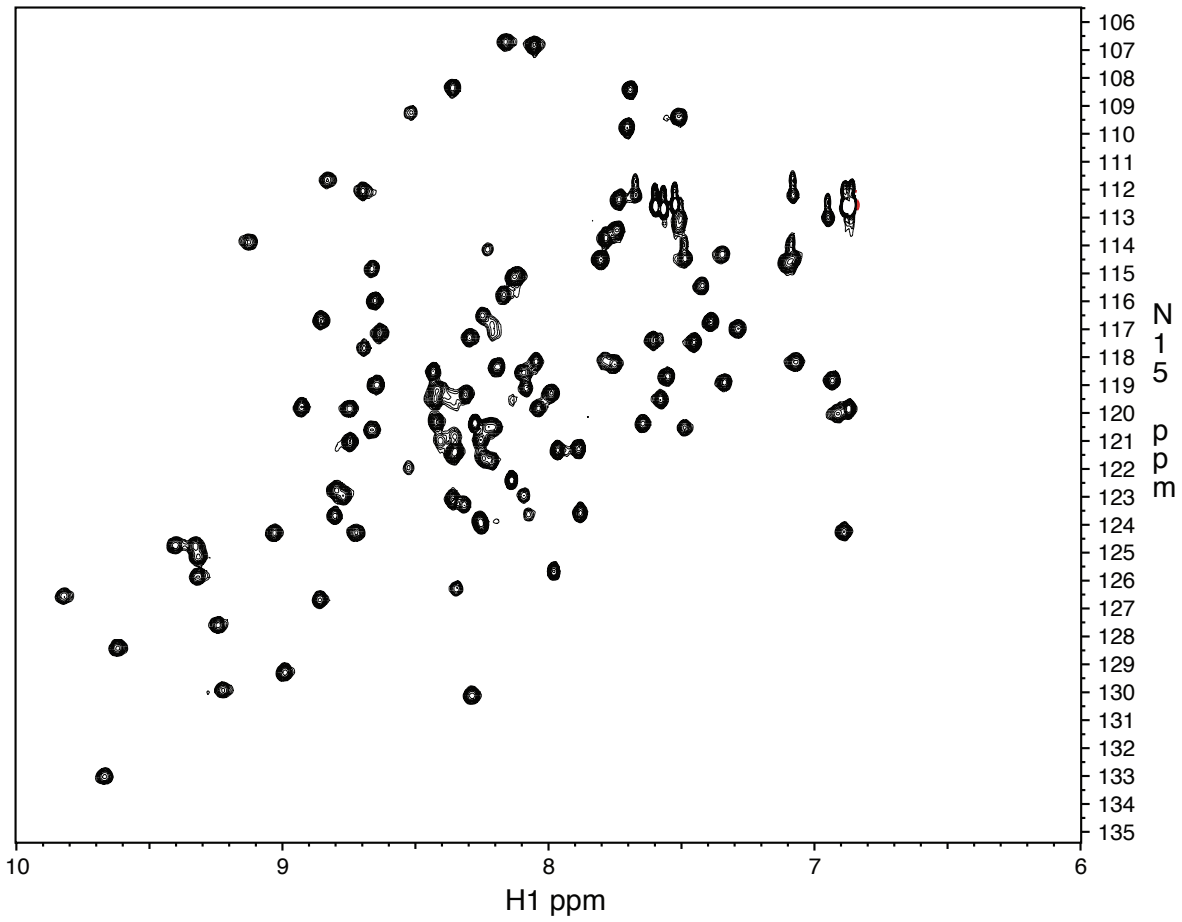
106
107
108
109
110
111
112
113
114
115
116
117
118
119
120
121
122
123
124
125
126
127
128
129
130
131
132
133
134
135
N
1
5
p
p
m
10
9
8
7
6
H1 ppm

FIG 4.6. Sequence and secondary structure alignment of $ChxR_{Eff}$ and other OmpR/PhoB subfamily members. The primary sequences of $ChxR_{Eff}$ (UniProt ID: B0B8K5), OmpR (PDB ID: 2JPB), and PhoB (PDB ID: 1GXP) were aligned using the multiple sequence alignment program ClustalW (Larkin, Blackshields et al. 2007). The secondary structures of each protein are displayed above their respective primary sequence. The secondary structure of $ChxR_{Eff}$ determined through crystallography or NMR is colored cyan or green, respectively. The secondary structures of OmpR and PhoB are colored yellow.

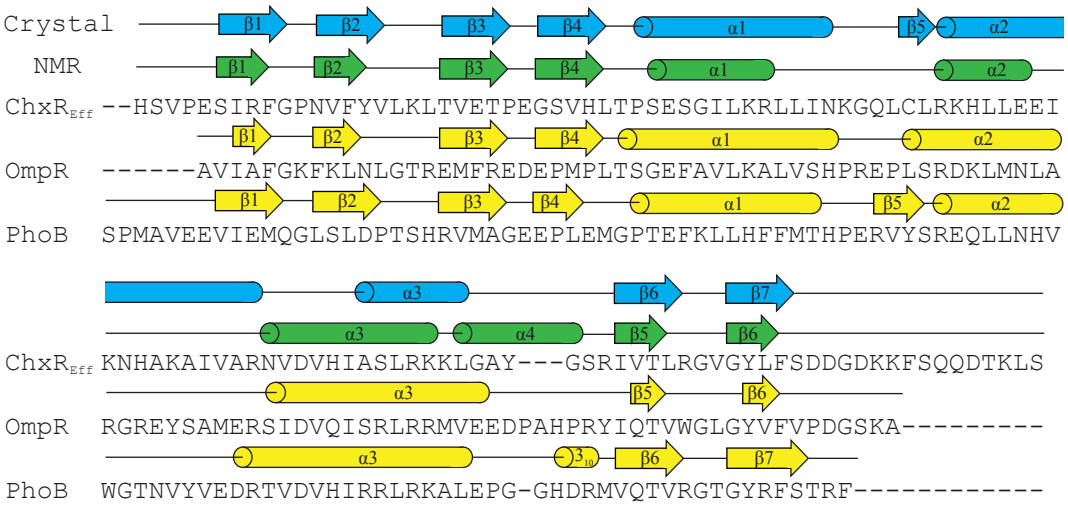
Crystal
β1 β2 β3 β4 α1 β5 α2
NMR
β1 β2 β3 β4 α1 α2
ChxR$_{Eff}$ --HSVPESIRFGPNVFYVLKLTVETPEGSVHLTPSESGILKRLLINKGQLCLRKHLLEEI
β1 β2 β3 β4 α1 α2
OmpR ------AVIAFGKFKLNLGTREMFREDEPMPLTSGEFAVLKALVSHPREPLSRDKLMNLA
β1 β2 β3 β4 α1 β5 α2
PhoB SPMAVEEVIEMQGLSLDPTSHRVMAGEEPLEMGPTEFKLLHFFMTHPERVYSREQLLNHV
α3 β6 β7
α3 α4 β5 β6
ChxR$_{Eff}$ KNHAKAIVARNVDVHIASLRKKLGAY---GSRIVTLRGVGYLFSDDGDKKFSQQDTKLS
α3 β5 β6
OmpR RGREYSAMERSIDVQISRLRRMVEEDPAHPRYIQTVWGLGYVFVPDGSKA---------
α3 3_{10} β6 β7
PhoB WGTNVYVEDRTVDVHIRRLRKALEPG-GHDRMVQTVRGTGYRFSTRF------------

(Kenney 2002; Gupta, Borin et al. 2009). The similarity between the $ChxR_{Eff}$ NMR secondary structure and other OmpR/PhoB subfamily members and the dissimilarity to the crystal structure leads us to speculate that the tertiary structure of monomeric $ChxR_{Eff}$ is homologous to the typical OmpR/PhoB effector domain structure.

Asn182, His186, and Lys192 in ChxR interact with DNA

NMR chemical shift titration was used to facilitate the identification of residues involved in interaction with DNA. A 28-bp fragment of double-stranded DNA corresponding to the DR2 binding site from the *chxR* promoter was titrated into a solution of ^{15}N-labeled $ChxR_{Eff}$ (Fig. 4.7A). A comparison of the HSQC spectra of $ChxR_{Eff}$ in the absence and at each concentration of DNA indicated that 20 residues were perturbed in the presence of DNA (Fig. 4.7B). Many of these residues reside in the regions known to interact with DNA in homologous effector domains (Gupta, Borin et al. 2009) and include the putative recognition helix (α3; Asn182, Asp184, His186, Ile187, Lys192) and minor groove-interacting wing (β5-β6 loop; Val207).

To begin to determine which of the perturbed residues might interact with DNA, Ala substitutions were generated in the full-length protein in the perturbed residues in α3 and the β5-β6 loop. The ability of each protein to bind DNA was tested through EMSAs. The amount of DNA shifted with each substitution was quantified and compared to wild-type ChxR (Fig. 4.7C). Substitutions in three (Asn182, His186, and Lys192) of the six residues significantly reduced DNA interaction. These three residues are located in α3 in $ChxR_{Eff}$, supporting that this helix is a region in ChxR that interacts with DNA.

We have previously determined a consensus DNA sequence recognized by ChxR (WHGAWNW) for which the central GAW nucleotides are critical for DNA binding

FIG 4.7. Identifying and testing DNA-binding residues. A) Chemical shift mapping of residues perturbed in the presence of DNA. To identify potential residues involved in interaction with DNA, increasing concentrations of cognate DNA were added to ^{15}N-labeled $ChxR_{Eff}$. The black, red, and blue peaks represent ^{15}N-labeled $ChxR_{Eff}$ at a concentration of 0.52 mM in the absence of DNA, in the presence of 0.52 mM DNA, and in the presence of 1.04 mM DNA, respectively. B) 20 residues (grey) were perturbed in the presence of DNA. Many of these residues are in the regions (α3 and the β5-β6 loop) known to interact with DNA in other effector domains from the OmpR/PhoP subfamily. C) The ability of the perturbed resides within α3 and the β5-β6 loop to bind DNA was quantified through a gel shift assay. The amount of DNA shifted from 3 of the 6 substitutions was significantly ($p < 0.001$ (***)) reduced relative to wild-type ChxR.

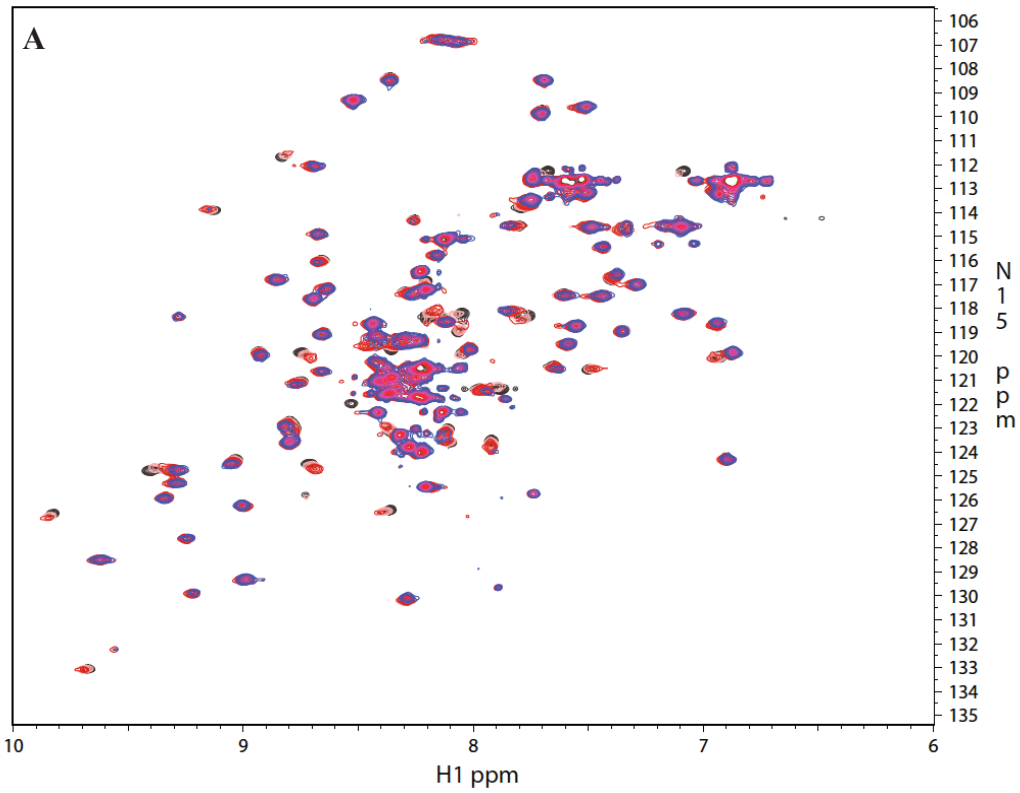
A
106
107
108
109
110
111
112
113
114
115
116
117
118
119
120
121
122
123
124
125
126
127
128
129
130
131
132
133
134
135
N
1
5
p
p
m
10
9
8
7
6
H1 ppm

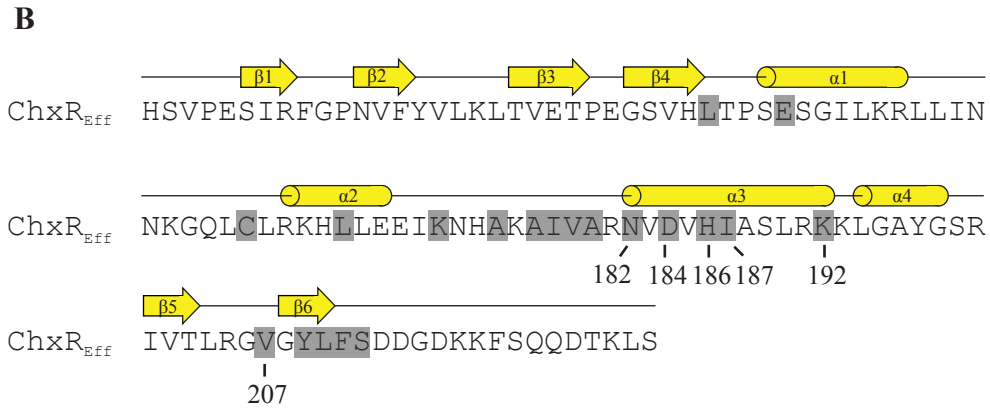
B
β1
β2
β3
β4
α1
ChxR$_{Eff}$ HSVPESIRFGPNVFYVLKLTVETPEGSVHLTPSESGILKRLLIN
α2
α3
α4
ChxR$_{Eff}$ NKGQLCLRKHLLEEIKNHAKAIVARNVDVHIASLRKKLGAYGSR
182 184 186 187 192
β5
β6
ChxR$_{Eff}$ IVTLRGVGYLFSDDGDKKFSQQDTKLS
207

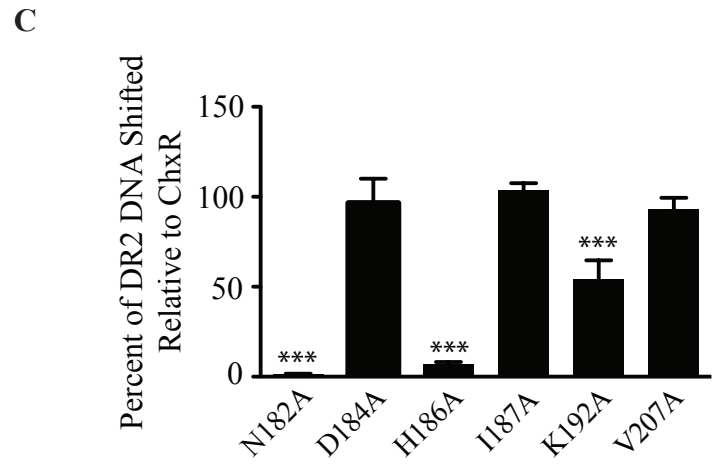
C
Percent of DR2 DNA Shifted
Relative to ChxR
150
100
50
0
***
***
***
N182A
D184A
H186A
I187A
K192A
V207A

(Hickey, Weldon et al. 2011 (Chapter 2)). Since substituting Asn182 or His186 essentially abolished DNA interaction, we speculate that these two residues specifically interact with the conserved adenine and guanine nucleotide, respectively. Asn or His is known to have the highest specificity for an adenine or guanine base, respectively (Suzuki 1994; Luscombe and Thornton 2002). For Asn182, the carboxamide side-chain could interact with both the phosphate backbone and the guanine base, providing two sites of interaction with the DNA, which could explain why substituting this residue had such a dramatic effect on DNA interaction. Additionally, substituting Lys192 reduced DNA interaction by ~45% but was not as dramatic as substitutions to Asn182 or His186, potentially suggesting that this residue is not making base-specific contact with the DNA, rather Lys192 may interact with the phosphate backbone of the variable nucleotide at positions 5 or 6 of the consensus sequence.

ChxR$_{Eff}$ interacts with the C-terminal domain of the α-subunit of RNA polymerase

To activate transcription, members of the OmpR/PhoB subfamily interact with either the σ factor or the α-subunit of RNA polymerase (Chen, Abdel-Fattah et al. 2004). Since our previous studies with ChxR indicated that the closest DNA binding site in the *chxR* promoter is 81 nucleotides upstream of the transcriptional start site (Hickey, Weldon et al. 2011 (Chapter 2)), we hypothesized that ChxR interacts with the C-terminal domain of the α-subunit of RNA polymerase (αCTD). To test this hypothesis, a co-immunoprecipitation was performed from a solution containing ChxR and αCTD (Fig. 4.8). In the absence of ChxR, a small amount of αCTD was detected, which was likely due to minor non-specific interactions between the αCTD and the antibodies or beads. In the presence of ChxR, a relatively large amount of αCTD was detected, which suggests that these two proteins interact. Given that both OmpR and PhoB have

FIG. 4.8. ChxR interacts with the αCTD. To determine of ChxR interacts with the αCTD, recombinant ChxR was immunoprecipitated in the presence (+) or absence (-) of αCTD using anti-ChxR antibodies (αChxR). The samples were subjected to SDS-PAGE and an immunoblot was performed using anti-ChxR and anti-RNA polymerase antibodies.

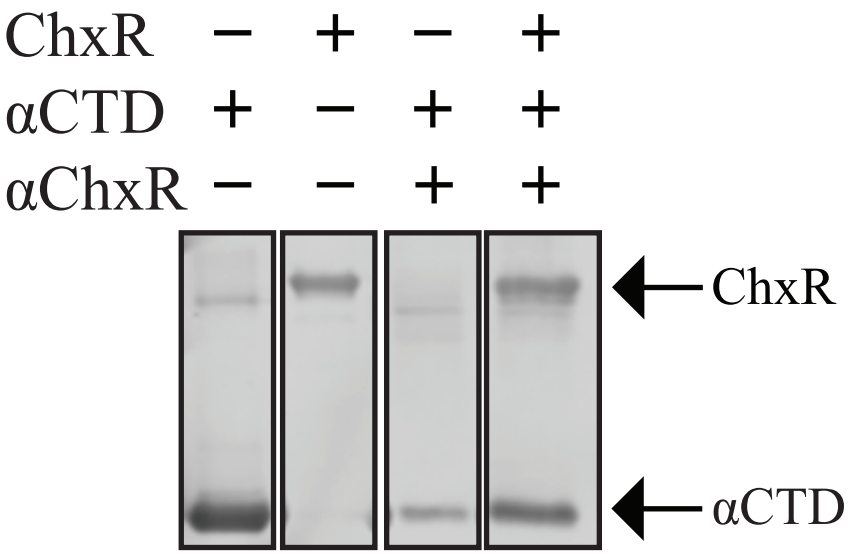
ChxR − + − +
αCTD + − + +
αChxR − − + +
ChxR
αCTD

been determined to interact with RNA polymerase machinery through their respective transactivation loops, we speculate that the residues that comprise the putative transactivation loop in ChxR (α2-α3) interact with the αCTD.

Chapter V

Discussion

OmpR/PhoB homologs activate transcription through a conserved mechanism (Stock, Robinson et al. 2000). Phosphorylation generally stabilizes the active conformation of the receiver domain, which promotes dimerization (Bachhawat and Stock 2007). This interaction allows the effector domain to bind to DNA and recruit RNA polymerase to activate transcription (Mack, Gao et al. 2009). ChxR was previously demonstrated to interact with its own promoter and activate the transcription of the *chxR* gene in the absence of phosphorylation (Koo, Walthers et al. 2006). The central hypothesis for this research was that the intra- and intermolecular interactions involved in forming a transcriptionally competent ChxR are distinct from the canonical phosphorylation (activation) paradigm in the OmpR/PhoB response regulator subfamily. The central aim of this work was to characterize each of the steps of activation (dimerization, DNA binding, and interaction with RNA polymerase) in order to begin to delineate the mechanism of ChxR transcriptional activation. This study expands upon a previous investigation into the ChxR-driven mechanism of transcriptional activation (Koo, Walthers et al. 2006) and facilitates the development of a working model of this mechanism (Fig. 5.1). The analysis of the structure-function relationships of ChxR are likely to aid in the rational design of small molecule compounds that inhibit the function of ChxR. Furthermore, the identification of the canonical DNA sequence recognized by ChxR could be used to identify potential binding sites within the promoters of its gene targets. The canonical sequence may also be used to identify additional gene targets, which will advance our knowledge of the functional role of ChxR in *Chlamydia*.

FIG. 5.1. A working model of ChxR interacting with DNA to activate transcription. A) ChxR forms a relatively stable homodimer through the α2-β5-α3 region of the receiver domain. The effector domain interacts with a direct repeat DNA sequence (WHGAWNH-N_{3-5}-WHGAWNH) in a head-to-tail fashion. B) Three residues (Asn182, His186, and Lys192; red) are proposed to make direct contact with DNA. C) ChxR potentially recruits RNA polymerase to the promoter through an interaction between the α7-α8 loop (red) and the αCTD. D) An overall model of a ChxR homodimer interacting with RNA to activate the transcription of a gene. The effector domains and DNA depicted within this figure are the PhoB effector domain bound to DNA (PDB ID 1GXP; (Blanco, Sola et al. 2002)).

A

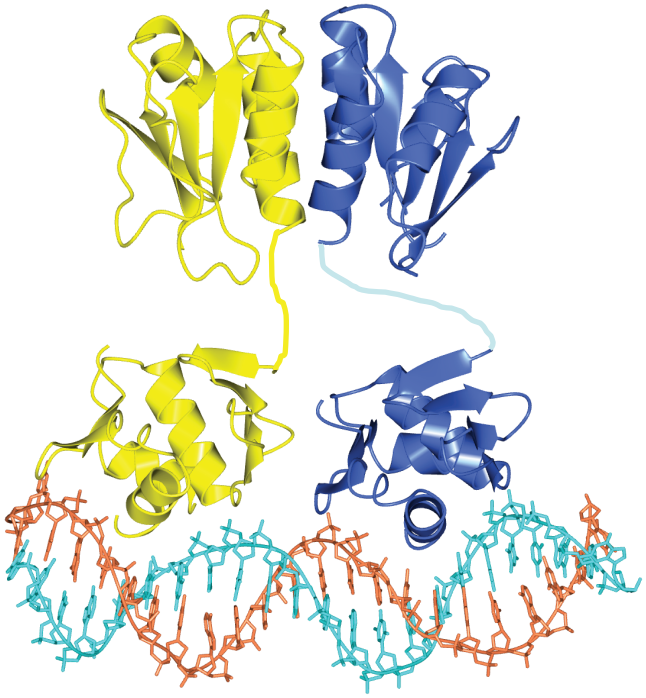

B

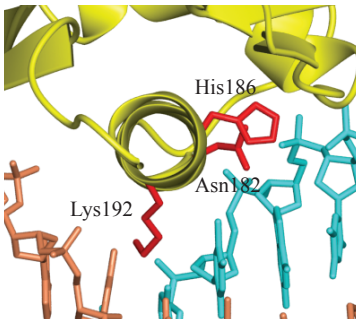
His186
Asn182
Lys192

C

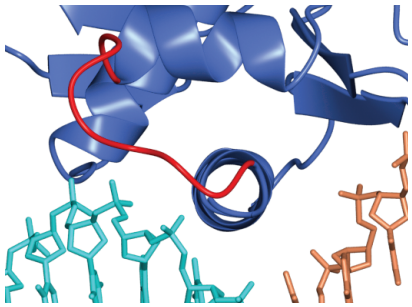

D

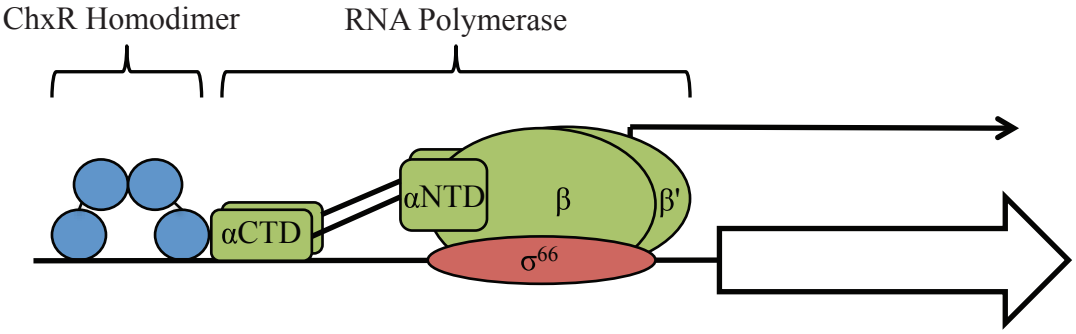
ChxR Homodimer
RNA Polymerase
αCTD
αNTD
β
β'
σ66

A working model of the mechanism of ChxR transcriptional activation

The results from this study, in conjunction with the findings of an earlier investigation (Koo, Walthers et al. 2006), have begun the process of elucidating the mechanism of ChxR transcriptional activation. Figure 5.1 depicts a working model of this mechanism, in which ChxR forms a stable homodimer through the receiver domain, binds to a direct repeat DNA sequence through specific residues within the recognition helix, and recruits the αCTD of RNA polymerase to the promoter in order to activate transcription. The mechanism of ChxR transcriptional regulation is likely much more complex than depicted in this simple model, given that ChxR recognizes six sites within the *chxR* promoter. Given the number and separation of these six binding sites, DNA bending and cooperative binding between dimers may also contribute to this mechanism. DNA bending and cooperative binding have been observed in other OmpR/PhoB response regulators that bind to multiple sites within a promoter (Makino, Amemura et al. 1996; Spencer, Siam et al. 2009). Future experiments will be designed to determine the contribution of each binding site to this process.

Functionally important regions in ChxR

ChxR forms stable homodimers primarily through hydrophobic interactions. Full-length ChxR was determined to form homodimers *in vivo* and *in vitro* through the use of a chemical crosslinker (Fig. 2.2). Additionally, ChxR was determined to form homodimers at concentrations from 100μM-1μM through analytical size exclusion chromatography (Fig. 3.3), which indicates that ChxR protomers form a stable complex. This stability originates from the relatively large

number of hydrophobic residues at the dimer interface. Hydrophobic interactions have been proposed to be the primary stabilizing force of protein-protein interactions (Tsai, Lin et al. 1997; Moreira, Fernandes et al. 2007). The observation that ChxR forms dimers primarily through hydrophobic interactions was further supported by subjecting proteins with residue substitutions within the receiver domain to size exclusion chromatography. The only substitution that abolished dimer formation was to a residue (W89E) within the hydrophobic core of the dimer interface (Fig. 3.7). Additionally, the ability of the W89E monomeric protein to bind DNA was significantly reduced compared to wild-type ChxR (Fig. 3.8). In combination, these results indicate that ChxR forms a stable dimer, which is critical to the functional activity of this transcription factor.

Interestingly, these findings are in stark contrast to other OmpR/PhoB response regulators. Phosphorylation-dependent OmpR/PhoB response regulators primarily interact through a highly conserved network of salt bridges and oligomerization is predominantly regulated through phosphorylation (Toro-Roman, Mack et al. 2005). In contrast, the oligomeric states of atypical OmpR/PhoB subfamily members and the interactions between these response regulators are not as well conserved. As stated above, ChxR forms stable homodimers through hydrophobic interactions. HP1043 (*Helicobacter pylori*) forms dimers through both hydrophobic interactions and salt bridges; although, the stability of this dimer has not been determined (Hong, Lee et al. 2007). In contrast to ChxR and HP1043, NblR (*Synechococcus elongates*) is monomeric in solution and does not appear to form dimers (Ruiz, Salinas et al. 2008). The oligomeric state of the three other atypical OmpR/PhoB homologs (JadR1 (*Streptomyces venezuelae*), HP1021 (*Helicobacter pylori*), and FrzS (*Myxococcus xanthus*)) has not been reported. These differing characteristics between ChxR, HP1043, and NblR are likely a result of

their affinity and specificity for DNA. Disrupting dimerization in HP1043 did not affect DNA binding (Hong, Lee et al. 2007); however, disrupting this protein-protein interaction in ChxR significantly reduced DNA binding (Fig. 3.8). This suggests that HP1043 forms dimers primarily to increase DNA specificity while ChxR forms dimers to increase both DNA affinity and specificity.

In contrast to the uncommon characteristics of the ChxR receiver domain, the effector domain appears to interact with DNA in a similar fashion to phosphorylation-induced and transcriptionally active OmpR/PhoB response regulators. For other OmpR/PhoB response regulators, the process of DNA binding is accomplished through the winged helix-turn-helix motif within the effector domain. The secondary structure of the ChxR effector domain was determined through NMR and contains a winged helix-turn-helix motif, similar to the typical OmpR/PhoB effector domain structure (Fig. 4.6). An NMR chemical shift titration experiment identified putative DNA-binding residues, many of which reside within the putative DNA binding winged helix-turn-helix motif (Fig. 4.7B). To determine which of the residues interact with DNA, Ala substitutions were generated for each putative DNA binding residue and the ability of each protein to bind DNA was tested through an electrophoretic mobility shift assay (Fig. 4.7C). Substitutions of three residues (Asn182, His186, and Lys192) significantly reduced DNA binding and suggest that these residues may interact with DNA (Fig. 5.1B). These results also support the conclusion that ChxR interacts with DNA in a similar manner to other OmpR/PhoB response regulators.

Additional support for this conclusion comes from the direct repeat DNA sequence recognized by ChxR. OmpR/PhoB response regulators generally recognizes a direct or inverted repeat DNA sequence, which ranges from 18–23 bp, containing two 6–10 bp DNA-binding sites

and is separated by 2–5 bp of intervening sequence (Harlocker, Bergstrom et al. 1995; Blanco, Sola et al. 2002; Kenney 2002). ChxR was found to bind to a direct repeat sequence, which consists of two 7 bp binding sites separated by 3-5 bp (Fig. 2.4). The length of each binding site and intervening sequence are analogous with other OmpR/PhoB homologs. Additionally, the direct repeat binding sequence indicates that the effector domain of ChxR binds the DNA in a head-to-tail fashion.

Once bound to DNA, members of the OmpR/PhoB subfamily have been reported to interact with either the σ factor or the α-subunit of RNA polymerase to activate transcription (Chen, Abdel-Fattah et al. 2004). ChxR was hypothesized to interact with the C-terminal domain of the α–subunit of RNA polymerase, given the location of the DR1 binding site within the *chxR* promoter. The detection of the αCTD from a co-immunoprecipitation with recombinant ChxR supports the hypothesis that these two proteins interact (Fig. 4.8). This finding also suggests that ChxR recruits the αCTD of RNA polymerase to the *chxR* promoter in order to activate transcription (Fig. 5.1D).

A potential regulatory mechanism

Recent studies of two atypical response regulators (JadR1 and NblR) have reported that their functional activity is regulated through an interaction with a small molecule ligand or another protein (Ruiz, Salinas et al. 2008; Wang, Tian et al. 2009). Similar to JadR1 and NblR, all of the data currently available indicates that the functional activity of ChxR is not regulated through phosphorylation. Therefore, ChxR could potentially be regulated through protein-ligand or protein-protein interactions.

If ChxR is regulated though either of these mechanisms, the two random coils in the receiver domain may serve as the site of this interaction. Many studies have reported that random coils in proteins can undergo conformational transitions into more rigid structures in the presence of binding partners (Sandhu and Dash 2007). RecA is an example of one of these proteins, as the helical content of the protein increases in the presence of DNA (Kumar, Mahalakshmi et al. 1993). The most commonly observed random coil-to-structured transition occurs in short (8-12 residues), hydrophilic regions that form a helix upon binding. Similarly, the two random coils in the ChxR receiver domain are short (8 and 11, residues respectively) and contain few hydrophobic residues (1 and 2, respectively). If ChxR is post-transcriptionally regulated, these similarities suggest that the two random coils in the receiver domain may participate in the regulation.

Post-translational regulation of ChxR would likely occur during chlamydial persistence. Persistent *Chlamydia* are non-replicating and do not convert into EB. Additionally, the expression of late stage genes decreases during persistence. A transcriptome analysis of persistent *C. trachomatis* at 12, 24, and 48 hpi revealed that the transcript levels of *chxR* are not altered relative to *chxR* transcript levels during a normal developmental cycle (Belland, Nelson et al. 2003). During normal growth, *chxR* transcripts are relatively low during the early stages of the developmental cycle but increase dramatically from 18-to-24 hpi and are sustained at an increased level throughout the rest of the developmental cycle (Fig. 1.5). The translational profile correlates with this observation, as ChxR is not detected until 24 hpi and increases in concentration at 36 hpi (Fig. 2.2). If the concentration of ChxR protein is unchanged during persistence, the activity of ChxR may be regulated through post-translational mechanisms given

that some of the late stage gene promoters' immunoprecipitated with ChxR and are therefore potential gene targets (Spedding 2009).

ChxR as a novel drug target

Due to the association between ChxR, and middle and late stage genes, which are likely essential for chlamydial viability, ChxR is an attractive target for the development of novel antimicrobial therapies. ChxR contains multiple regions that appear to be critical to its function, including the dimer interface and the DNA binding motif. Given the structural similarity of the ChxR effector domain and other OmpR/PhoB subfamily members, a compound that would inhibit either the DNA binding or RNA polymerase interaction activity of the ChxR effector domain may also be effective in inhibiting the activity of OmpR/PhoB response regulators in other pathogenic bacteria. In contrast, a compound that would inhibit the formation of ChxR dimers would likely be specific to this response regulator since the ChxR receiver domain has many unique features not found in many other OmpR/PhoB response regulators. The ample number of OmpR/PhoB effector domain structures currently available and the experimentally determined structure of the ChxR receiver domain described within this study will likely facilitate the rational design of these inhibitory compounds.

Currently, research on other OmpR/PhoB transcriptional regulators in pathogenic bacteria has identified a promising binding site for an inhibitory compound. The effector domain of WalR, an essential transcription factor in *Staphylococcus aureus*, was recently experimentally determined (Doi, Okajima et al. 2010). A cavity near the DNA recognition helix was discovered that is conserved in the WalR orthologs from *Bacillus subtilis* and *Enterococcus faecalis*.

Furthermore, the residues surrounding this cavity are highly conserved among pathogenic bacteria and are required for interaction with DNA. Interestingly, many of these residues are shared in ChxR and include: Asp184, Ile187A, Arg191, and Tyr209. Additionally, a residue (Lys192) in ChxR that is not shared but is in the same position as one of the conserved residues in WalR was determined to be important for ChxR-DNA interaction (Fig. 4.7C). These findings could indicate that this cavity is present in ChxR and a compound that would inhibit DNA interaction in ChxR would be effective at inhibiting the activity of WalR and other OmpR/PhoB homologs in pathogenic bacteria.

Identifying putative ChxR binding sites within the promoters of additional gene targets

Extensive analysis of the association between ChxR and the *chxR* promoter revealed that ChxR recognizes six binding sites within the promoter. These six DNA sequences were used to generate a consensus recognition sequence (WHGAWNW-N_{3-5}-WHGAWNW), which occurs at 3303 sites within the chlamydial genome (*C. trachomatis* L2/434/Bu). The GA nucleotides are generally conserved in all of the recognition sites and triple mutations to the central GAW dramatically reduce ChxR-DNA interaction, suggesting that these two nucleotides are critical for recognition. As stated in Chapter I, ChxR could be immunoprecipitated with promoter regions for many chlamydial genes (*chxR*, *CT084*, *CT091*, *CT322*, *CT323*, *CT444*, *CT480*, *CT557*, *CT559*, *CT576*, *CT619/620*, and *CT733/734*). The ChxR recognition sequence was used to search the 300bp upstream regions of these genes to identify putative ChxR binding sites. As Table 5.1 demonstrates, putative ChxR binding sites were identified within the promoters of these genes. The distances of the putative binding sites relative to their transcriptional start sites (-172 to -71 bp) suggest that ChxR might activate the expression of these genes by interacting

with the αCTD of RNA polymerase. It is expected that additional gene targets of ChxR will be identified using this consensus sequence in combination with ChIP-PCR and other experimental analyses.

ChxR was found to be associated with the predicted promoter regions of two diverging genes (*CT619* and *CT620*) through a ChIP-PCR assay (Spedding 2009). However, the overlap of these two promoters prevents a direct linkage of ChxR with either of these genes. As a result, the only conclusion that could be drawn from this analysis is that ChxR binds to DNA between these two genes. Interestingly, no ChxR binding sites were identifiable in the 300bp upstream region of *CT620* but two putative binding sites were identified for the *CT619* upstream region. This suggests that *CT619* is the gene target of ChxR from this region but experimental evidence is clearly needed to correlate ChxR with the promoter of *CT619*.

Table 5.1 Putative ChxR recognition sites

Open Reading Frame	Binding Site[1]	Binding Site[2]	Sequence[3]
CT084	-154 to -136	-269 to -251	CTGAATG-N4-ATGAAAC
	-123 to -105	-238 to -220	AGGAAGT-N4-CTGATGA
CT091	-162 to -144	-194 to -176	AAGAAAT-N4-AAGAAAA
	-151 to -134	-183 to -166	AAGAAAA-N3-AAGATTA
CT322	ND	-199 to -183	GAGAAAA-N3-TTGAGGC
	ND	-162 to -147	GGGAAAG-N3-CCGATGC
CT323	-126 to -108	-236 to -218	TTGAGTC-N5-AGGACAA
CT444	-128 to -112	-219 to -203	CGGATTC-N3-GAGATAA
CT480	-174 to -158	-266 to -250	GAGATCC-N3-TCGATAG
	-119 to -102	-211 to -194	GAGAATC-N4-AAGAAAA
CT557	-162 to -145	-290 to -273	TAGATGT-N4-GCGATTC
	-103 to -86	-231 to -214	TCGAATG-N4-GGGAGAG
CT559	-248 to -231	-266 to -249	TCGAAAG-N4-GGGAGAC
	-157 to -138	-175 to -156	CGGATTC-N5-TTGAAGC
CT576	-197 to -181	-237 to -221	GAGACAG-N3-GAGAGAA
	-173 to -158	-213 to -198	GCGAAAG-N3-TGGACTT
CT619	-202 to -186	-226 to -210	TTGATTC-N3-CAGAAAG
	-107 to -89	-131 to -113	GAGATGT-N5-ATGAACA
CT733	-87 to -71	-279 to -263	AGGATAG-N3-GGGATTG
CT734	-188 to -172	-215 to -199	TGGATTC-N3-GAGAGAT

[1] Binding site relative to the transcriptional start site (Albrecht, Sharma et al. 2010)
[2] Binding site relative to the translational start site (Thomson, Holden et al. 2008)
[3] DNA sequences from *C. trachomatis* L2/434/Bu genome

Evolution of ChxR

The structure of the ChxR receiver domain revealed many contrasting features to both the typical and atypical OmpR/PhoB response regulators. Features distinct to ChxR include: the unique residue composition of the canonical site of phosphorylation, the "inactive" orientation of the conformational switch residues, the relatively large number of hydrophobic residues at the dimer interface, and the absence of two α-helices present in all other OmpR/PhoB response regulators (Fig. 3.5). The atypical characteristics of ChxR relative to other OmpR/PhoB response regulators could be a result of the evolutionary divergence of pathogenic chlamydiae.

As stated in Chapter I, chlamydiae diverged from other bacteria approximately two billion years ago and became obligate intracellular pathogens approximately 700 million years ago (Horn, Collingro et al. 2004). Genomes of pathogenic chlamydiae, which are approximately 1-1.2 Mbp, are half as large and highly reorganized compared to environmental chlamydiae (Stephens, Kalman et al. 1998; Horn, Collingro et al. 2004). ChxR is conserved among all pathogenic chlamydiae but absent in environmental chlamydiae (*Parachlamydia acanthamoebae* and *Protochlamydia amoebophila*). Interestingly, these environmental chlamydiae encode a OmpR/PhoB response regulator that appears to be regulated through phosphorylation, as both the phospho-accepting Asp and a cognate sensor kinase are present in their genomes. Given these findings, a possible theory for the atypical nature of ChxR is that it originated from a typical, phospho-accepting OmpR/PhoB response regulator that was present in a common chlamydial ancestor. As the ancestor evolved into the pathogenic chlamydiae of today, the stimuli sensed by a ChxR cognate sensor kinase may not have been present or was present but at a static concentration, which would essentially abolish the transcriptional response of the two-

component system. Therefore, as the organism evolved, the sensor kinase was lost and the response regulator was modulated into the atypical OmpR/PhoB transcriptional regulator in present-day *Chlamydia*.

This theory that ChxR evolved from a phospho-accepting OmpR/PhoB ancestor is supported through the evolution of pathogenic chlamydiae. Very little evidence exists of lateral gene transfer events in pathogenic chlamydiae (Horn, Collingro et al. 2004), indicating that after their separation from environmental chlamydiae ~700 million years ago, the organisms evolved through vertical gene transfer. This suggests that ChxR was not acquired from another organism; rather, ChxR arose from chlamydiae adapting to their animal hosts. This is exemplified in the genetic variation of ChxR in *C. trachomatis* and *C. pneumoniae* in which phylogenetic analysis indicates that the two species of *Chlamydia* diverged approximately 60-100 million years ago (Stephens, Myers et al. 2009). ChxR from *C. trachomatis* (L2/434/Bu) is 48.5% identical and 64.3% similar to ChxR from *C. pneumoniae* (AR39), demonstrating that *chxR* has undergone extensive mutagenesis from a common ancestor.

References

Abdelrahman, Y. M. and R. J. Belland (2005). "The chlamydial developmental cycle." FEMS Microbiol Rev **29**(5): 949-959.

Abdelrahman, Y. M., L. A. Rose and R. J. Belland (2010). "Developmental expression of non-coding RNAs in Chlamydia trachomatis during normal and persistent growth." Nucleic Acids Res.

Adams, P. D., P. V. Afonine, G. Bunkoczi, V. B. Chen, I. W. Davis, N. Echols, J. J. Headd, L. W. Hung, G. J. Kapral, R. W. Grosse-Kunstleve, A. J. McCoy, N. W. Moriarty, R. Oeffner, R. J. Read, D. C. Richardson, J. S. Richardson, T. C. Terwilliger and P. H. Zwart (2010). "PHENIX: a comprehensive Python-based system for macromolecular structure solution." Acta Crystallogr D Biol Crystallogr **66**(Pt 2): 213-221.

Ainsa, J. A., H. D. Parry and K. F. Chater (1999). "A response regulator-like protein that functions at an intermediate stage of sporulation in Streptomyces coelicolor A3(2)." Mol Microbiol **34**(3): 607-619.

Akers, J. C. and M. Tan (2006). "Molecular mechanism of tryptophan-dependent transcriptional regulation in Chlamydia trachomatis." J Bacteriol **188**(12): 4236-4243.

al-Rifai, K. M. (1988). "Trachoma through history." Int Ophthalmol **12**(1): 9-14.

Albrecht, M., C. M. Sharma, R. Reinhardt, J. Vogel and T. Rudel (2010). "Deep sequencing-based discovery of the Chlamydia trachomatis transcriptome." Nucleic Acids Res **38**(3): 868-877.

Appelt, D. M., M. R. Roupas, D. S. Way, M. G. Bell, E. V. Albert, C. J. Hammond and B. J. Balin (2008). "Inhibition of apoptosis in neuronal cells infected with Chlamydophila (Chlamydia) pneumoniae." BMC Neurosci **9**: 13.

Appleby, J. L. and R. B. Bourret (1998). "Proposed signal transduction role for conserved CheY residue Thr87, a member of the response regulator active-site quintet." J Bacteriol **180**(14): 3563-3569.

Arribas-Bosacoma, R., S. K. Kim, C. Ferrer-Orta, A. G. Blanco, P. J. Pereira, F. X. Gomis-Ruth, B. L. Wanner, M. Coll and M. Sola (2007). "The X-ray crystal structures of two constitutively active mutants of the Escherichia coli PhoB receiver domain give insights into activation." J Mol Biol **366**(2): 626-641.

Bachhawat, P. and A. M. Stock (2007). "Crystal structures of the receiver domain of the response regulator PhoP from Escherichia coli in the absence and presence of the phosphoryl analog beryllofluoride." J Bacteriol **189**(16): 5987-5995.

Bachhawat, P., G. V. Swapna, G. T. Montelione and A. M. Stock (2005). "Mechanism of activation for transcription factor PhoB suggested by different modes of dimerization in the inactive and active states." Structure **13**(9): 1353-1363.

Baikalov, I., I. Schroder, M. Kaczor-Grzeskowiak, K. Grzeskowiak, R. P. Gunsalus and R. E. Dickerson (1996). "Structure of the Escherichia coli response regulator NarL." Biochemistry **35**(34): 11053-11061.

Barnard, A., A. Wolfe and S. Busby (2004). "Regulation at complex bacterial promoters: how bacteria use different promoter organizations to produce different regulatory outcomes." Curr Opin Microbiol **7**(2): 102-108.

Beatty, W. L., R. P. Morrison and G. I. Byrne (1994). "Persistent chlamydiae: from cell culture to a paradigm for chlamydial pathogenesis." Microbiol Rev **58**(4): 686-699.

Bebear, C. and B. de Barbeyrac (2009). "Genital Chlamydia trachomatis infections." Clin Microbiol Infect **15**(1): 4-10.

Beck, T., A. Krasauskas, T. Gruene and G. M. Sheldrick (2008). "A magic triangle for experimental phasing of macromolecules." Acta Crystallogr D Biol Crystallogr **64**(Pt 11): 1179-1182.

Beier, D. and R. Frank (2000). "Molecular characterization of two-component systems of Helicobacter pylori." J Bacteriol **182**(8): 2068-2076.

Belland, R. J., D. E. Nelson, D. Virok, D. D. Crane, D. Hogan, D. Sturdevant, W. L. Beatty and H. D. Caldwell (2003). "Transcriptome analysis of chlamydial growth during IFN-gamma-mediated persistence and reactivation." Proc Natl Acad Sci U S A **100**(26): 15971-15976.

Belland, R. J., G. Zhong, D. D. Crane, D. Hogan, D. Sturdevant, J. Sharma, W. L. Beatty and H. D. Caldwell (2003). "Genomic transcriptional profiling of the developmental cycle of Chlamydia trachomatis." Proc Natl Acad Sci U S A **100**(14): 8478-8483.

Bergstrom, L. C., L. Qin, S. L. Harlocker, L. A. Egger and M. Inouye (1998). "Hierarchical and co-operative binding of OmpR to a fusion construct containing the ompC and ompF upstream regulatory sequences of Escherichia coli." Genes Cells **3**(12): 777-788.

Blanco, A. G., M. Sola, F. X. Gomis-Ruth and M. Coll (2002). "Tandem DNA recognition by PhoB, a two-component signal transduction transcriptional activator." Structure **10**(5): 701-713.

Blasi, F. (2004). "Atypical pathogens and respiratory tract infections." Eur Respir J **24**(1): 171-181.

Bohm, G., R. Muhr and R. Jaenicke (1992). "Quantitative analysis of protein far UV circular dichroism spectra by neural networks." Protein Eng **5**(3): 191-195.

Bourret, R. B. (2010). "Receiver domain structure and function in response regulator proteins." Curr Opin Microbiol **13**(2): 142-149.

Brennan, R. G. (1993). "The winged-helix DNA-binding motif: another helix-turn-helix takeoff." Cell **74**(5): 773-776.

Brickman, T. J., C. E. Barry, 3rd and T. Hackstadt (1993). "Molecular cloning and expression of hctB encoding a strain-variant chlamydial histone-like protein with DNA-binding activity." J Bacteriol **175**(14): 4274-4281.

Burton, M. J., S. N. Rajak, J. Bauer, H. A. Weiss, S. B. Tolbert, A. Shoo, E. Habtamu, A. Manjurano, P. M. Emerson, D. C. Mabey, M. J. Holland and R. L. Bailey (2011). "Conjunctival transcriptome in scarring trachoma." Infect Immun **79**(1): 499-511.

Cai, S. J. and M. Inouye (2002). "EnvZ-OmpR interaction and osmoregulation in Escherichia coli." J Biol Chem **277**(27): 24155-24161.

Campbell, L. A. and C. C. Kuo (2004). "Chlamydia pneumoniae--an infectious risk factor for atherosclerosis?" Nat Rev Microbiol **2**(1): 23-32.

Case, E. D., E. M. Peterson and M. Tan "Promoters for Chlamydia type III secretion genes show a differential response to DNA supercoiling that correlates with temporal expression pattern." J Bacteriol **192**(10): 2569-2574.

CDC (2010). "Summary of notifiable diseases-United States, 2008." Morbidity and Mortality Weekly Report **57**(54).

Chater, K. F. (1972). "A morphological and genetic mapping study of white colony mutants of Streptomyces coelicolor." J Gen Microbiol **72**(1): 9-28.

Chen, Y., W. R. Abdel-Fattah and F. M. Hulett (2004). "Residues required for Bacillus subtilis PhoP DNA binding or RNA polymerase interaction: alanine scanning of PhoP effector domain transactivation loop and alpha helix 3." J Bacteriol **186**(5): 1493-1502.

Chen, Y., C. Birck, J. P. Samama and F. M. Hulett (2003). "Residue R113 is essential for PhoP dimerization and function: a residue buried in the asymmetric PhoP dimer interface determined in the PhoPN three-dimensional crystal structure." J Bacteriol **185**(1): 262-273.

Collaborative Computational Project, N. (1994). "The CCP4 suite: programs for protein crystallography." Acta Crystallogr D Biol Crystallogr **50**(Pt 5): 760-763.

Cowtan, K. (2006). "The Buccaneer software for automated model building. 1. Tracing protein chains." Acta Crystallogr D Biol Crystallogr **62**(Pt 9): 1002-1011.

Crooks, G. E., G. Hon, J. M. Chandonia and S. E. Brenner (2004). "WebLogo: a sequence logo generator." Genome Res **14**(6): 1188-1190.

Delaglio, F., S. Grzesiek, G. W. Vuister, G. Zhu, J. Pfeifer and A. Bax (1995). "NMRPipe: a multidimensional spectral processing system based on UNIX pipes." J Biomol NMR **6**(3): 277-293.

Delany, I., G. Spohn, R. Rappuoli and V. Scarlato (2002). "Growth phase-dependent regulation of target gene promoters for binding of the essential orphan response regulator HP1043 of Helicobacter pylori." J Bacteriol **184**(17): 4800-4810.

Doi, A., T. Okajima, Y. Gotoh, K. Tanizawa and R. Utsumi (2010). "X-ray crystal structure of the DNA-binding domain of response regulator WalR essential to the cell viability of staphylococcus aureus and interaction with target DNA." Biosci Biotechnol Biochem **74**(9): 1901-1907.

Dong, F. and H. X. Zhou (2002). "Electrostatic contributions to T4 lysozyme stability: solvent-exposed charges versus semi-buried salt bridges." Biophys J **83**(3): 1341-1347.

Eckmann, L., M. F. Kagnoff and J. Fierer (1993). "Epithelial cells secrete the chemokine interleukin-8 in response to bacterial entry." Infect Immun **61**(11): 4569-4574.

Emsley, P. and K. Cowtan (2004). "Coot: model-building tools for molecular graphics." Acta Crystallogr D Biol Crystallogr **60**(Pt 12 Pt 1): 2126-2132.

Evans, P. (2006). "Scaling and assessment of data quality." Acta Crystallogr D Biol Crystallogr **62**(Pt 1): 72-82.

Fahr, M. J., A. L. Douglas, W. Xia and T. P. Hatch (1995). "Characterization of late gene promoters of Chlamydia trachomatis." J Bacteriol **177**(15): 4252-4260.

Fraser, J. S., J. P. Merlie, Jr., N. Echols, S. R. Weisfield, T. Mignot, D. E. Wemmer, D. R. Zusman and T. Alber (2007). "An atypical receiver domain controls the dynamic polar localization of the Myxococcus xanthus social motility protein FrzS." Mol Microbiol **65**(2): 319-332.

Friedland, N., T. R. Mack, M. Yu, L. W. Hung, T. C. Terwilliger, G. S. Waldo and A. M. Stock (2007). "Domain orientation in the inactive response regulator Mycobacterium tuberculosis MtrA provides a barrier to activation." Biochemistry **46**(23): 6733-6743.

Galperin, M. Y. (2005). "A census of membrane-bound and intracellular signal transduction proteins in bacteria: bacterial IQ, extroverts and introverts." BMC Microbiol **5**: 35.

Galperin, M. Y. (2006). "Structural classification of bacterial response regulators: diversity of output domains and domain combinations." J Bacteriol **188**(12): 4169-4182.

Gao, R., T. R. Mack and A. M. Stock (2007). "Bacterial response regulators: versatile regulatory strategies from common domains." Trends Biochem Sci **32**(5): 225-234.

Gao, R., A. Mukhopadhyay, F. Fang and D. G. Lynn (2006). "Constitutive activation of two-component response regulators: characterization of VirG activation in Agrobacterium tumefaciens." J Bacteriol **188**(14): 5204-5211.

Gao, R. and A. M. Stock (2009). "Biological insights from structures of two-component proteins." Annu Rev Microbiol **63**: 133-154.

Gaydos, C. A., C. P. Cartwright, P. Colaninno, J. Welsch, J. Holden, S. Y. Ho, E. M. Webb, C. Anderson, R. Bertuzis, L. Zhang, T. Miller, G. Leckie, K. Abravaya and J. Robinson (2010). "Performance of the Abbott RealTime CT/NG for detection of Chlamydia trachomatis and Neisseria gonorrhoeae." J Clin Microbiol **48**(9): 3236-3243.

Gaydos, C. A., J. T. Summersgill, N. N. Sahney, J. A. Ramirez and T. C. Quinn (1996). "Replication of Chlamydia pneumoniae in vitro in human macrophages, endothelial cells, and aortic artery smooth muscle cells." Infect Immun **64**(5): 1614-1620.

Gerbase, A. C., J. T. Rowley and T. E. Mertens (1998). "Global epidemiology of sexually transmitted diseases." Lancet **351 Suppl 3**: 2-4.

Gooderham, W. J. and R. Hancock (2008). "Regulation of virulence and antibiotic resistance by two-component regulatory systems in Pseudomonas aeruginosa." FEMS microbiology reviews **33**: 279-294.

Gotoh, Y., Y. Eguchi, T. Watanabe, S. Okamoto, A. Doi and R. Utsumi (2010). "Two-component signal transduction as potential drug targets in pathogenic bacteria." Curr Opin Microbiol **13**(2): 232-239.

Grayston, J. T. (2000). "Background and current knowledge of Chlamydia pneumoniae and atherosclerosis." J Infect Dis **181 Suppl 3**: S402-410.

Gupta, S. S., B. N. Borin, T. L. Cover and A. M. Krezel (2009). "Structural analysis of the DNA-binding domain of the Helicobacter pylori response regulator ArsR." J Biol Chem **284**(10): 6536-6545.
Haddad, D. (2010). "Ten years left to eliminate blinding trachoma." Community Eye Health **23**(73): 38.
Harlocker, S. L., L. Bergstrom and M. Inouye (1995). "Tandem binding of six OmpR proteins to the ompF upstream regulatory sequence of Escherichia coli." J Biol Chem **270**(45): 26849-26856.
Hatch, T. P. (1999). "Developmental biology, in Chlamydia: Intracellular Biology, Pathogenesis, and Immunity." American Society of Microbiology: Washington, D.C.: 47-76.
Hatch, T. P., I. Allan and J. H. Pearce (1984). "Structural and polypeptide differences between envelopes of infective and reproductive life cycle forms of Chlamydia spp." J Bacteriol **157**(1): 13-20.
Head, C. G., A. Tardy and L. J. Kenney (1998). "Relative binding affinities of OmpR and OmpR-phosphate at the ompF and ompC regulatory sites." J Mol Biol **281**(5): 857-870.
Hefty, P. S. and R. S. Stephens (2007). "Chlamydial type III secretion system is encoded on ten operons preceded by sigma 70-like promoter elements." J Bacteriol **189**(1): 198-206.
Hickey, J. M., P. S. Hefty and A. L. Lamb (2009). "Expression, purification, crystallization and preliminary X-ray analysis of the DNA-binding domain of a Chlamydia trachomatis OmpR/PhoB-subfamily response regulator homolog, ChxR." Acta Crystallogr Sect F Struct Biol Cryst Commun **65**(Pt 8): 791-794.
Hickey, J. M., L. Weldon and P. S. Hefty (2011). "The atypical OmpR/PhoB response regulator ChxR from Chlamydia trachomatis forms homodimers in vivo and binds a direct repeat of nucleotide sequences." J Bacteriol **193**(2): 389-398.
Hoch, J. A. (2000). "Two-component and phosphorelay signal transduction." Curr Opin Microbiol **3**(2): 165-170.
Hogan, R. J., S. A. Mathews, S. Mukhopadhyay, J. T. Summersgill and P. Timms (2004). "Chlamydial persistence: beyond the biphasic paradigm." Infect Immun **72**(4): 1843-1855.
Hong, E., H. M. Lee, H. Ko, D. U. Kim, B. Y. Jeon, J. Jung, J. Shin, S. A. Lee, Y. Kim, Y. H. Jeon, C. Cheong, H. S. Cho and W. Lee (2007). "Structure of an atypical orphan response regulator protein supports a new phosphorylation-independent regulatory mechanism." J Biol Chem **282**(28): 20667-20675.
Horn, M., A. Collingro, S. Schmitz-Esser, C. L. Beier, U. Purkhold, B. Fartmann, P. Brandt, G. J. Nyakatura, M. Droege, D. Frishman, T. Rattei, H. W. Mewes and M. Wagner (2004). "Illuminating the evolutionary history of chlamydiae." Science **304**(5671): 728-730.
Hybiske, K. and R. S. Stephens (2007). "Mechanisms of host cell exit by the intracellular bacterium Chlamydia." Proc Natl Acad Sci U S A **104**(27): 11430-11435.
Itzhaki, R. F., M. A. Wozniak, D. M. Appelt and B. J. Balin (2004). "Infiltration of the brain by pathogens causes Alzheimer's disease." Neurobiol Aging **25**(5): 619-627.
Jelesarov, I. and A. Karshikoff (2008). Defining the Role of Salt Bridges in Protein Stability. **490:** 1-34.
Jones, B. D. (2005). "Salmonella invasion gene regulation: a story of environmental awareness." J Microbiol **43 Spec No**: 110-117.
Kato, H., T. Chibazakura and H. Yoshikawa (2008). "NblR is a novel one-component response regulator in the cyanobacterium Synechococcus elongatus PCC 7942." Biosci Biotechnol Biochem **72**(4): 1072-1079.
Kenney, L. J. (2002). "Structure/function relationships in OmpR and other winged-helix transcription factors." Curr Opin Microbiol **5**(2): 135-141.
King-Scott, J., E. Nowak, E. Mylonas, S. Panjikar, M. Roessle, D. I. Svergun and P. A. Tucker (2007). "The structure of a full-length response regulator from Mycobacterium tuberculosis in a stabilized three-dimensional domain-swapped, activated state." J Biol Chem **282**(52): 37717-37729.
Klose, K. E., D. S. Weiss and S. Kustu (1993). "Glutamate at the site of phosphorylation of nitrogen-regulatory protein NTRC mimics aspartyl-phosphate and activates the protein." J Mol Biol **232**(1): 67-78.

Kondo, H., A. Nakagawa, J. Nishihira, Y. Nishimura, T. Mizuno and I. Tanaka (1997). "Escherichia coli positive regulator OmpR has a large loop structure at the putative RNA polymerase interaction site." Nat Struct Biol **4**(1): 28-31.

Koo, I. C. and R. S. Stephens (2003). "A developmentally regulated two-component signal transduction system in Chlamydia." J Biol Chem **278**(19): 17314-17319.

Koo, I. C., D. Walthers, P. S. Hefty, L. J. Kenney and R. S. Stephens (2006). "ChxR is a transcriptional activator in Chlamydia." Proc Natl Acad Sci U S A **103**(3): 750-755.

Kumar, K. A., S. Mahalakshmi and K. Muniyappa (1993). "DNA-induced conformational changes in RecA protein. Evidence for structural heterogeneity among nucleoprotein filaments and implications for homologous pairing." J Biol Chem **268**(35): 26162-26170.

Langer, G., S. X. Cohen, V. S. Lamzin and A. Perrakis (2008). "Automated macromolecular model building for X-ray crystallography using ARP/wARP version 7." Nat Protoc **3**(7): 1171-1179.

Larkin, M. A., G. Blackshields, N. P. Brown, R. Chenna, P. A. McGettigan, H. McWilliam, F. Valentin, I. M. Wallace, A. Wilm, R. Lopez, J. D. Thompson, T. J. Gibson and D. G. Higgins (2007). "Clustal W and Clustal X version 2.0." Bioinformatics **23**(21): 2947-2948.

Lejona, S., M. E. Castelli, M. L. Cabeza, L. J. Kenney, E. Garcia Vescovi and F. C. Soncini (2004). "PhoP can activate its target genes in a PhoQ-independent manner." J Bacteriol **186**(8): 2476-2480.

Liu, Y. and D. Eisenberg (2002). "3D domain swapping: as domains continue to swap." Protein Sci **11**(6): 1285-1299.

Lozada-Chavez, I., V. E. Angarica, J. Collado-Vides and B. Contreras-Moreira (2008). "The role of DNA-binding specificity in the evolution of bacterial regulatory networks." J Mol Biol **379**(3): 627-643.

Luscombe, N. M. and J. M. Thornton (2002). "Protein-DNA interactions: amino acid conservation and the effects of mutations on binding specificity." J Mol Biol **320**(5): 991-1009.

Mack, T. R., R. Gao and A. M. Stock (2009). "Probing the roles of the two different dimers mediated by the receiver domain of the response regulator PhoB." J Mol Biol **389**(2): 349-364.

Makino, K., M. Amemura, T. Kawamoto, S. Kimura, H. Shinagawa, A. Nakata and M. Suzuki (1996). "DNA binding of PhoB and its interaction with RNA polymerase." J Mol Biol **259**(1): 15-26.

Maris, A. E., M. R. Sawaya, M. Kaczor-Grzeskowiak, M. R. Jarvis, S. M. Bearson, M. L. Kopka, I. Schroder, R. P. Gunsalus and R. E. Dickerson (2002). "Dimerization allows DNA target site recognition by the NarL response regulator." Nat Struct Biol **9**(10): 771-778.

Maris, A. E., D. Walthers, K. Mattison, N. Byers and L. J. Kenney (2005). "The response regulator OmpR oligomerizes via beta-sheets to form head-to-head dimers." J Mol Biol **350**(5): 843-856.

Marley, J., M. Lu and C. Bracken (2001). "A method for efficient isotopic labeling of recombinant proteins." J Biomol NMR **20**(1): 71-75.

Martinez-Hackert, E. and A. M. Stock (1997). "The DNA-binding domain of OmpR: crystal structures of a winged helix transcription factor." Structure **5**(1): 109-124.

Martinez-Hackert, E. and A. M. Stock (1997). "Structural relationships in the OmpR family of winged-helix transcription factors." J Mol Biol **269**(3): 301-312.

Mathews, S. A. and P. Timms (2000). "Identification and mapping of sigma-54 promoters in Chlamydia trachomatis." J Bacteriol **182**(21): 6239-6242.

McCoy, A. J., R. W. Grosse-Kunstleve, P. D. Adams, M. D. Winn, L. C. Storoni and R. J. Read (2007). "*Phaser* crystallographic software." J. Appl. Cryst. **40**: 658-674.

McCoy, A. J., R. W. Grosse-Kunstleve, P. D. Adams, M. D. Winn, L. C. Storoni and R. J. Read (2007). "Phaser crystallographic software." J Appl Crystallogr **40**(Pt 4): 658-674.

Mittal, S. and L. Kroos (2009). "A combination of unusual transcription factors binds cooperatively to control Myxococcus xanthus developmental gene expression." Proc Natl Acad Sci U S A **106**(6): 1965-1970.

Moreira, I. S., P. A. Fernandes and M. J. Ramos (2007). "Hot spots--a review of the protein-protein interface determinant amino-acid residues." Proteins **68**(4): 803-812.

Mukhopadhyay, S., D. Good, R. D. Miller, J. E. Graham, S. A. Mathews, P. Timms and J. T. Summersgill (2006). "Identification of Chlamydia pneumoniae proteins in the transition from reticulate to elementary body formation." Mol Cell Proteomics **5**(12): 2311-2318.

Murshudov, G. N., A. A. Vagin and E. J. Dodson (1997). "Refinement of macromolecular structures by the maximum-likelihood method." Acta Crystallogr D Biol Crystallogr **53**(Pt 3): 240-255.

Nicholson, T. L., L. Olinger, K. Chong, G. Schoolnik and R. S. Stephens (2003). "Global stage-specific gene regulation during the developmental cycle of Chlamydia trachomatis." J Bacteriol **185**(10): 3179-3189.

Niehus, E., E. Cheng and M. Tan (2008). "DNA supercoiling-dependent gene regulation in Chlamydia." J Bacteriol **190**(19): 6419-6427.

O'Connor, T. J. and J. R. Nodwell (2005). "Pivotal roles for the receiver domain in the mechanism of action of the response regulator RamR of Streptomyces coelicolor." J Mol Biol **351**(5): 1030-1047.

Otwinowski, Z. and W. Minor (1997). "Processing of X-ray diffraction data collected in oscillation mode." Macromolecular Crystallography, Pt A **276**: 307-326.

Painter, J. and E. A. Merritt (2006). "Optimal description of a protein structure in terms of multiple groups undergoing TLS motion." Acta Crystallogr D Biol Crystallogr **62**(Pt 4): 439-450.

Pflugrath, J. W. (1999). "The finer things in X-ray diffraction data collection." Acta Crystallogr D Biol Crystallogr **55**(Pt 10): 1718-1725.

Polack, S., S. Brooker, H. Kuper, S. Mariotti, D. Mabey and A. Foster (2005). "Mapping the global distribution of trachoma." Bull World Health Organ **83**(12): 913-919.

Potterton, L., S. McNicholas, E. Krissinel, J. Gruber, K. Cowtan, P. Emsley, G. N. Murshudov, S. Cohen, A. Perrakis and M. Noble (2004). "Developments in the CCP4 molecular-graphics project." Acta Crystallogr D Biol Crystallogr **60**(Pt 12 Pt 1): 2288-2294.

Rasmussen, S. J., L. Eckmann, A. J. Quayle, L. Shen, Y. X. Zhang, D. J. Anderson, J. Fierer, R. S. Stephens and M. F. Kagnoff (1997). "Secretion of proinflammatory cytokines by epithelial cells in response to Chlamydia infection suggests a central role for epithelial cells in chlamydial pathogenesis." J Clin Invest **99**(1): 77-87.

Resnikoff, S., D. Pascolini, D. Etya'ale, I. Kocur, R. Pararajasegaram, G. P. Pokharel and S. P. Mariotti (2004). "Global data on visual impairment in the year 2002." Bull World Health Organ **82**(11): 844-851.

Reynolds, C., D. Damerell and S. Jones (2009). "ProtorP: a protein-protein interaction analysis server." Bioinformatics **25**(3): 413-414.

Rhee, J. E., W. Sheng, L. K. Morgan, R. Nolet, X. Liao and L. J. Kenney (2008). "Amino acids important for DNA recognition by the response regulator OmpR." J Biol Chem **283**(13): 8664-8677.

Roan, N. R. and M. N. Starnbach (2008). "Immune-mediated control of Chlamydia infection." Cell Microbiol **10**(1): 9-19.

Rotter, C., S. Muhlbacher, D. Salamon, R. Schmitt and B. Scharf (2006). "Rem, a new transcriptional activator of motility and chemotaxis in Sinorhizobium meliloti." J Bacteriol **188**(19): 6932-6942.

Ruiz, D., P. Salinas, M. L. Lopez-Redondo, M. L. Cayuela, A. Marina and A. Contreras (2008). "Phosphorylation-independent activation of the atypical response regulator NblR." Microbiology **154**(Pt 10): 3002-3015.

Salinas, P., D. Ruiz, R. Cantos, M. L. Lopez-Redondo, A. Marina and A. Contreras (2007). "The regulatory factor SipA provides a link between NblS and NblR signal transduction pathways in the cyanobacterium Synechococcus sp. PCC 7942." Mol Microbiol **66**(6): 1607-1619.

Sandhu, K. S. and D. Dash (2007). "Dynamic alpha-helices: conformations that do not conform." Proteins **68**(1): 109-122.

Schaaf, S. and M. Bott (2007). "Target genes and DNA-binding sites of the response regulator PhoR from Corynebacterium glutamicum." J Bacteriol **189**(14): 5002-5011.

Schachter, J. (1999). Infection and disease epidemiology. In Chlamydia: Intracellular Biology, Pathogenesis and Immunity. S. R.S. Washington D.C., ASM**:** 139-169.

Schar, J., A. Sickmann and D. Beier (2005). "Phosphorylation-independent activity of atypical response regulators of Helicobacter pylori." J Bacteriol **187**(9): 3100-3109.
Schaumburg, C. S. and M. Tan (2006). "Arginine-dependent gene regulation via the ArgR repressor is species specific in chlamydia." J Bacteriol **188**(3): 919-927.
Scidmore, M. A. (2005). "Cultivation and Laboratory Maintenance of Chlamydia trachomatis." Curr Protoc Microbiol **Chapter 11**: Unit 11A 11.
Sheldrick, G. M. (2008). "A short history of SHELX." Acta Crystallogr A **64**(Pt 1): 112-122.
Siam, R. and G. T. Marczynski (2003). "Glutamate at the phosphorylation site of response regulator CtrA provides essential activities without increasing DNA binding." Nucleic Acids Res **31**(6): 1775-1779.
Sippel, K. H., A. H. Robbins, R. Reutzel, J. Domsic, S. K. Boehlein, L. Govindasamy, M. Agbandje-McKenna, C. J. Rosser and R. McKenna (2008). "Structure determination of the cancer-associated Mycoplasma hyorhinis protein Mh-p37." Acta Crystallogr D Biol Crystallogr **64**(Pt 11): 1172-1178.
Sola, M., F. X. Gomis-Ruth, L. Serrano, A. Gonzalez and M. Coll (1999). "Three-dimensional crystal structure of the transcription factor PhoB receiver domain." J Mol Biol **285**(2): 675-687.
Spedding, L. (2009). "Novel effector protein and transcriptional regulation of the type three secretion system in *Chlamydia trachomatis*." Unpublished Masters Thesis **University of Kansas**.
Spencer, W., R. Siam, M. C. Ouimet, D. P. Bastedo and G. T. Marczynski (2009). "CtrA, a global response regulator, uses a distinct second category of weak DNA binding sites for cell cycle transcription control in Caulobacter crescentus." J Bacteriol **191**(17): 5458-5470.
Stephens, R. S. (2002). Chlamydia evolution: A billion years and counting. Proceeding of the tenth international symposium on human chlamydial infections., Antalya, Turkey, International Chlamydia Symposium.
Stephens, R. S. (2003). "The cellular paradigm of chlamydial pathogenesis." Trends Microbiol **11**(1): 44-51.
Stephens, R. S., S. Kalman, C. Lammel, J. Fan, R. Marathe, L. Aravind, W. Mitchell, L. Olinger, R. L. Tatusov, Q. Zhao, E. V. Koonin and R. W. Davis (1998). "Genome sequence of an obligate intracellular pathogen of humans: Chlamydia trachomatis." Science **282**(5389): 754-759.
Stephens, R. S., G. Myers, M. Eppinger and P. M. Bavoil (2009). "Divergence without difference: phylogenetics and taxonomy of Chlamydia resolved." FEMS Immunol Med Microbiol **55**(2): 115-119.
Stevens-Simon, C. and J. Sheeder (2005). "Chlamydia trachomatis: common misperceptions and misunderstandings." J Pediatr Adolesc Gynecol **18**(4): 231-243.
Stock, A. M., V. L. Robinson and P. N. Goudreau (2000). "Two-component signal transduction." Annu Rev Biochem **69**: 183-215.
Stock, J. B., A. J. Ninfa and A. M. Stock (1989). "Protein phosphorylation and regulation of adaptive responses in bacteria." Microbiol Rev **53**(4): 450-490.
Suzuki, M. (1994). "A framework for the DNA-protein recognition code of the probe helix in transcription factors: the chemical and stereochemical rules." Structure **2**(4): 317-326.
Thomson, N. R., M. T. Holden, C. Carder, N. Lennard, S. J. Lockey, P. Marsh, P. Skipp, C. D. O'Connor, I. Goodhead, H. Norbertzcak, B. Harris, D. Ormond, R. Rance, M. A. Quail, J. Parkhill, R. S. Stephens and I. N. Clarke (2008). "Chlamydia trachomatis: genome sequence analysis of lymphogranuloma venereum isolates." Genome Res **18**(1): 161-171.
Thylefors, B., A. D. Negrel, R. Pararajasegaram and K. Y. Dadzie (1995). "Global data on blindness." Bull World Health Organ **73**(1): 115-121.
Toro-Roman, A., T. R. Mack and A. M. Stock (2005). "Structural analysis and solution studies of the activated regulatory domain of the response regulator ArcA: a symmetric dimer mediated by the alpha4-beta5-alpha5 face." J Mol Biol **349**(1): 11-26.
Toro-Roman, A., T. Wu and A. M. Stock (2005). "A common dimerization interface in bacterial response regulators KdpE and TorR." Protein Sci **14**(12): 3077-3088.

Tsai, C. J., S. L. Lin, H. J. Wolfson and R. Nussinov (1997). "Studies of protein-protein interfaces: a statistical analysis of the hydrophobic effect." Protein Sci **6**(1): 53-64.

Vandahl, B. B., S. Birkelund and G. Christiansen (2004). "Genome and proteome analysis of Chlamydia." Proteomics **4**(10): 2831-2842.

Villareal, C., J. A. Whittum-Hudson and A. P. Hudson (2002). "Persistent Chlamydiae and chronic arthritis." Arthritis Res **4**(1): 5-9.

Wade, J. T., K. Struhl, S. J. Busby and D. C. Grainger (2007). "Genomic analysis of protein-DNA interactions in bacteria: insights into transcription and chromosome organization." Mol Microbiol **65**(1): 21-26.

Wang, L., X. Tian, J. Wang, H. Yang, K. Fan, G. Xu, K. Yang and H. Tan (2009). "Autoregulation of antibiotic biosynthesis by binding of the end product to an atypical response regulator." Proc Natl Acad Sci U S A **106**(21): 8617-8622.

Wang, S., J. Engohang-Ndong and I. Smith (2007). "Structure of the DNA-binding domain of the response regulator PhoP from Mycobacterium tuberculosis." Biochemistry **46**(51): 14751-14761.

Wedel, A. and S. Kustu (1995). "The bacterial enhancer-binding protein NTRC is a molecular machine: ATP hydrolysis is coupled to transcriptional activation." Genes Dev **9**(16): 2042-2052.

West, A. H. and A. M. Stock (2001). "Histidine kinases and response regulator proteins in two-component signaling systems." Trends Biochem Sci **26**(6): 369-376.

Yoshida, T., L. Qin, L. A. Egger and M. Inouye (2006). "Transcription regulation of ompF and ompC by a single transcription factor, OmpR." J Biol Chem **281**(25): 17114-17123.

Yu, H. H., D. Kibler and M. Tan (2006). "In silico prediction and functional validation of sigma28-regulated genes in Chlamydia and Escherichia coli." J Bacteriol **188**(23): 8206-8212.

Yu, H. H. and M. Tan (2003). "Sigma28 RNA polymerase regulates hctB, a late developmental gene in Chlamydia." Mol Microbiol **50**(2): 577-584.

Yucesan, C. and S. Sriram (2001). "Chlamydia pneumoniae infection of the central nervous system." Curr Opin Neurol **14**(3): 355-359.

Z. Otwinowski and W. Minor (1997). Processing of X-ray Diffraction Data Collected in Oscillation Mode. Methods in Enzymology, Macromolecular Crystallography, part A. C. W. Carter and R. M. Sweet. New York, Academic Press. **276:** 307-326.

Zhao, H., A. Heroux, R. D. Sequeira and L. Tang (2009). "Preliminary crystallographic studies of the regulatory domain of response regulator YycF from an essential two-component signal transduction system." Acta Crystallogr Sect F Struct Biol Cryst Commun **65**(Pt 7): 719-722.